Single-domain Antibody Inhibitors of *Clostridium difficile* Toxins

By

Greg Hussack

Thesis submitted to the

Faculty of Graduate and Postdoctoral Studies

In partial fulfillment of the requirements

For the PhD degree in Microbiology and Immunology

Department of Biochemistry, Microbiology and Immunology

Faculty of Medicine

University of Ottawa

ABSTRACT

Clostridium difficile is a leading cause of nosocomial infection in North America and a considerable challenge to healthcare professionals in hospitals and nursing homes. The Gram-positive bacterium produces two exotoxins, toxin A (TcdA) and toxin B (TcdB), which are the major virulence factors responsible for *C. difficile*-associated disease (CDAD) and are targets for CDAD therapy. In this work, recombinant single-domain antibody fragments (V_HHs) which target the cell receptor binding domains of TcdA or TcdB were isolated from an immune, llama phage display library and characterized. Four V_HHs (A4.2, A5.1, A20.1, and A26.8) were potent neutralizers of the cytopathic effects of TcdA in an *in vitro* assay and the neutralizing potency was enhanced when V_HHs were administered in combinations. Epitope mapping experiments revealed that some synergistic combinations consisted of V_HHs recognizing overlapping epitopes, an indication that factors other than mere epitope blocking are responsible for the increased neutralization. Binding assays revealed TcdA-specific V_HHs neutralized TcdA by binding to sites other than the carbohydrate binding pocket of the toxin. The TcdB-specific V_HHs failed to neutralize TcdB, as did a panel of human V_L antibodies isolated from a synthetic library. To enhance the stability of the *C. difficile* TcdA-specific V_HHs for oral therapeutic applications, the V_HHs were expressed with an additional disulfide bond by introducing Ala/Gly54Cys and Ile78Cys mutations. The mutant V_HHs were found to be well expressed, were non-aggregating monomers, retained low nM affinity for TcdA, and were capable of *in vitro* TcdA neutralization. Digestion of the V_HHs with the major gastrointestinal proteases, at biologically relevant concentrations,

revealed a significant increase in pepsin resistance for all mutants and an increase in chymotrypsin resistance for the majority of mutants without compromising inherent V_HH trypsin resistance. Collectively, the second disulfide not only increased V_HH thermal stability at neutral pH, as previously shown, but also represents a generic strategy to increase V_HH stability at low pH and impart protease resistance. These are all desirable characteristics for the design of protein-based oral therapeutics. In conclusion, llama V_HHs represent a class of novel, non-antibiotic inhibitors of infectious disease virulence factors such as *C. difficile* toxins.

ACKNOWLEDGEMENTS

To my dearest family, friends, and colleagues. Thank you for all of your support!

TABLE OF CONTENTS

LIST OF ABBREVIATIONS

Ab	antibody
Ag	antigen
AP	alkaline phosphatase
BIC	bovine immunoglobulin concentrate
BSA	bovine serum albumin
CD	circular dichroism
CDAD	*Clostridium difficile*-associated disease
CD-grease	α-Gal-(1,3)-β-Gal-(1,4)-β-GlcNAcO$(CH_2)_8CO_2CH_3$
cDNA	complementary DNA
CDR	complementarity-determining region
C_H	constant heavy
CID	collision induced dissociation
CNBr	cyanogen bromide
CP	cysteine protease domain
DDA	data dependent analysis
dsDNA	double-stranded DNA
EDTA	ethylenediaminetetraacetic acid
ELISA	enzyme-linked immunosorbent assay
ESI	electrospray ionization
F80	80 amino acid fragment of TcdB

Fab	fragment antigen binding
Fc	fragment crystallizable
FCA	Freund's complete adjuvant
FcRn	neonatal IgG Fc receptor
FDA	United States Food and Drug Administration
FF	fraction folded
FIA	Freund's incomplete adjuvant
FR	framework region
Fv	fragment variable
GI	gastrointestinal
GST	glutathione-S-transferase
GT	glucosyltransferase domain
HLF	human lung fibroblast
HPLC	high performance liquid chromatography
HRP	horseradish peroxidase
IgG	immunoglobulin G
IgM	immunoglobulin M
IgNAR	immunoglobulin new antigen receptor
IgY	immunoglobulin Y
IMAC	immobilized-metal affinity chromatography
IMGT	international immunogenetics information system
Ins6P	inositol hexakisphosphate

I.P.	intraperitoneal
I.V.	intravenous
IVIG	intravenous immunoglobulin
K_D	equilibrium dissociation constant
k_{off}	dissociation rate constant
k_{on}	association rate constant
Le^X-AmHex	Gal-β1,4-(Fuc-α1,3)-GlcNAc-$(CH_2)_6$-NH_2-HOAc
mAb	monoclonal antibody
mdeg	millidegrees
MI	membrane insertion domain
mRNA	messenger RNA
MRW	mean residue weight
MS	mass spectrometry
Mut	mutant
MW	molecular weight
NaPi	sodium phosphate buffer
OD	optical density
PAGE	polyacrylamide gel electrophoresis
PaLoc	*Clostridium difficile* pathogenicity locus
PBS	phosphate-buffered saline
PCG-4	antitoxin A monoclonal antibody
PCR	polymerase chain reaction

pGEX-6P-2	GST-containing expression vector
pMED1	phagemid vector
pMED2	V_HH expression vector
pSJF2H	V_HH expression vector
PVDF	polyvinylidene difluoride
pyro-Q	pyro-glutamic acid
rAb	recombinant antibody
RBD	cell receptor binding domain
RPLC-ESI-MS	reversed-phase HPLC mass spectrometry
RU	resonance unit
scFv	single-chain variable fragment antibody
sdAb	single-domain antibody
SDS	sodium dodecyl sulfate
SEC	size exclusion chromatography
sIgA	secretory immunoglobulin A
SLP	surface layer protein
SOC	super optimized culture medium
SOE	splice overlap extension
SPR	surface plasmon resonance
TcdA	*Clostridium difficile* toxin A
TcdB	*Clostridium difficile* toxin B
T_m	thermal unfolding midpoint temperature

T_{onset}	thermal unfolding onset temperature
TMB	3,3′,5,5′-tetramentylbenzidine
TRE	thermal refolding efficiency
V_HH	heavy-chain antibody variable domain
V_H	heavy chain variable domain
V_L	light chain variable domain
V_{NAR}	IgNAR variable domain
WT	wild-type

LIST OF FIGURES

LIST OF TABLES

1.0 INTRODUCTION

Therapeutic agents targeting bacterial virulence factors are gaining interest as non-antibiotic alternatives for the treatment of infectious diseases. *C. difficile* is a Gram-positive, anaerobic, endospore-forming gastrointestinal pathogen responsible for *C. difficile*-associated disease (CDAD) in humans and animals with symptoms ranging in severity from mild cases of antibiotic-associated diarrhea to fatal pseudomembranous colitis (93, 112, 157, 169). Each year in North America, 1-3% of hospitalized patients receiving antibiotics become infected with *C. difficile*, leading to thousands of deaths and over $1 billion in associated costs to the health-care system (93, 109, 202). *C. difficile* produces two primary virulence factors, toxin A (TcdA) and toxin B (TcdB), which are large (308 kDa and 269 kDa, respectively), single-polypeptide chain exotoxins composed of a catalytic, a translocation and a cell receptor binding domain (RBD) (80, 81). It has been suggested TcdB is solely responsible for *C. difficile* virulence (126) although a recent study found both TcdA- and TcdB-knockout *C. difficile* strains are capable of causing mortality in hamsters (106). This later finding is in agreement with earlier work that showed both anti-TcdA and anti-TcdB mAbs were required for full protection of hamsters from CDAD (11, 99) and anti-TcdA mAbs were required for protection in mice from CDAD (26).

Patients suffering from CDAD are most commonly treated with metronidazole or vancomycin antibiotics (112). However, there are several emerging challenges warranting the development of novel therapeutics. First, there is no acute CDAD treatment targeting TcdA/B. These toxins are responsible for loss of epithelial barrier function in the colon by disrupting tight junctions and increasing membrane

permeability, causing diarrhea and promoting severe inflammation (80, 157). Second, hypervirulent strains of *C. difficile*, such as the NAP1/027 isolate, over-express TcdA and TcdB (197) and have been associated with increased mortality rates and disease severity (140, 148). Third, an estimated 20-25% of patients suffering from CDAD experience symptomatic relapse after the initial infection is cleared, with 45% of these patients prone to subsequent relapses (85).

Taken together, there is a need for non-antibiotic based reagents which target and inhibit TcdA and TcdB for CDAD therapy. Antibodies specific for TcdA and TcdB have been shown to effectively treat CDAD and prevent disease relapse in animal models and in humans (Table 1.1, Table 1.2, Table 1.3).

This opening chapter reviews *C. difficile* toxin structure and function, highlights the various toxin-specific antibody formats and strategies under development for treating CDAD, and discusses future directions for CDAD immunotherapy, including the use of engineered antibody fragments with robust biophysical properties for systemic and oral delivery.

1.1 *C. difficile*

C.difficile is a Gram-positive, endospore-forming, anaerobic, gastrointestinal pathogen that is a leading cause of nosocomial infections in developed nations. The bacterium is transmitted by the fecal-oral route and can readily colonize persons with suppressed microbiota as a result of antibiotic usage. The symptoms of *C. difficile* infection range from mild cases of diarrhea to fatal pseudomembranous colitis and are collectively known as *C. difficile*-associated disease (CDAD) (112, 140, 157). The recent

emergence of hypervirulent and antibiotic-resistant *C. difficile* strains with increased morbidity, mortality and recurrence rates (129, 197) have warranted the development of novel, non-antibiotic based treatment regimes. *C. difficile* exerts its pathological effects by colonizing luminal surfaces of the colon and secreting two high-molecular weight exotoxins. With their causative role in CDAD firmly established (11, 97, 123, 126), these two virulence factors have been identified as targets for therapeutic intervention. With the continued rise of antibiotic resistance, the development of novel, non-antibiotic agents which target bacterial virulence factors and reduce the selection pressure normally placed upon pathogens by antibiotics are highly desirable (16, 23, 153). These agents, such as antibodies (Abs), may also be useful to control the recurrence of infection after antibiotic treatment has been terminated.

1.2 *C. difficile* colonization and toxin production

Before *C. difficile* can exert a physiological effect on a host, the pathogen must colonize the host. It is believed that *C. difficile* spores are consumed orally and travel to the large intestine where they flourish in environments lacking competition from normal gut microbiota. Surface layer proteins (SLPs), which decorate the pathogen's surface, are involved in adherence to the human intestinal epithelium and are thought to be a critical step in gut colonization (18). Quorum sensing molecules have been shown to play an important role in transcriptional regulation of toxin production (111) suggesting toxin production is a cell-density dependent process. Whether *C. difficile* toxin production and secretion occurs during or after colonization of the host is unknown.

1.2.1 Toxin structure and function

TcdA and TcdB are single-polypeptide chain, high-molecular weight exotoxins (308 kDa and 269 kDa, respectively) organized into multi-domain structures (4, 80). The genes encoding TcdA and TcdB, *tcdA* and *tcdB*, are located in the 19.6 kb *C. difficile* pathogenicity locus (PaLoc) and are positively regulated at the protein level by TcdR, a sigma factor (192). Like other members of the large clostridial toxin family, TcdA and TcdB are organized as modular domains with each domain performing a distinct function (Figure 1.1). Similar to other members of the large clostridial family of toxins, TcdA and TcdB target the Rho/Ras superfamily of GTPases by irreversible modification through glucosylation (80, 192). Since GTPases are key cellular regulatory proteins, their permanent inactivation causes disruptions in essential cell signaling pathways that are critical for transcriptional regulation, apoptosis, cytoskeleton integrity, and eventually colonic epithelial cell barrier function (81, 150).

The C-terminal region of TcdA/B is responsible for toxin binding to the surface of epithelial cells possibly via multi-valent interactions with putative cell-surface carbohydrate receptors (34, 53). Structural studies of this receptor binding domain (RBD) region from TcdA and TcdB revealed a β-solenoid fold (4, 70) with 7 carbohydrate binding sites identified for receptor binding in TcdA (53, 70). While the C-terminal region of TcdA has been shown to bind various oligosaccharides, including the trisaccharide α-Gal-(1,3)-β-Gal-(1,4)-β-GlcNac (103), the native human ligand has not been positively identified. The TcdB host cell receptor also remains unknown. Binding of TcdA/B via the RBD to epithelial cells induces receptor-mediated endocytosis, permitting entry of the endosome-encapsulated toxin into the cytoplasm (Figure 1.2).

Once internalized, the toxins require an acidic endosome for transport to the cytosol. A decrease in endosomal pH is thought to induce a conformational change, resulting in exposure of the hydrophobic membrane insertion (MI) domain and insertion of the N-terminus (catalytic domain and cysteine protease domain) into and through the endosomal membrane via pore formation [reviewed in (80)]. Recently, Reineke *et al* (156) showed inositol hexakisphosphate (InsP6) from the host cell induces the autocatalytic cleavage of the N-terminal region at the cysteine protease (CP) site, freeing the N-terminal glucosyltransferase (GT) domain into the cytosol while the remaining portions of the toxin are left in the endosome. This finding was later supported by evidence from Egerer *et al* (38). Upon cleavage, the GT domain is capable of transferring glucose residues from UDP-glucose to Rho-GTPases (89), locking the important cell signaling mechanism in an inactive conformation. Inhibition of Rho-GTPases causes a series of cascading effects, including dysregulation of actin cytoskeleton and tight junction integrity. Collectively, these events lead to increased membrane permeability and loss of barrier function (66), diarrhea, inflammation, and a massive influx of neutrophils and other mediators of the innate immune response (112).

Figure 1.1. Schematic representation of *C. difficile* toxins A and B.
(**A**) For illustration purposes, only one toxin is shown. Toxin A (TcdA, 308 kDa) and toxin B (TcdB, 269 kDa) are each composed of four domains which perform distinct functions. The schematic illustrates each domain, their function, and site of action. GT = glucosyltransferase domain, CP = cysteine protease domain, MI = hydrophobic membrane insertion domain, RBD = cell receptor binding domain. (**B**) 3D reconstruction of TcdA and organization of the four functional domains. Red = glucosyltransferase domain, blue = cysteine protease domain, yellow = hydrophobic membrane insertion domain, green = cell receptor binding domain. Image adopted from Pruitt et al (152).

A

Domain:	Glucosyltransferase	Cysteine protease	Membrane insertion	Cell receptor binding domain
Function:	Glucosylation of Rho GTPase	Cleavage of GT from toxin	N-terminal toxin entry into cytosol	Binding of toxin to and entry into epithelial cell
Site of action:	Cytosol	Cytosol	Endosome	Extracellular

B

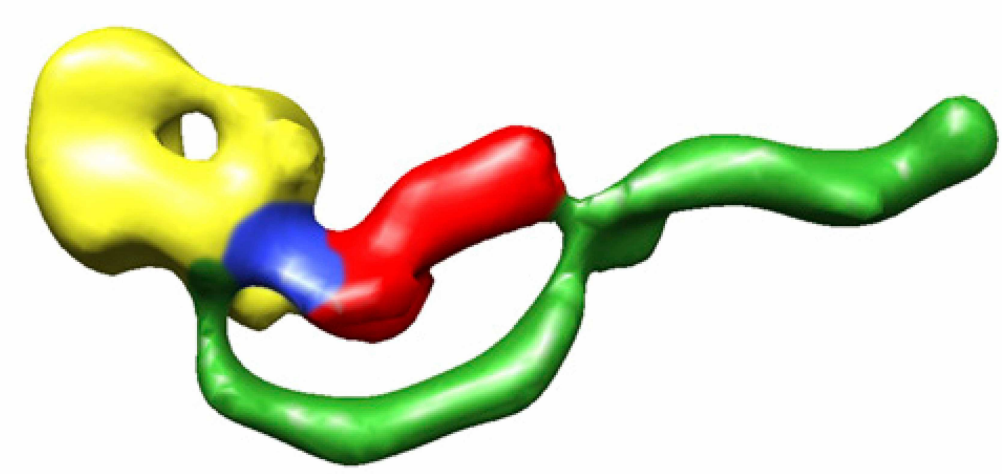

Figure 1.2. Schematic illustration of *C. difficile* toxin mechanism of action.
TcdA or TcdB first binds the surface of epithelial cells via the RBD region of the toxin, promoting receptor-mediated endocytosis. Acidification of the endosome-encapsulated toxin promotes a conformational change in which the N-terminal region of the toxin is extended through the endosomal membrane into the cytoplasm. Cellular inositol hexakisphosphate (InsP6) promotes cleavage at the start of the CP domain, releasing the GT domain into the cytoplasm. The GT domain transfers a glucose moiety from UDP-glucose to a threonine (T) residue on Rho-GTPase, trapping the signaling enzyme in an inactive conformation. Targeting the RBD domain with antibodies and antibody fragments may block toxin binding to cell-surface receptors or prevent internalization of the toxin.

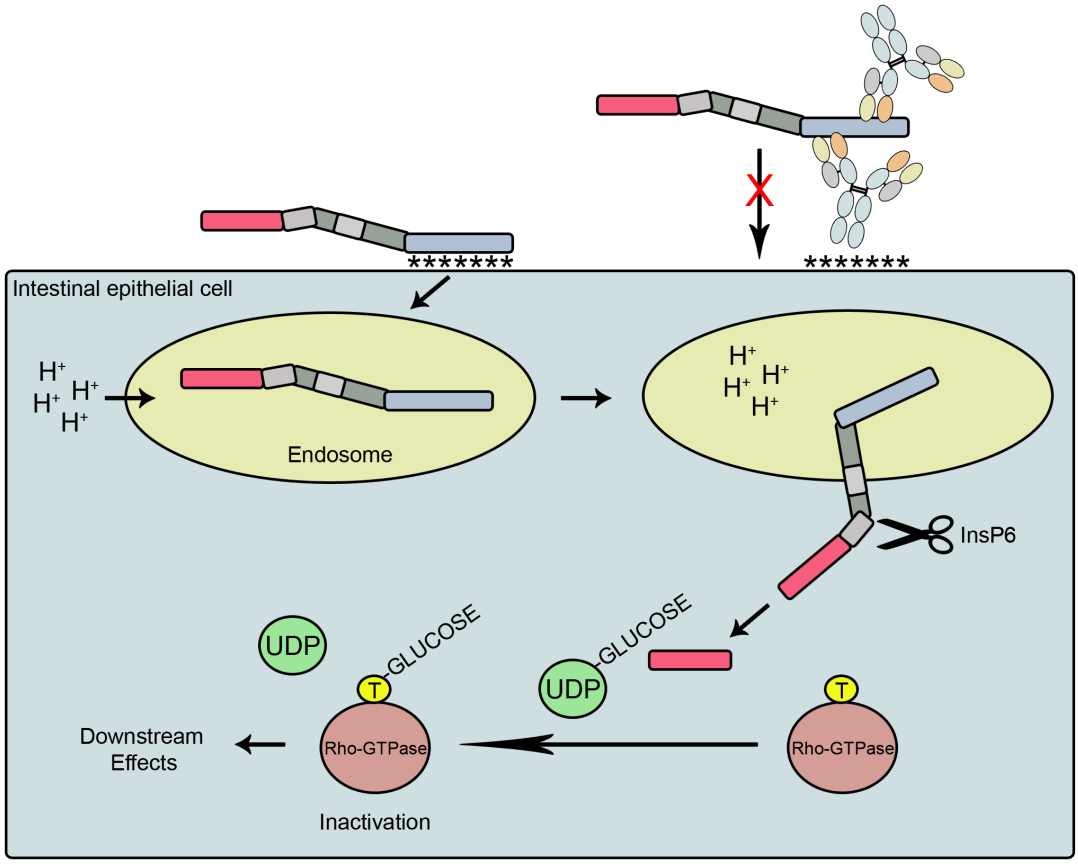
****
****
Intestinal epithelial cell
H+ H+ H+ H+
Endosome
H+ H+ H+ H+
InsP6
UDP
GLUCOSE
T
Rho-GTPase
UDP
GLUCOSE
T
Rho-GTPase
Downstream Effects
Inactivation

1.3 Treatment of CDAD

The most common treatment for *C. difficile* infection currently involves discontinuing the original antibiotic in use at the time of diagnosis followed by administration of vancomycin or metronidazole antibiotics. However, resistant strains to both antibiotics have been reported (48, 147). In addition, increased CDAD recurrence rates and the prominence of hypervirulent strains over expressing TcdA and TcdB (129, 197) highlight the need for novel approaches to treatment. There are several strategies under development for the treatment of CDAD (Table 1.1), including: various antibiotics, antimicrobial peptides, replenishment of patient microbiota with oral probiotic therapy or fecal-transplantation therapy, development of toxin binding resins and polymers, vaccines, and toxin-specific antibodies and recombinant antibody fragments (14, 85, 112, 141, 146). The remainder of this opening chapter is focused on the literature describing efforts to develop anti-TcdA/B antibodies for CDAD immunotherapy, reports the successes and failures, and describes the challenges that lie ahead.

Table 1.1. Therapeutic strategies under development for the treatment of CDAD.

Type of therapy	Description	Reference
Antibiotic	Nitazoxanide	(134)
	Rifaximin	(47)
	Ramoplanin	(41)
	Difimicin	(178)
	Fidamoxicin	(117)
Antimicrobial peptide	Thuricin CD	(154)
Probiotic	*Saccharomyces boulardii*	(186)
	Lactobacillus spp.	(56)
Fecal transplantation	Stool replacement therapy	(1)
Toxin binding agent	Cholestyramine	(131)
	Tolevamer	(164)
Vaccine	Toxoid-based	(170)
	SLP-based	(137)
	DNA-based	(46)
Antibody	IgG, IgA, IgY, polyclonal	Table 1.2 and 1.3
	scFv	(32)
	V_HH	(77)

1.4 Toxin specific antibodies

The field of antibody engineering has rapidly expanded over the past few decades, proving itself as a source for high-affinity, high-specificity, protein-based binding reagents for a myriad of applications (72). From polyclonal antibody production in animals, to hybridoma cell culture of IgG antibodies, to the rational design of high-affinity antibodies and antibody fragments via display techniques and site-directed mutagenesis, antibodies have been produced by numerous methods and against countless targets of therapeutic importance. Of the US Food and Drug Administration (FDA)-approved therapeutic antibodies on the market, most are for the treatment of cancer and autoimmune disorders, although numerous antibodies targeting the

virulence factors of disease-causing bacteria are in development and in clinical trials (http://www.fda.gov).

With respect to *C. difficile*, administering toxin-neutralizing antibodies for CDAD therapy is supported by numerous studies which have shown that patients with low antitoxin IgG titers are more likely to experience severe effects from *C. difficile* infection and are more likely to develop recurrent rounds of CDAD (Table 1.3).

1.4.1 Role of antibodies in CDAD

Persons infected with *C. difficile* experience a broad-spectrum of symptoms, ranging from asymptomatic carriage to life-threatening pseudomembraneous colitis. The reasons for such varied symptoms, or lack thereof, are not fully understood. It is thought that patients who experience mild cases of CDAD (tend to) possess high antitoxin A IgG serum titers (110, 191, 198). Conversely, patients susceptible to relapsing *C. difficile* infection have demonstrated low anti-TcdA Ig titers, specifically IgM, IgG2 and IgG3 isotypes (91, 110, 113). TcdA-neutralizing secretory IgA (sIgA) antibodies are also thought to play a role in regulating CDAD severity in the colonic mucosa (84, 94). Furthermore, many individuals develop antitoxin A/B antibodies (i.e., IgG, IgA) in the serum (86, 191) and stool after a symptomatic CDAD infection (49). The importance of antitoxin Abs in regulating CDAD severity and relapse is highlighted by the number of experimental vaccines under development. For example, toxoid-based vaccines have protected animals against *C. difficile* challenge (49). Others have shown antibody-mediated protection can be transferred from adult hamsters to offspring through milk (97, 98). Therefore, the introduction of antitoxin antibodies to patients suffering from

severe *C. difficile* infection may be a useful approach to treat severe CDAD or reduce the incidence of recurrent CDAD infection.

1.4.2 Experimental animal studies

Over the past 30 years, a number of antibodies have been isolated against *C. difficile* toxins and their efficacy evaluated in various animal models (Table 1.2). Some of the earliest evidence that antitoxin antibodies may be useful agents for *C. difficile* therapy was demonstrated by Allo *et al* (5) who isolated *C. sordellii* toxin-specific polyclonal Abs and found intraperitoneal (I.P.) injection of these Abs into hamsters prevented clindamycin-induced *C. difficile*-associated colitis. The earliest animal study involving monoclonal antibodies (mAbs) specific for TcdA and TcdB was performed by Lyerly *et al* (122). This group demonstrated that pre-mixing anti-TcdA mAb PCG-4 with TcdA and orally administering the mixture completely protected hamsters from fatal doses of TcdA. However, administration of G-2 IgG, an antibody which cross-reacted with both toxins, failed to protect hamsters against oral TcdA challenge and was not capable of TcdB neutralizing *in vitro*. Elsewhere, Kamiya *et al* (90) isolated a panel of nine TcdA-specific mAbs from hybridoma cell lines, but found none were capable of preventing mouse lethality upon I.P. co-injection of TcdA and mAb. Corthier *et al* (26) later isolated three TcdA-specific mAbs (A9, 141-2, and C11) and found the antibodies completely protected mice when injected intravenously four days prior to *C. difficile* challenge. This panel of mAbs was not tested in *C. difficile* post-challenge treatment models however. Interestingly, these three mAbs and PCG-4 produced by Lyerly *et al* (122) were shown to recognize the C-terminal cell receptor binding domain region of TcdA, indicating the

antibodies may have blocked toxin-cell contacts or prevented internalization of the toxin (Figure 1.2).

In another early study examining oral administration of antitoxin Abs, Lyerly *et al* (119) showed hamsters could be protected prophylactically from the effects of *C. difficile* with orally administered bovine immunoglobulin G concentrate (BIC), which was generated from the colostrum of cows vaccinated with *C. difficile* culture filtrates. In the post infection model, however, the antibodies had no effect on hamsters. Several years later, Kelly *et al* (95) produced two bovine IgG preparations by immunizing cattle with *C. difficile* culture filtrates and formalin inactivated TcdA (toxoid A). Both preparations were capable of inhibiting TcdA-induced cytotoxicity in *in vitro* cell assays, as well as inhibiting the enterotoxic effects of TcdA on rat intestinal loops. The study did not assess the efficacy of bovine IgG preparations in either prophylactic or treatment models.

Table 1.2. Animal studies involving *C. difficile* toxin-specific antibodies.

Antibody	Specificity	Immunogen	Antibody source	Animal model	Challenge type	Ab administration route	Treatment type	Outcome	Ref
PCG-4 IgG	TcdA	Culture filtrate	Mouse	Hamster	Oral TcdA administration	Oral	Ab + TcdA co-administered	Protection	(122)
G-2 IgG	TcdA and B	Toxoid B	Mouse hybridoma	Hamster	Oral TcdA administration	Oral	Ab + TcdA co-administered	No protection	(122)
37B5 IgG	TcdA	Toxoid A	Hybridoma	Mouse	I.P. TcdA administration	I.P.	Ab + TcdA co-administered	No protection	(90)
A9, 141-2, C11 IgGs	TcdA	Toxoid A	Mouse	Mouse	Oral *C. difficile*[1]	I.V.	Prophylactic	Protection	(26)
Bovine Ig	TcdA and B	Culture filtrate	Cow colostrum	Hamster	Oral *C. difficile* (10^8 cells)	Oral	Prophylactic	Protection	(119)
Bovine Ig	TcdA and B	Culture filtrate	Cow colostrum	Rat	CD filtrate into ileum[2]	Ileum injection[2]	Ab + toxin co-injected[2]	Protection	(95)
Anti-TcdA bovine Ig	TcdA	Toxoid A	Cow colostrum	Rat	CD filtrate into ileum[2]	Ileum injection[2]	Ab + toxin co-injected[2]	Protection	(95)
Anti-TcdA IgY	TcdA	rTcdA fragment	Chicken	Hamster	Oral *C. difficile* (10^4 cells)	Oral	Treatment and relapse	Protection	(50)
Anti-TcdB IgY	TcdB	rTcdB fragment	Chicken	Hamster	Oral *C. difficile* (10^4 cells)	Oral	Treatment and relapse	Protection	(99)
Polyclonal	TcdA and B	rTcdA/B toxoid	Mouse	Hamster	Oral *C. difficile* (10^5 cells)	I.P.	Prophylactic	Protection	(50)
Bovine immune whey	TcdA and B	Culture filtrate	Cow	Hamster	Oral *C. difficile* (10^4 cells)	Oral	Prophylactic and treatment	Protection	(190)
CDA1 IgG	TcdA	Toxoid A	Mouse hybridoma[3]	Hamster	Oral *C. difficile* spores (140)[4]	I.P.	Treatment and relapse	Protection	(11)
MDX-1388 IgG	TcdB	rTcdB fragment	Mouse hybridoma[3]	Hamster	Oral *C. difficile* spores (140K)[4]	I.P.	Treatment and relapse	Protection	(11)

1. Number of *C. difficile* cells administered was not given.
2. *C. difficile* (CD) culture filtrates containing TcdA and TcdB were co-injected into rat ileal loops with antitoxin bovine Ig.
3. Mouse hybridoma cells were generated from HuMAb™ mice. HuMAb™ mice are transgenic mice containing human immunoglobulin genes.
4. One-hundred forty (140) *C. difficile* spores were given orally in the treatment model, while 140,000 *C. difficile* spores were given orally in the relapse model.
I.P. = intraperitoneal.
I.V. = intravenous.

In a seminal study, Kink and Williams (99) demonstrated that hens immunized with recombinant TcdA and TcdB fragments could yield potent toxin-neutralizing IgY antibodies. As with other studies noted above, only anti-TcdA was required for prophylactic protection. However, when IgY antibodies specific to both toxins were administered orally to hamsters, the effects were profound: hamsters suffering from CDAD were successfully treated and did not show signs of CDAD relapse. This study indicated, for the first time, that neutralization of TcdB was important in treatment of CDAD and prevention of CDAD relapse. Furthermore, this was one of the most successful examples of oral antibody administration, likely due to the robustness of IgY antibodies in withstanding the harsh pH and protease-rich gastrointestinal (GI) tract. Elsewhere, Giannasca *et al* (50) demonstrated that passive immunization of hamsters with immune hamster sera and polyclonal ascites fluid via the I.P. route resulted in full protection when administered two days before oral *C. difficile* challenge. This study was one of the first to show systemically delivered antitoxin antibodies could offer mucosal protection from CDAD in hamsters. From this work and that of others, it became obvious that antitoxin A and B Abs were required for treatment of CDAD. More recently, van Dissel *et al* (190) showed bovine immune whey preparations containing toxin-specific sIgA and IgG antibodies from immunized cattle were effective at preventing *C. difficile*-induced hamster mortality when administered orally before and after bacterial challenge. Compared to control animals, 80 – 90% of hamsters receiving the immune whey survived.

Most of the antitoxin Ab work reviewed thus far involved antibodies produced from animal sources, but for systemic human therapeutics, antibodies should be humanized or of

human origin to reduce potential immunogenicity. Antibody immunogenicity, however, should not be a concern in the oral therapy approach. The first human antitoxin mAbs specific to TcdA and TcdB were isolated in 2006 and reported by Babcock *et al* (11). The group evaluated several antibodies, and found that I.P. administration of their best TcdA-binding candidate (CDA1) combined with their top TcdB-binder (MDX-1388, later referred to as "CDB1") significantly reduced hamster mortality in the primary CDAD treatment model and CDAD relapse model, relative to either mAb alone. Similar to the most efficacious antibodies reported before, both CDA1 and MDX-1388 (CDB1) recognized the C-terminal host-cell receptor binding domains of TcdA and TcdB, respectively. This work has led to the testing of CDA1 and MDX-1388 (CDB1) in the first human clinical trial for the treatment of recurrent CDAD, which is discussed below.

1.4.3 Experimental human studies

A number of studies and case reports have indicated that passive immunotherapy is a successful therapy for human patients suffering from chronic relapsing *C. difficile* infection who did not respond to standard treatment (i.e., antibiotic therapy). In contrast to animal studies where antibodies were delivered orally or systemically, the majority of human studies thus far have used the systemic delivery route.

The earliest reports of treating relapsing CDAD in humans with antibodies were based on intravenous immunoglobulin (IVIG) therapy (Table 1.3). IVIG involves injecting high doses of human Ig's (300 – 400 mg Ig/kg of body weight) from healthy donors, which

are thought to contain TcdA- and TcdB-specific antibodies, into patients suffering from CDAD. The first data showing successful treatment of relapsing CDAD with IVIG were from Leung *et al* (113) who reported five out of five children were cleared of their symptoms upon receiving 400 mg IVIG/kg. Others have reported similar findings using IVIG therapy in adults with patient survival rates ranging from 60% - 100%, although these studies lacked control subjects (15, 21, 65, 102, 130, 132, 161, 201). Conversely, a retrospective analysis performed by Juang *et al* (87) concluded that patients administered IVIG (n = 18) showed no statistical advantages over control groups (n = 18). More recently, Abougergi *et al* (3) reported 9 of 21 patients (43%) receiving IVIG for severe CDAD survived, indicating one of the highest mortality rates of IVIG thus far.

The first case of orally delivered antitoxin therapy was reported by Tjellström *et al* (183) who successfully treated a 3½ year old boy with purified human IgA. Recently, a study by van Dissel *et al* (190) demonstrated the effectiveness of orally delivered bovine immune whey to CDAD patients. Whey protein enriched in bovine immunoglobulins was prepared from cattle immunized with inactivated *C. difficile* culture filtrates. Of 15 patients receiving the oral immunoglobulin mixture, 14 were completely cured of *C. difficile*-associated diarrhea. The same group then conducted a larger study and found their immune whey treatment successfully prevented CDAD relapse in 98 out of 109 patients (139). Later, Mattila *et al* (128) used a similar approach of orally administering bovine immune whey to patients suffering from CDAD and found a 55% success rate, although the clinical trial was prematurely terminated. The discrepancies between the success rates of the first two immune whey studies (139, 190) and that conducted by Mattila *et al* (128) may be

due to differences in the immune whey product, patient selection criteria, previous antibiotic usage, and overall study design.

Collectively, these studies illustrated the effectiveness of polyclonal antitoxin antibody preparations on severe CDAD when administered intravenously or orally to patients. However, a major issue with IVIG therapy or bovine immune concentrates is the quantity, quality and variability of toxin-specific antibodies contained within these preparations. As such, comparisons of the effectiveness of each of these studies should be treated with caution.

In a landmark study, Lowy *et al* (118) recently provided data on the largest clinical trial involving CDAD therapy and the efficacy of human antitoxin mAbs. The study intravenously administered specific doses of both anti-TcdA mAb CDA1 and anti-TcdB mAb CDB1 or placebo control to 200 patients with recurrent CDAD symptoms. The authors found a significant reduction in CDAD recurrence compared to controls, with only 7% of those receiving the mAb therapy relapsing compared to a 25% relapse rate among patients receiving placebo.

1.4.4 Antibody mechanism of action

How systemically-administered antitoxin antibodies can neutralize TcdA and TcdB, which are found primarily in the colon, is not well understood. Two possible explanations have been proposed. First, antitoxin antibodies administered systemically are thought to migrate to the GI tract through a leaky mucosal barrier (49, 108). With many immune

centers located in close proximity to the mucosa barrier, inflamed or disrupted epithelial cells may allow easy access of systemic Abs to the lumen. Alternatively, IgGs may be actively transported from systemic circulation to the lumen via the neonatal IgG Fc receptor (FcRn) which is expressed by colonic epithelial cells (108, 206). Both cases are supported by an increase in the levels of IgG in the stools from infected patients (198). It is possible that administered Abs may bind and neutralize TcdA/B in the bloodstream, although the principal sight of action is believed to be in the GI tract. Regardless of administration route, systemic or oral, at the molecular level the mechanism of antibody-based toxin-neutralization *in vivo* appears to involve inhibition of the binding of toxin to target cells, a critical first step in the toxins' mechanism of action (Figure 1.2).

Table 1.3. Therapeutic human studies involving *C. difficile* toxin-specific antibodies.

Antibody	Specificity	Source	Administration route	Number of treated patients	Treatment success rate (%)	Ref
IVIG prep	TcdA	Human	I.V.	5	100	(113)
IVIG prep	TcdA and B	Human	I.V.	2	100	(161)
IVIG prep	Unknown	Human	I.V.	4	100	(15)
IVIG prep	Unknown	Human	I.V.	5	60	(201)
IVIG prep	Unknown	Human	I.V.	14	64	(130)
IVIG prep	Unknown	Human	I.V.	1	100	(132)
IVIG prep	Unknown	Human	I.V.	18	83	(87)
IVIG prep	Unknown	Human	I.V.	1	100	(65)
IVIG prep	Unknown	Human	I.V.	1	100	(102)
IVIG prep	Unknown	Human	I.V.	2	100	(21)
IVIG prep	Unknown	Human	I.V.	21	43	(3)
IgA	Unknown	Human	Oral	1	100	(183)
Bovine immune whey	TcdA and B	Cow	Oral	15	93	(190)
Bovine immune whey	TcdA and B	Cow	Oral	101	90	(139)
Bovine immune whey	TcdA and B	Cow	Oral	20	55	(128)
CDA1 IgG	TcdA	Mouse hybridoma[1]	I.V.	101	93	(118)
CDB1 IgG	TcdB	Mouse hybridoma[1]	I.V.	101	93	(118)

1. Mouse hybridoma cells were generated from HuMAb™ mice. HuMAb™ mice are transgenic mice containing human immunoglobulin genes.

IVIG = intravenous immunoglobulin; I.P. = intraperitoneal; I.V. = intravenous.

1.5 Future perspectives for CDAD immunotherapy

Many cases documenting the successful treatment of relapsing CDAD with antibody-based reagents have relied on systemically-delivery antibody administration. As mentioned above, these antibodies likely need to reach the GI tract to work effectively. This brings forth the question: Is systemic delivery the most efficacious method for antitoxin therapy?

Conceivably, oral-administered toxin-neutralizing antibodies would bypass the need for systemically delivered Abs to traverse the mucosal barrier to the GI tract. Currently, there are only a handful of examples in the literature suggesting oral therapy may be effective. This may be largely due to the sensitivitiy of conventional IgGs to the extreme pH and protease-rich environment of the stomach and small intestine. Bovine immune Ig preparations (196) and IgA preparations (183) appear to survive the GI tract as oral administration has proven effective and functional toxin-specific antibodies have been recovered after GI tract passage (183, 196). To enhance the efficacy of orally delivered Abs, the exploration of protective antibody formulations and engineered antibodies with robust biophysical properties may be warranted.

1.5.1 Recombinant antibody fragments

Antibody fragments (Figure 1.3) are smaller versions of parent antibodies (i.e., IgGs) that lack one or more C_H domains while retaining antigen binding capacity. In contrast to conventional antibodies (i.e., IgGs) which are produced by traditional immunization

approaches, antibody fragments are routinely generated through *in vitro* selection procedures from synthetic/semi-synthetic, naïve, or immune display libraries [reviewed in (72, 74)]. While both methods of antibody generation are equally important for generating therapeutic antibodies, recombinant antibody (rAb) fragments (i.e., Ab production through genetic engineering approaches) offer some advantages over conventional Abs. The main advantages of rAb fragments are their amenability to *in vitro* display selection, which circumvents the need for animal immunization and allows for the generation of antibodies against targets that are toxic or infectious to the host. In addition, rAbs can be engineered for greater efficacy, used as scaffolds or building blocks to generate multi-specific antibodies, and used as carriers of therapeutic payloads such as radionuclides and toxins. Furthermore, some rAb formats have been shown to bind epitopes that are inaccessible with conventional Abs. The most common rAb formats include Fab (fragment antigen binding), scFv (single chain variable fragments), and single-domain antibodies (Figure 1.3). Numerous fusion derivatives of these fragments have also been engineered (151, 208).

There are several reports in the literature of potent toxin neutralization with recombinant antibodies, including botulinum toxin, cholera toxin, and ricin. With respect to *C. difficile* toxins, there has only been one publication describing the isolation of TcdB binding scFv antibodies (32). In this work, a hyperimmunized scFv library was constructed and provided a source of toxin binders; however, the work did not progress beyond binding assays.

1.5.2 Single-domain antibodies

In recent years, smaller antibody fragments have been developed that show considerable promise as human therapeutic and diagnostic agents (72, 158, 188, 200). Single-domain antibodies (sdAbs) are recombinant, *in vitro* selected fragments and include the V_H and V_L domains of conventional Igs (73, 184, 194), the V_HH domain from *Camelidae* species' heavy-chain IgGs (10, 28, 58), and the V_{NAR} domain (similar to V_HH, *see* Figure 1.3) from cartilaginous shark IgNAR antibodies (35). The unique feature of these antibodies compared to conventional antibodies is their small size (13 – 15 kDa) and single-domain nature which consists of only the antigen recognition domain. In addition, sdAbs possess desirable characteristics [reviewed in (59)] such as high tissue penetrating properties, high chemical, thermal and proteolytic stability, high level expression in microorganisms, ease of genetic manipulation and library construction, and amenability to *in vitro* library screening and selection under harsh conditions such as proteases (64), acidic pH (39), and heat (83). Single-domain antibodies, which possess extended complementarity-determining region 3 (CDR3) loops, are also known to access immunosilent cavities (175) or cryptic epitopes in receptors, enzymes, and infectious agents (29, 33, 172) that conventional mAbs cannot access, making them novel and potent inhibitors.

Figure 1.3. Various antibody formats for anti-toxin therapy.
Traditional antibody formats (i.e., IgY, IgG, IgA) targeting *C. difficile* toxins have been produced primarily from immunized animals. Smaller recombinant antibody binding fragments (i.e., Fab, scFv, V_L, V_H, V_HH) produced from *in vitro* selection procedures may be useful agents to explore for CDAD immunotherapy. Of these recombinant fragments, single-domain antibodies (i.e., V_HH) from *Camelidae* heavy-chain IgGs possess inherent thermal and protease stability and have been shown to bind cryptic epitopes or pockets on proteins that cannot be accessed by traditional antibodies. As such, these single-domain antibodies may be potent toxin neutralizers and promising therapeutic agents for CDAD immunotherapy. Black bars represent disulfide bonds, grey bars represent hinge regions, and the red bar represents a synthetic linker. Some Igs have more than two inter-heavy chain disulfide linkages.

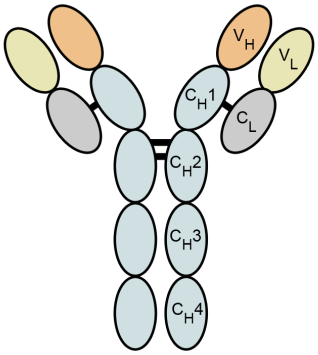

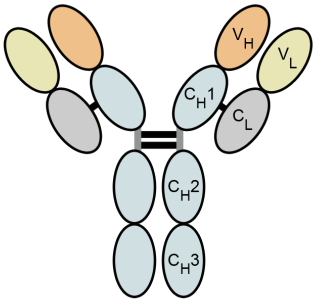

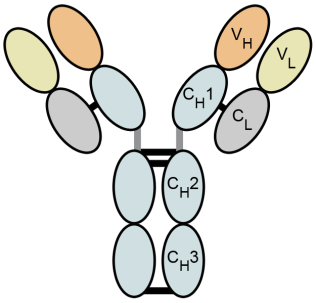

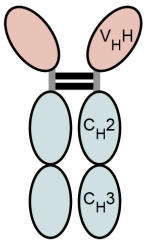

Format:	IgY	IgG	IgA1	Heavy Chain IgG
Source:	Chicken	Human, Mouse, Cow	Human, Mouse, Cow	*Camelidae*
MW (kDa):	170 - 190	150	~160 (monomer) ~335 (dimer) ~380-420 (secretory IgA)	~90

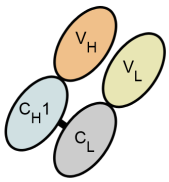

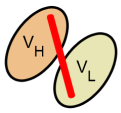

Format:	Fab	scFv	V_H	V_L	V_HH or Nanobody
Source:	Recombinant, IgG digestion	Recombinant, Library selection	Recombinant, Library selection	Recombinant, Library selection	Recombinant, Library selection
MW (kDa):	50	25-27	13-15	13-15	13-15

Several V_HHs or 'Nanobodies' have been isolated against targets relevant to infection and immunity (200). Many of these V_HHs were effective neutralizers of bacterial toxins, viruses, and enzymes, such as: scorpion toxin AahI' (68); *E. coli* heat-labile toxin (62); foot and mouth disease virons (60); ART2.2, an ecto-enzyme related to ADP-ribosylating bacterial toxins (100); verotoxin 1 (176); HIV-1 envelope protein gp 120 (43) and rotovirus (45, 189). With strong binding affinity which can be well into the low picomolar range (2, 25, 30, 69, 101, 114, 160), and the desirable biophysical properties listed above, sdAbs could be promising *C. difficile* toxin-neutralizing agents that may exhibit superior efficacy within the GI tract compared to conventional formats (i.e., IgG). In addition, the efficacy of these compact antibody formats could be further increased by increasing their tolerance to extreme pH and proteolytic degradation through engineering and selection-based approaches.

1.6 Conclusions

With broad-spectrum antibiotic therapy known to promote *C. difficile* infection and TcdA/B firmly established as the causative agents of *C. difficile*-associated disease, the development of non-antibiotic agents to treat CDAD is of considerable importance. The encouraging results from the first human clinical trial involving two antitoxin mAbs demonstrated their efficacy in reducing CDAD relapse (118) and further established the importance of antitoxin neutralizing Abs in controlling CDAD severity. Recently, Demarest *et al* (31) showed a panel of mAbs targeting TcdA were potent toxin neutralizers, suggesting

oligoclonal mixtures of mAbs or Ab fragments targeting unique epitopes may be superior toxin neutralizers compared to single mAbs targeting a single epitope. Indeed, this has been shown with a panel of anti-botulinum toxin mAbs (138).

Pharmacokinetics, affinity, specificity, and stability are key determinants of antibody efficacy in CDAD therapy. Higher affinity antibodies, preferably with at least picomolar K_Ds, should be aimed for, and with respect to specificity, those capable of blocking toxin binding to the host epithelia or preventing toxin internalization may prove to be most efficacious. Antibody stability, one of the determinants of antibody efficacy in systemic therapy, may be the determining factor of antibody efficacy in the oral therapy approach, given that antibodies have to face the hostile environment of the GI tract with acid-induced denaturing and protease degradation capabilities. Recombinant antibody fragments - in particular single-domain antibodies - lend themselves readily to efficacy improvement with regards to all four of the aforementioned antibody characteristics, thanks to major advances in the past decades within the field of antibody engineering and evolutionary display technologies. Formulation may further protect toxin-specific Abs against the deactivating conditions of the GI tract. It is also possible that probiotic bacteria secreting or displaying recombinant antibody fragments (104, 145) specific for TcdA/B could deliver their toxin-neutralizing payloads directly to the lower GI tract, bypassing adverse GI tract conditions and the requirement for purified antibodies altogether.

2.0 HYPOTHESIS AND RESEARCH OBJECTIVES

2.1 Hypothesis

Single-domain antibodies, isolated from an immune llama phage display library and targeting the cell receptor binding domain of *C. difficile* toxins A and B, will effectively neutralize the cytotoxicity of the *C. difficile* toxins and form the basis for developing non-antibiotic therapeutics targeting bacterial virulence factors.

2.2 Research objectives

1. To generate a large and diverse immune llama phage display library by hyper-immunizing a llama with recombinant fragments of *C. difficile* toxins.
2. To isolate high-affinity llama V_HH single-domain antibodies specific for *C. difficile* toxins' cell receptor binding domain from the immune llama phage display library.
3. To functionally characterize the llama V_HHs with respect to tendency for aggregation, affinity and specificity for *C. difficile* toxins A or B, nature of the toxin epitope, epitope mapping, and toxin neutralizing efficacy *in vitro*.
4. To explore the use of a synthetic human V_L single-domain antibody library as a source of high-affinity, toxin B neutralizing agents.
5. To increase the thermal, chemical, and protease stability of the *C. difficile* toxin-specific antibodies through protein engineering.

6. To characterize the stability-enhanced llama VHHs with respect to expression yield, aggregation status, affinity for TcdA, far-UV and near-UV CD spectroscopy signatures, thermal refolding efficiency, thermal stability, protease resistance, and in vitro functionality.
7. To produce VHH variants suitable for VHH:TcdA co-crystal structure determination with our collaborators.

3.0 MATERIALS AND METHODS

For all buffer and medium recipes, please refer to Appendix 1. For the amino acid sequences of all toxins, recombinant toxins, and isolated antibodies, please refer to Appendix 2.

3.1 Isolation of *C. difficile* toxin A- and B-specific V_HHs

3.1.1 TcdA and TcdB antigen preparation

Recombinant fragments of TcdA (amino acid residues 2304 - 2710) and TcdB (amino acid residues 2286 - 2366), which are fragments of the RBD, were cloned (as a *Bam*HI-*Hin*dIII fragment for *tcdA* and a *Bam*HI-*Eco*RI fragment for *tcdB*) into pTrcHisB (Invitrogen, Carlsbad, CA), transforming *E. coli* DH5αMCR. Expression was induced by IPTG, cells harvested and lysed in a French pressure cell, and proteins TcdA-RBD-f1 and TcdB-RBD-f1 were purified by immobilized metal-affinity chromatography (IMAC). Recombinant RBD fragments were dialyzed into PBS pH 7.3 and stored at 4°C. TcdA and TcdB were isolated from *C. difficile* strain 10463 (ATCC, Manassas, VA) as described previously (92) and were stored in 50 mM Tris-HCl buffer pH 7.5 at 4°C. Briefly, supernatant from dialysis bags containing *C. difficile* cultures (92) were centrifuged (15,000 x *g*, 20 min, 4°C) and the toxins purified using a DAEA-sepharose ion-exchange column. TcdA was eluted with a gradient of 0.05 - 0.25 M NaCl in 50 mM Tris-HCl buffer at pH 7.5. TcdB was eluted with a gradient of 0.25 - 0.5 M NaCl in 50 mM Tris-HCl buffer at pH 7.5.

3.1.2 Llama immunization, serum fractionation, and serum response monitoring

3.1.2.1 Llama immunization

One male llama was immunized by sub-cutaneous, lower-back injection with both recombinant toxin antigens simultaneously, using the schedule shown in Table 3.1. On day 1, 200 μg of each antigen (diluted in PBS to 1 mL total and filter-sterilized) and 1 mL of Freund's complete adjuvant (FCA) was injected for a total immunization volume of 2 mL. On days 22, 36, and 50, 100 μg of each antigen (diluted in PBS to 1 mL total) and 1 mL of Freund's incomplete adjuvant (FIA) was injected. On day 77, 100 μg of each antigen (diluted in PBS to 1 mL total) was injected with no adjuvant. Blood (10 – 15 mL) was collected into heparin-coated tubes on days 29, 43, 57, and 84 and immediately stored on ice. A pre-immune bleed on day 1 was also performed (this serves as a non-immunized control for a subsequent ELISA). After each collection, blood was stored overnight at 4°C. The next day, serum was prepared by centrifugation at 2,700 *g* for 10 min at 4°C and stored at 4°C. The lymphocytes were isolated from blood collected on day 84 and used for phage display library construction (*see* below).

Table 3.1. Llama immunization and blood collection schedule.

Day	Antigen injected	Adjuvant	Blood collection
1	200 μg of each[1]	Freund's complete	Yes (pre-immune)
22	100 μg of each	Freund's incomplete	No
29	-	-	Yes
36	100 μg of each	Freund's incomplete	No
43	-	-	Yes
50	100 μg of each	Freund's incomplete	No
57	-	-	Yes
77	100 μg of each	No adjuvant	No
84	-	-	Yes

1. "Each" refers to TcdA-RBD-f1 and TcdB-RBD-f1 antigens.

3.1.2.2 Serum fractionation

The serum prepared from blood on day 57 and day 84 bleeds was fractionated in order to separate conventional IgG from heavy-chain IgG (hcIgG) (Figure 3.1) (36, 136). Briefly, 1 – 2 mL of the llama serum (dialysed against NaPi buffer and clarified by sterile filtration) was loaded onto a 1 mL HiTrap™ Protein G HP column (GE Healthcare, Baie-d'Urfé, QC, Canada) previously equilibrated with 10 mL of filter-sterilized NaPi buffer, all separated using an ÄKTA™ FPLC purification system (GE Healthcare). The flow-through was collected and set aside at 4°C for a second round of purification. The Protein G column was washed with 10 mL of filter-sterilized NaPi buffer and 1 – 2 mL of citrate buffer (pH 3.5) added to elute the hcIgG3 fraction (Figure 3.1). The eluted fraction was immediately neutralized by adding 1 M Tris-HCl buffer (pH 8.8) until a pH of at least 6.0 is reached. A second elution was then performed with 2 – 4 mL of glycine buffer (pH 2.7) to elute the conventional IgG1 fraction (Figure 3.1) and the eluted fraction neutralized as above. Next, the flow-through from the Protein G column was loaded onto a 1 mL HiTrap™ Protein A

Figure 3.1. Overview of the serum fractionation process.
Overview of the serum fractionation procedure to separate conventional IgG (IgG1) and hcIgGs (IgG2a/b/c, IgG3) from serum using Protein G and Protein A affinity columns. Minor amounts of IgM may co-elute with the IgG2a/b/c fraction.

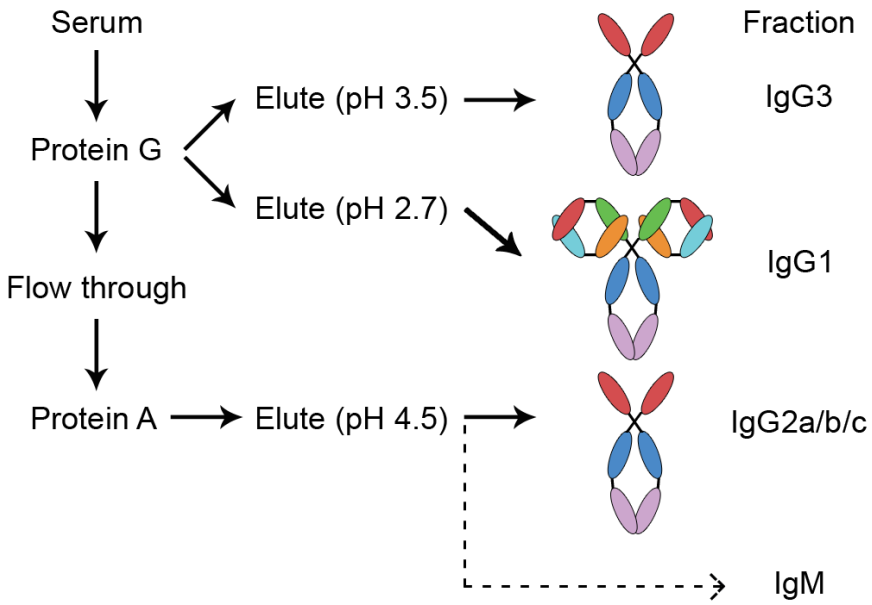
Serum
Protein G
Flow through
Protein A
Elute (pH 3.5)
Elute (pH 2.7)
Elute (pH 4.5)
Fraction
IgG3
IgG1
IgG2a/b/c
IgM

HP column previously equilibrated with 10 mL of filter-sterilized NaPi buffer. After loading, the Protein A column (GE Healthcare) was washed with 10 mL of NaPi buffer and 1 – 2 mL of sodium acetate buffer (pH 4.5) applied to elute the hcIgG2 fraction (Figure 3.1), which consists of IgG2a, IgG2b and IgG2c isotypes. The fraction was neutralized as above. The eluted fractions were analyzed on an SDS-PAGE gel under non-reducing and reducing conditions. Eluted fractions were stored at 4°C for further analysis by serum ELISA.

3.1.2.2 Serum response monitoring

ELISA was performed on total and fractionated sera to determine if a toxin A/B-specific heavy-chain antibody immune response was obtained. To do this, 96-well microtiter plates were coated with rTcdA, rTcdB, and BSA (control) overnight at 4°C, all at 1 – 5 μg/well diluted in a total of 100 μL of PBS. Another control well contained PBS alone. The wells were blocked with blocking buffer A (200 μL/well) for 2 h at 37°C. Serial dilutions of pre-immune total serum (collected on day 1), post-immune total serum from various bleeds (collected on days 29, 43, 57, and 84), and fractionated serum (IgG3, IgG1, and IgG2a/b/c fractions) from day 57 and day 84 bleeds diluted in a total of 100 μL of PBS were added to wells for 1.5 h at room temperature. The last well contained PBS only. The wells were washed with PBS-T (5 x 300 μL) and 100 μL/well of goat anti-llama IgG (Cedarlane, Burlington, ON, Canada; previously diluted 1:1,000 in PBS) was added for 1 h at 37°C. The wells were then washed as above and 100 μL/well of swine anti-goat IgG-HRP (Cedarlane; previously diluted 1:3,000 in PBS) was added for 1 h at 37°C. After another set of washes,

HRP substrate (100 μL/well) was added and incubated at room temperature for 5 – 10 min. The reaction was stopped with 1 M H_3PO_4 (100 μL/well) and the absorbance of each well read at 450 nm with a microtiter plate reader.

3.1.3 Library construction

In this step, leukocytes were isolated from the serum prepared from day 84 blood and used as a source of mRNA for library construction. cDNA was synthesized from the mRNA and used to produce dsDNA. V_HH dsDNA was inserted into a phagemid vector and transformed into *E. coli*, creating the phage display library.

First, total lymphocyte RNA was isolated from 2 mL of llama blood drawn on day 84 by using the QIAamp RNA Blood Mini™ kit (Qiagen, Streetsville, ON, Canada) according to the manufacturer's instructions. The RNA concentration and purity was measured at $A_{260\ nm}$ and $A_{280\ nm}$, respectively, with a spectrophotometer. A total of 3 – 5 μg of RNA was used in 20 μL of ddH_2O to synthesize cDNA in a total reaction volume of 33 μL, using the First-Strand cDNA Synthesis™ kit (Promega, Madison, WI) and C_H2-specific primers, CH2FORTA4 and CH2B3-F (Table 3.2), according to the manufacturer's instructions. Test polymerase chain reactions (PCRs) were performed using various amounts of the cDNA reaction mix ranging in volume from 0.5 μL to 5 μL and using an equimolar mix of framework 1-specific primers MJ1, MJ2, and MJ3 with either CH2FORTA4 or CH2B3-F primer (Table 3.2). The PCR reaction was set up as follows:

10x buffer	5 μL
MJ1 – 3 primer mix (10 pmol/μL each)	0.5 μL
CH2FORTA4 or CH2B3-F primer	0.5 μL
dNTPs	1 μL
cDNA	0.5–5 μL
Taq DNA polymerase	0.5 μL
ddH_2O	add to 50 μL

The PCR was performed using a program consisting of an initial step of 94°C for 3 min, 30 cycles of 94°C for 1 min, 55°C for 30 s, and 72°C for 30 s and a final extension of 72°C for 7 min. Approximately 5 μL of the PCR reaction was analyzed on a 1% agarose gel (163). The cDNA volume that gave the best yield in terms of amplifying the V_HH genes was identified and the remaining cDNA mixture was PCR amplified under those same conditions. Gel-purified V_HH bands were extracted from a 1% agarose gel using the QIAquick Gel Extraction™ kit (Qiagen). The DNA was pooled and the concentration measured as described for mRNA.

Table 3.2. Oligonucleotides used in this work.

Name	Sequence (5′ → 3′)	Purpose
MJ1	GCC CAG CCG GCC ATG GCC SMK GTG CAG CTG GTG GAK TCT GGG GGA	Library construction
MJ2	GCC CAG CCG GCC ATG GCC CAG GTA AAG CTG GAG GAG TCT GGG GGA	Library construction
MJ3	GCC CAG CCG GCC ATG GCC CAG GCT CAG GTA CAG CTG GTG GAG TCT	Library construction
CH2FORTA4	CGC CAT CAA GGT ACC AGT TGA	Library construction
CH2B3-F	GGG GTA CCT GTC ATC CAC GGA CCA GCT GA	Library construction
MJ7	CAT GTG TAG ACT CGC GGC CCA GCC GGC CAT GGC C	Library construction
MJ8	CAT GTG TAG ATT CCT GGC CGG CCT GGC CTG AGG AGA CGG TGA CCT GG	Library construction
BbsI-V_HH	TAT GAA GAC ACC AGG CCC AGG TAA AGC TGG AGG AGT CT	Subcloning
BbsI2-V_HH	TAT GAA GAC ACC AGG CCC AGG TGC AGC TGG TGG AGT CT	Subcloning
BamHI-V_HH	TTG TTC GGA TCC TGA GGA GAC GGT GAC CTG	Subcloning
-96gIII	CCC TCA TAG TTA GCG TAA CGA TCT	Colony-PCR, sequencing
M13FP	GTA AAA CGA CGG CCA GT	Colony-PCR, sequencing
M13RP	CAG GAA ACA GCT ATG AC	Colony-PCR, Sequencing
5′pGEX	GGG CTG GCA AGC CAC GTT TGG TG	Colony-PCR, sequencing
3′pGEX	CCG GGA GCT GCA TGT GTC AGA GG	Colony-PCR, Sequencing
T7 For	TAA TAC GAC TCA CTA TAG GG	Colony-PCR, sequencing
T7 Rev	GCT AGT TAT TGC TCA GCG G	Colony-PCR, Sequencing
FdTet	GTG AAA AAA TTA TTA TTC GCA ATT CCT	Colony-PCR
HVL24-BamHI	TTG TTC GGA TCC TAG GAC GGT CAC CT	Subcloning
HVL24-BbsI	TAT GAA GAC ACC AGG CCG ACA TCC AG	Subcloning
A4.2mR-Cys	AGT CTG CAT AGT ATG TGC TAC CAC CAC TCC GGC TAA CAG CGC AAA CAA ACT C	A4.2m, cloning
A4.2mF-Cys	TAG CAC ATA CTA TGC AGA CTC CGT GAA GGG CCG ATT CAC CTG CTC CAG AGA C	A4.2m/A5.1m, cloning
A5.1mR-Cys	AGT CTG CAT AGT ATG TGC TAC TAC CAT TCC GGG TAA TAA CGC ATA CAA ACT C	A5.1m, cloning
A19.2mR-Cys	ACT CTA CAT AGG CAC TAT TAC CAC CAC GCC GGC TAA TAC CGC ATA CAA ACT C	A19.2m cloning
A19.2mF-Cys	TAA TAG TGC CTA TGT AGA GTC CGT GAA GGG CCG ATT CAC CTG CTC CAG AGA C	A19.2m, cloning
A20.1mSfiI-F	ACC GTT GCG CAG GCC CAG CCG GCC ATG GCC CAG GTA CAG C	A20.1m/A24.1m, cloning
A20.1mR-Cys	TGT CTG CAT AGT ATG TGG TCC GCC CCG TAG AAC TCC CCG CGC ATA CAA ACT C	A20.1m, cloning
A20.1mF-Cys	GAC CAC ATA CTA TGC AGA CAG CGT GAA GGG CCG ATT CAC CTG CTC CAG AGA C	A20.1m, cloning
A20.1mSfiI-R	GTT CGG ATC CCT GGC CGG CCT GGC CTG AGG AGA CGG TGA CC	A20.1m/A24.1m, cloning
A24.1mR-Cys	AGT CTG CAT AGC GTG TGC TAC CTC CAC CCC AGC TAA TAC CGC ATA CAA ACT C	A24.1m, cloning
A24.1mF-Cys	TAG CAC ACG CTA TGC AGA CTC CGT GAA GGG CCG ATT CAC CTG CTC CAG AGA C	A24.1m, cloning
A26.8mR-Cys	AGT CTG CAT AGT ATG TGC TCG TAC CAG TCG AGC TAA TAA CGC ATA CAA ACT C	A26.8m, cloning
A26.8mF-Cys	GAG CAC ATA CTA TGC AGA CTC GGT GAA GGG CCG GTT CAC CTG CTC CAG AGA C	A26.8m, cloning

The purified product (10 – 20 ng of the amplified cDNA/reaction tube) was re-amplified in a second PCR under the exact same conditions above, using sense and framework 4 (FR4)-specific primers MJ7 and MJ8, respectively. A total of 20 PCR reactions were performed. A small amount of the PCR reaction was analyzed on a 1% agarose gel, with the expectation of seeing bands ranging from 400 – 450 bp, which corresponds to the V_HH fragments. The PCR products were de-salted with the QIAquick PCR Purification™ kit (Qiagen) and the concentration determined. The PCR products were then digested with *Sfi*I (5 units/μg DNA) restriction enzymes overnight at 50°C and a few microliters subsequently analyzed on a 1% agarose gel to ensure that it was of the proper size. The digested DNA was re-purified with the QIAquick PCR Purification™ kit (Qiagen) and its concentration measured. Approximately 30 μg of pMED1 phagemid vector (courtesy of Dr. Mehdi Arbabi-Ghahroudi) was digested with *Sfi*I (5 units/μg DNA) for 5 h at 50°C. The next day, 1 μL (10 units) of each of *Xho*I and *Pst*I enzymes were added for an additional 2 h at 37°C to reduce self ligation of pMED1. The digested pMED1 was analyzed on a 1% agarose gel against the undigested control vector to ensure that the vector was completely linearized. The digested vector was purified with the QIAquick PCR Purification™ kit and its concentration measured. Using the LigaFast™ Rapid DNA Ligation System (Promega), the *Sfi*I-digested V_HH DNA was ligated with *Sfi*I-digested pMED1 vector as follows:

Digested vector	20 μg
Digested V_HH insert	3.5 μg
2x T4 DNA ligase buffer	50 μL
T4 DNA ligase	8 μL
Sterile ddH_2O	add to 100 μL

The ligation was performed at room temperature for 60 min and the ligated materials were purified with the QIAquick PCR Purification™ kit using two spin columns. The DNA was eluted in a final volume of 35 µL of sterile ddH_2O per column. The eluted material was pooled and its concentration measured. Next, 50 µL of electrocompetent TG1 *E. coli* cells were transformed with 3 µL of the purified ligated material using a MicroPulser™ electroporator (187). The electroporated cells were transferred into a tube containing 1 mL of SOC medium and incubated for 1 h at 37°C and 180 rpm. The transformation was repeated for the remaining DNA for a total of 20 transformations. The transformed cells were pooled, and a small aliquot was used to carry out 10^3-, 10^4-, and 10^5-fold dilutions in 2xYT. Next, 100 µL of the diluted cells were spread on 2xYT-Amp plates and incubated overnight at 32°C.

The library was amplified by transferring the transformed cells into 500 mL of 2xYT-Amp-Glu and incubating overnight at 220 rpm and 37°C. In the morning, the cells were centrifuged at 5,000 *g* for 20 min at 4°C. The supernatant was discarded and the cells resuspend in 50 mL of 2xYT-Amp-Glu. Next, dilutions of the cells were made in 2xYT, the absorbance measured at $A_{600\ nm}$ and this value was used to calculate the cell density (# of cells/mL) in the stock solution (1 $A_{600\ nm} \cong 10^9$ cells). Next, 50 mL of sterile 70% glycerol was added to the cell stock, several aliquots of 10^{10} bacterial cells/vial were made, and finally frozen at -80°C. The colonies on the titer plates were counted to determine the total library size. A colony-PCR was then performed on the colonies from the titer plates in a total volume of 15 µL. A master mix for 50 PCR reactions was prepared as follows:

10x PCR buffer	80 μL
dNTPs (25 mM of each)	16 μL
-96gIII primer (10 pmol/μL)	8 μL
M13RP primer (10 pmol/μL)	8 μL
Taq DNA polymerase (Roche)	8 μL
ddH_2O	680 μL

Volumes of 15 μL from the master mix were added to each of 50 PCR tubes. Single colonies from the titer plates were touched with a P10 pipette tip and then swirled in the PCR tubes. The PCR reaction tubes were then placed in a thermal cycler and a PCR performed with a program consisting of a preheating step at 94°C for 5 min followed by 30 cycles of 94°C for 30 s, 55°C for 30 s, and 72°C for 1 min and a final step of 72°C for 7 min. Next, a few microliters of each PCR reaction were analyzed on a 1% agarose gel to identify the clones with full inserts (≅600 bp band). Approximately 0.5 μL of the PCR mixture and M13RP primer (Table 3.2) were used to sequence the clones and identify those expressing V_HH sequences (61, 135). The functional library size was determined by multiplying the percentage of the 50 clones with V_HH sequences by the total library size.

To produce the phage library, 1 – 2 mL of frozen library cells were thawed and grown in 200 mL of 2xYT-Amp-Glu at 37°C and 220 rpm until the cell culture density reached an $A_{600\ nm}$ of 0.5 (2 – 3 h). The cells were infected with a 20x excess of M13KO7 helper phage (2 x 10^{12} plaque-forming units, pfu) for 1 h at 37°C. The infected cells were pelleted by centrifugation at 5,000 x *g* for 10 min at 4°C. The pellets were resuspended in 200 mL of 2xYT-Amp-Kan and grown overnight at 37°C and 250 rpm. To purify the phage, the overnight cultures were centrifuged (10,000 x *g*, 15 min, 4°C), the supernatant filtered through a 0.2 μm filter unit, and then 1/5 the volume of PEG/NaCl was added to the filtrate.

The mixture was incubated for 1 h on ice, centrifuged as above and the supernatant discarded. The pelleted phage was then resuspended in 1.5 mL of sterile PBS, its titer determined, and stored at -80°C. The purified phage was then used as the input phage for round 1 of library screening.

3.1.4 V_HH phage display library screening

The library was screened for phage displaying V_HHs with specificity to rTcdA or rTcdB. A phage ELISA was then performed to identify individual phage displaying V_HHs specific to whole TcdA or TcdB toxins.

Panning was performed (Figure 3.2) by coating a 96 well microtiter plate with 20 μg of recombinant rTcdA or rTcdB fragments (100 μL/well diluted in PBS) overnight at 4°C. The contents of the coated wells were removed the next day, washed with 300 μL of PBS, and blocked for 2 h at 37°C with 200 μL/well of blocking buffer B. At that time, 10 mL of exponentially growing TG1 *E. coli* cells were started in a sterile 50-mL Falcon tube. The blocking buffer was removed and ≅10^{12} input phages in 100 μL of PBS were added to the blocked wells for 2 h at 37°C. The unbound phage were removed, washed 10x with PBS-T (300 μL per wash) and the bound phage eluted by incubating with 0.1 M triethylamine (100 μL/well) for exactly 10 min at room temperature. The elution solution was pipetted up and down several times in the well before removing the contents and neutralizing the phage with 50 μL of 1 M Tris-HCl, pH 7.4, in a separate tube. Next, 100 μL of the exponentially growing TG1 cells were kept for the negative control titer (*see* below) and the remaining

cells infected with 100 μL of the eluted phage by incubating the mixture at 37°C for 15 min without shaking and for 1 h with shaking at 220 rpm (the remaining phage were stored at -80°C for future reference). The infected cells were then titrated. A super infection step of the infected bacterial cells (≈10 mL) with 10^{11} pfu of M13KO7 helper phage was performed. Subsequently, kanamycin was added at a final concentration of 50 μg/mL and incubated overnight at 37°C and 250 rpm. The next day, the phage was purified in a final volume of 200 μL of PBS and the phage titer determined as described above. The purified phage was used as the input phage for the next round of panning. To assess the progress of the panning, colony-PCR and DNA sequencing of titer plate colonies was performed as described above. Fifteen to twenty clones in each of the first 2 rounds, 25 clones in the third round, and 50 – 100 clones in the fourth round were sequenced.

The entire panning process was repeated for 3 more rounds using the amplified phage from the previous round as the input phage for the next round and reduce the amount of coated antigen by 5 μg for each subsequent round (e.g., 15 μg of rTcdA or rTcdB in round 2). After 4 rounds of selection, a phage ELISA was performed on colonies containing unique V_HH DNA sequences (determined by colony-PCR and sequencing) to identify toxin binding V_HH phages.

Figure 3.2. Overview of the phage display library screening procedure.
Phage displaying VHHs were screened against rTcdA-f1 and rTcdB-f1 to isolate toxin-specific VHHs. By screening with the recombinant toxin fragments, selection was driven for binders that target the C-terminal cell receptor binding domains of the toxins. Four rounds of selection were performed in total. After selection, VHHs were screened by phage ELISA with positive, unique binders subcloned into high-yielding expression vectors. TEA: triethylamine.

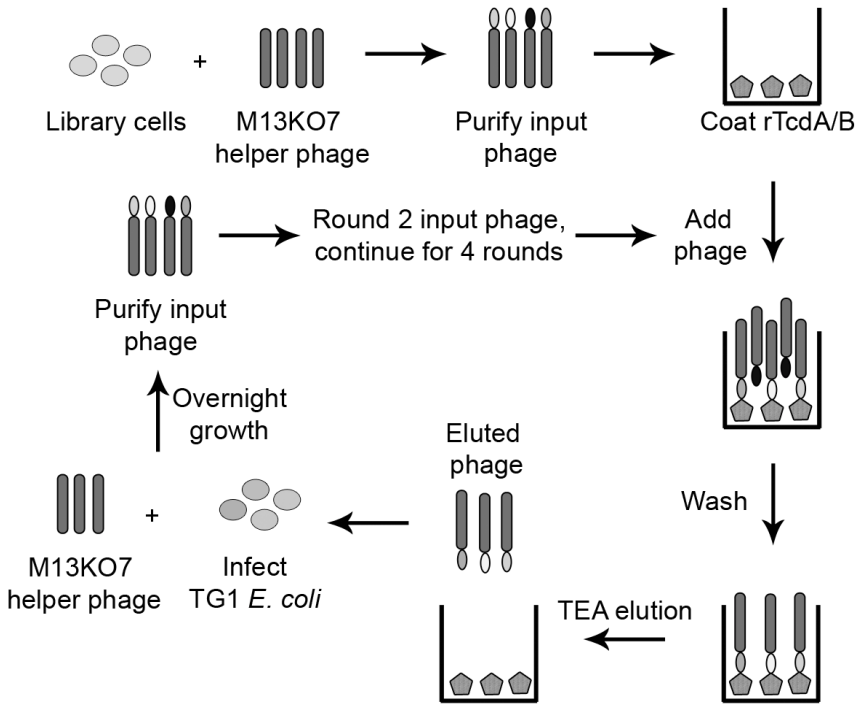
Library cells
+
M13KO7
helper phage
Purify input
phage
Coat rTcdA/B
Add
phage
Round 2 input phage,
continue for 4 rounds
Purify input
phage
Overnight
growth
Eluted
phage
Wash
M13KO7
helper phage
+
Infect
TG1 E. coli
TEA elution

In the phage ELISA, the binding of V_HH-displaying phages to toxins was detected colorimetrically by adding a secondary anti-phage antibody-HRP conjugate and HRP substrate. Briefly, microtiter wells were coated with toxin (TcdA or TcdB), recombinant fragments (rTcdA or rTcdB), and BSA as described above. Next, 1 mL of 2xYT-Amp-Glu was added into sterile 15-mL Falcon tubes. A small colony of TG1 cells containing the V_HH-phagemid (that was previously screened by colony-PCR and DNA sequencing) was added to the medium. The cell culture was grown at 37°C and 250 rpm until the $A_{600\ nm}$ of the culture reached 0.5. The cells were then infected with 10^{10} pfu of M13KO7, kanamycin added, and then grown overnight as described above. The next day, each well was blocked with blocking buffer B. While blocking, the overnight cultures were centrifuged at 10,000 x *g* for 20 min in microfuge tubes at 4°C. Carefully, the supernatant which contains the V_HH-displaying phage particles was removed and decanted into new microfuge tubes. The blocking agent was then removed and each well washed with PBS-T (5 x 300 μL). Next, 100 μL/well of phage supernatants were added to the appropriate wells for 1.5 h at room temperature. A negative control well was included in duplicate, with 10^9 M13KO7 helper phage replacing the phage supernatant. The unbound phage particles were removed and wells were washed with PBS-T (6 x 300 μL). Next, 100 μL/well of anti-M13 IgG-HRP conjugate (GE Healthcare; previously diluted 1:5,000 in PBS) was added and incubated for 1 h at room temperature. The ELISA-positive phages were stored at -20°C for future reference.

3.1.5 V_HH subcloning, soluble expression, and purification

3.1.5.1 V_HH subcloning

While it is an option to express the V_HHs in the pMED1 phagemeid vector in an amber non-suppressor *E. coli* strain, subcloning the V_HHs into a dedicated expression vector was performed to obtain higher protein expression yields. To subclone positive V_HH binders for soluble expression, the V_HH gene was amplified directly from TG1 colonies containing the V_HH gene in the pMED1 phagemid vector by colony-PCR (as above) in a total volume of 50 μL using either the BbsI-V_HH or BbsI2-V_HH framework 1-specific primer and BamHI-V_HH framework 4-specific primer (Table 3.2). A small amount of the PCR reaction was analyzed by agarose gel, looking for the correct size of 400 – 450 bp. The PCR fragment was purified with a QIAquick PCR Purification™ kit and its concentration determined. The purified V_HH DNA and pSJF2H vector were digested with *Bbs*I as follows:

V_HH fragment or pSJF2H	80 ng or 500 ng, respectively
10x *Bbs*I buffer	10 μL
*Bbs*I (5 units/μL)	5 μL
ddH_2O	add to 100 μL

The reactions were incubated at 37°C for 12 h. The digested fragment and vector were then purified with the QIAquick PCR Purification™ kit and its concentration determined. The purified *Bbs*I-digested fragment or vector (conditions as above) were digested with *Bam*HI as follows:

V_HH fragment or pSJF2H	60 ng or 400 ng, respectively
10x *Bam*HI buffer	10 μL
*Bam*HI (10 units/μL)	2 μL (fragment) or 6 μL (vector)
ddH_2O	add to 100 μL

The *Bbs*I/*Bam*HI digested insert (fragment) and vector were then ligated as follows:

Digested pSJF2H	100 ng
Digested insert	20 ng
10x ligase buffer	0.5 μL
T4 DNA ligase (5 units/μL)	0.5 μL
ddH_2O	add to 5 μL

A vector-only control reaction mixture where insert is replaced with water was also included. The reaction mixtures were incubated at room temperature for 2 h. Next, 50 μL of electrocompetent TG1 *E. coli* cells were transformed with 1.2 μL of ligation reaction (~30 ng DNA). Following incubation in SOC medium, 50 μL of cells were spread on prewarmed LB-Amp plates and incubated overnight at 32°C. The next day, the number of colonies on LB-Amp plates were counted, including control ligation/transformation reactions containing vector-only. At least 10 colony-PCRs (as before) were performed to screen for colonies with inserts using the primer pair M13FP and M13RP. The same P10 pipette tip which was used to introduce colonies into the PCR reaction tubes was used to make a reference plate of the colonies being screened. Next, 5 μL of each PCR reaction was analyzed on a 1% agarose gel to identify clones with insert (≅600 bp) or without insert (≅200 bp) and positive PCR products were sequenced directly. After sequencing and identification of positive clones, permanent stocks of the positive clones were prepared for long term storage at -80°C.

3.1.5.2 Soluble V_HH expression and purification

V_HHs were expressed using the 5-day M9 minimal media method (8). After induction of protein expression, cell cultures were harvested at 6,000 *g* for 30 min at 4°C, the

supernatant decanted and the periplasmic contents extracted from the cell pellet. Briefly, each pellet was resuspended in 30 mL of ice-cold TES buffer (0.2 M Tris-HCl buffer pH 8.0, 20% (w/v) sucrose, 0.5 mM EDTA) and incubated on ice for 30 min. Next, 40 mL of ice-cold 1/8 TES was added, incubated an additional 30 min on ice and the slurry centrifuged at 12,000 *g* for 30 min at 4°C. The resulting supernatant was dialysed overnight into IMAC buffer A and purified as previously described (78). Eluted fractions were analyzed by SDS-PAGE and Western blotting before being dialysed into PBS. V_HH concentrations were determined by absorbance measurements at $A_{280\ nm}$ using theoretical molecular weight (MW) and extinction coefficients calculated with the ExPASy ProtParam Tool (http://expasy.org/tools/protparam.html) (143).

3.1.6 Characterizing V_HH binding by ELISA

ELISA was used to determine if the purified antitoxin V_HHs recognized native TcdA or TcdB and recombinant TcdA-RBD-f1 or TcdB-RBD-f1 fragments. Equivalent molar concentrations of proteins (BSA, TcdA, TcdB, TcdA-RBD-f1, and TcdB-RBD-f1) were coated overnight in 96 well microtiter plates at 4°C. The next day, wells were blocked with 3% (w/v) skim milk diluted in PBS-T. After washing with PBS-T, purified V_HHs at concentrations as high as 10 μg/mL were added to wells with the various coated antigens for 1 h at 37°C. Wells were washed with PBS-T and rabbit anti-His_6 IgG conjugated to HRP (Cedarlane) diluted 1:2,500 in PBS was added for 1 h at room temperature before another set of 5 washes. Rabbit anti-His_6 IgG-HRP did not recognize the N-terminal His_6 epitope tags

on recombinant RBD fragments (data not shown). Binding was detected with TMB substrate (KPL, Gaithersburg, MD), the reactions were stopped with 1 M H_3PO_4, and absorbance read at $A_{450\ nm}$. All conditions were performed in triplicate and the reported values are representative of two independent experiments.

A second ELISA was performed with differentially temperature-treated TcdA to determine if the V_HHs recognized linear or conformational epitopes. Briefly, TcdA (5 μg/mL) was exposed to the following conditions for 30 min: 4°C, 20°C, 37°C, 50°C, 60°C, and 70°C. After temperature treatment, 100 μL of TcdA was coated in 96 well microtiter plates overnight at 4°C and the assay performed essentially as described above, except that 0.05 – 1 μg/mL of V_HH was used. All conditions were performed in duplicate and the reported values are representative of two independent experiments.

3.1.7 Western blotting

Western blots containing TcdA were probed with anti-TcdA V_HHs or control anti-TcdA IgG (PCG4; Novus Biologicals, Littleton, CO) to determine if the V_HHs recognized linear or conformational epitopes. For denaturing SDS-PAGE Western blots, TcdA (0.75 μg/lane), A4.2 V_HH (1 μg/lane) and PCG4 IgG (1 μg/lane) were separated on 12.5% SDS-PAGE gels under reducing conditions and transferred to PVDF membranes at 100 V for 1 h. Membranes were blocked for 1 h with 5% (w/v) BSA diluted in PBS-T followed by probing with various V_HHs (25 μg/10 mL blocking buffer) or PCG4 (10 μg/10 mL blocking buffer) for 1 h. Membranes were washed 4x in PBS-T followed by addition of either: (i) mouse anti-His_6 IgG-alkaline phosphatase (AP) conjugate (Abcam, Cambridge, MA) diluted 1:5,000 in

blocking buffer, or (ii) HisDetector™ Nickel-AP conjugate (Mandel Scientific, Guelph, ON, Canada) diluted 1:5,000 in blocking buffer, or (iii) goat anti-mouse IgG-AP conjugate (Cederlane) diluted 1:10,000 in blocking buffer for 1 h. After a final set of 4 washes, membranes were subjected to AP substrate (BioRad, Hercules, CA) for 7 min, washing in dH_2O and air drying.

For native PAGE Western blots, TcdA, V_HH and PCG4 (concentrations as above) were separated on 8% PAGE gels (without SDS) at 100 V for 2 h on ice. Next, gels were transferred to PVDF membranes at 20 V for 14 h at 4°C. Membranes were blocked, probed, washed and detected using the same protocol as for SDS-PAGE Western blots.

3.1.8 Size exclusion chromatography (SEC)

SEC was performed on all purified V_HHs using a Superdex™ 75 column (GE Healthcare) as described (184) and HBS-EP buffer, all under the control of an ÄKTA™ FPLC. Fractions from the SEC column were then used for affinity measurements.

3.1.9 Surface plasmon resonance (SPR) analysis

The binding kinetics for the interaction of antitoxin V_HHs and TcdA or TcdB were determined by SPR using a Biacore 3000 biosensor system (GE Healthcare). A total of 10,377 resonance units (RUs) of TcdA and 5,980 RUs of mouse IgG 13D9 control (116) were immobilized on a CM5 sensor chip (GE Healthcare). Anti-TcdA V_HH affinity measurements were carried out in HBS-EP running buffer at a flow rate of 40 μL/min. Surfaces were

regenerated by washing with either running buffer or 10 mM glycine pH 2.0. Initial attempts to immobilize TcdB directly onto a CM5 sensor chip (GE Healthcare) were unsuccessful due to the toxin's low pI (theoretical pI = 4.42). TcdB was biotinylated with the EZ-Link Sulfo-NHS-LC-LC-Biotin kit from Pierce (Rockford, IL) and 825 RUs were immobilized onto a streptavidin-coated CM5 sensor chip. However, due to the size difference of TcdB-biotin (269 kDa) compared to streptavidin (53 kDa), not all streptavidin sites were occupied and roughly 1 TcdB-biotin was immobilized for every 7 streptavidin molecules. Furthermore, no binding was observed between the anti-TcdB VHHs and immobilized TcdB-biotin. Data was collected on the VHH-TcdB-RBD-f1 interaction by immobilizing TcdB-specific VHHs onto the CM5 sensor chip (RUs ranging from 215 to 1,209) and injecting TcdB-RBD-f1 at 20 μL/min. The IgG 13D9 or human single-domain antibody HVHP420 (184) served as controls. In all cases, data were analyzed with BIAevaluation 4.1 software (GE Healthcare).

In addition to obtaining binding kinetic data, SPR co-injection experiments were performed to determine if the VHHs could bind unique, non-overlapping epitopes on TcdA. Briefly, 80 μL of the first VHH diluted in HBS-EP buffer to a concentration of 20x its K_D was injected over 10,287 RUs of immobilized TcdA at 40 μL/min. Following injection of the first VHH, buffer or a second VHH (80 μL total volume, at 20x K_D) were injected at 40 μl/min over the TcdA surface already saturated with the first VHH. Data were collected on all possible paired combinations of A4.2, A5.1, A20.1, and A26.8, in both orientations (i.e., each VHH acted as the first and second VHH). Data were collected and evaluated as described above.

Using SPR, attempts to inhibit the V_HH-TcdA interaction with two trisaccharides known to bind TcdA-RBD were also performed, in order to gain insight into the TcdA epitope recognized by the V_HHs. CD-grease (α-Gal-(1,3)-β-Gal-(1,4)-β-GlcNAcO$(CH_2)_8CO_2CH_3$; (53)) and Le^X-AmHex (Gal-β1,4-(Fuc-α1,3)-GlcNAc-$(CH_2)_6$-NH_2-HOAc; P. Zhang and C.C. Ling, unpublished) are two trisaccharides known to interact with the carbohydrate binding pockets of TcdA-RBD ((34, 53, 185) and present study). Briefly, 4 V_HHs (i.e., A4.2, A5.1, A20.1, and A26.8) at K_D concentrations were injected alone or in the presence of trisaccharide (2 mM) over immobilized TcdA (≅8000 RUs). The response obtained from the interaction of trisaccharide with TcdA was subtracted from response generated by V_HH + trisaccharide co-injection experiments. Then, the response of each V_HH to TcdA in the presence of trisaccharide was compared to the response generated by the V_HH-TcdA interaction.

3.1.10 Toxin neutralization assay

Human lung fibroblast (HLF) cells are sensitive to both TcdA and TcdB, and the HLF cell rounding assay is routinely used for analyzing the presence of *C. difficile* toxins in biological samples (11). The assay was used here to determine if antitoxin V_HHs could neutralize the cytopathic effects of TcdA and TcdB. HLF cells (IMR-90: ATCC#CCL-186) were purchased from ATCC (Manassas, VA) and maintained in Eagle's minimal medium (Invitrogen, Carlsbad, CA) supplemented with 10% fetal bovine serum (Invitrogen) at 37°C with 5% CO_2. Cells were seeded in sterile 96 well microtiter plates (2 x 10^4 cells per well in

200 µl) for 20 h, allowing for the formation of confluent monolayers. Initially, a dose-response experiment was conducted to find the minimum concentration of TcdA and TcdB which induced 100% HLF cell rounding after 24 h post toxin addition. To do so, sterile filtered TcdA or TcdB were added to wells containing confluent monolayers, giving final toxin A concentrations ranging from 500 ng/mL (1.6 nM) to 0.5 ng/mL (1.6 pM) and final toxin B concentrations ranging from 500 ng/mL (1.9 nM) to 0.5 ng/mL (1.9 pM). Each concentration was performed in triplicate and the assay performed twice. HLF cells were scored visually for rounding at various time points over 24 h. For all subsequent assays, 100 ng/mL (325 pM) of TcdA and 10 ng/mL (37 pM) of TcdB were used.

For experiments involving VHHs, 20 µL of purified and sterile filtered VHHs were added to HLF cells with 10 µL TcdA/B or 10 µL PBS. For experiments involving 2 and 3 VHHs the concentration of each VHH was reduced by 1/2 and 1/3, respectively, giving the same final concentrations as experiments involving only a single VHH. Importantly, VHHs and toxin were not pre-incubated; rather, each added directly to HLF monolayers at time = 0 h. HLF cells containing PBS, VHH, toxin, or VHH + toxin were scored visually for cell rounding using a confocal microscope at 24 h post antibody/toxin addition. Assays were performed in triplicate and repeated twice. Each assay was performed on fresh preparations of HLF cells and VHHs were from separate purifications. The purified TcdA and TcdB stock remained the same for all assays. Cell rounding was assessed using the cytopathic effect (CPE) scoring system previously described (11). Briefly, the CPE scoring system examines the amount of cell rounding in a microscope field of view and reports a value of between 0

and 4. A score of 0 = 0% cell rounding, a score of 1 = 25% rounding, a score of 2 = 50% rounding, a score of 3 = 75% rounding, and a score of 4 = 100% rounding.

3.1.11 Production of V_HH variants for crystallography

The long N-terminal epitope tag (c-Myc + His_6) present on antibodies expressed within the pMED2 and pSJF2H vectors can effect V_HH crystal formation (personal communication, K-K. Ng, University of Calgary). To initiate co-crystallization studies of various antitoxin V_HHs and V_Ls in complex with TcdA or TcdB, several antibodies were cloned and expressed with a short, N-terminal His_6 tail immediately following the antibody FR4 region. Both wild-type antibodies (containing the long tags) and shorter variants were expressed in *E. coli* and purified, as described above. Approximately 20 – 30 mg of each purified antibody was sent to collaborators at the University of Calgary for co-crystallization trials.

3.2 Isolation of *C. difficile* toxin B-specific V_Ls

Despite isolating high-affinity llama V_HHs targeting *C. difficile* TcdB, the antibodies failed to neutralize TcdB in cell-based assays (*see* below). As such, selection and isolation of human V_L single-domain antibodies from a novel synthetic library was undertaken in an attempt to find toxin B-neutralizing antibodies. In addition to using a V_L library, a novel antigen and panning scheme was employed to overcome the instability issues facing the

recombinant TcdB fragment used for V_HH selection. This section describes the materials and methods utilized in isolating and characterizing TcdB-binding V_Ls.

3.2.1 Synthetic V_L display library construction

A synthetic V_L display library was constructed and kindly donated by Dr. Jamshid Tanha and Artine Keklikian (NRC). This library was panned for toxin B specific V_L antibodies.

3.2.2 Assembly of the GST-TcdB-F80 fusion protein

Two DNA constructs encoding the C-terminal 80 amino acids of TcdB (*see* Appendix 2) were synthesized and assembled by GeneArt (Regensburg, Germany), for use as targets for V_L library panning. The first construct encoded the 80 amino acid TcdB fragment, denoted TcdB-F80, in the pET-21b(+) expression vector with a C-terminal His_6 epitope tag. The second construct encoded TcdB-F80 as a C-terminal fusion to GST, all in the pGEX-6P-2 expression vector (GE Healthcare). The GST-TcdB-F80 construct contained a PreScission™ protease site (GE Healthcare) and linker between GST and TcdB-F80. The second construct did not contain a C-terminal His_6 epitope tag. Upon arrival, the constructs were resuspended in nuclease-free ddH_2O and electrocompetent TG1 E. *coli* cells were transformed with 40 ng of each construct. A third construct, pGEX-6P-2 containing only the GST and the protease cleavage site, was also transformed into TG1 cells to serve as a source of GST.

Colony-PCR and DNA sequencing was performed to identify TG1 colonies harboring GST, TcdB-F80, or GST-TcdB-F80. The primers used for the amplification of GST or GST-TcdB-F80 in pGEX-6P-2 (i.e., 5′ pGEX and 3′ pGEX) are listed in Table 3.2. Amplification of TcdB in pET-21b(+) was performed using the T7 For and T7 Rev primer pair (Table 3.2). Colony-PCR reaction mixtures and the thermocycler program were the same as described earlier (*see* section 3.1.3).

3.2.2.1 Expression and purification of GST-TcdB-F80

The proteins GST, GST-TcdB-F80, and TcdB-F80 were expressed according to the following protocol. Single TG1 colonies were used to inoculate 100 mL of LB/Amp media contained within a 250 mL baffled flask and grown for 20 h at 37°C and 220 rpm. The next day, the 100 mL of overnight culture was added to 1 L of LB/Amp media contained in a 4 L baffled flask and grown for 3 h at 37°C and 220 rpm before the addition of 400 μL of 1 M IPTG and grown an additional 18 h at 37°C and 220 rpm.

Cells were harvested by centrifugation at 6,000 *g* for 10 min and lysed using a lysozyme total cell lysis protocol as follows. Upon centrifugation, cell pellets were resuspended in 100 mL of ice-cold lysis buffer and stored at -20°C overnight. The next day the pellets were thawed, 1 mL of 100 mM PMSF and 200 μL of 1 M DTT were added and mixed. The cells were lysed by addition of 5 mL of freshly prepared lysozyme (5 mg/mL stock prepared in PBS) and incubating at room temperature for 1 h. Next, 300 μL of DNase I (Sigma, Mississauga, ON, Canada; 15 units/μL stock prepared in 1 M $MgCl_2$) was added

and incubated for 30 min before a final centrifugation step at 12,000 *g* for 30 min. The resulting supernatants (soluble fractions) were dialyzed overnight against PBS pH 7.3. Dialyzed soluble supernatants were examined by SDS-PAGE and Western blotting. A mouse anti-His6 IgG (GE Healthcare) and a goat-anti-mouse IgG conjugated to alkaline phosphotase (Cedarlane) were used for the detection of TcdB-F80, whereas GST and GST-TcdB-F80 were detected with polyclonal rabbit anti-GST (GenScript, Piscataway, NJ) and a goat-anti-rabbit IgG conjugated to AP (Cedarlane).

GST and GST-TcdB-F80 were purified using a 1 mL GSTrap column (GE Healthcare) according to the manufacturer's instructions. Briefly, PBS pH 7.3 was used as a loading and washing buffer while a reduced glutathione elution buffer was used for elution. Eluted and purified fractions were analyzed by SDS-PAGE and Western blotting, as above, before dialysis against PBS pH 7.3. Tcd-F80 could not be expressed despite two attempts.

3.2.2.2 GST-TcdB-F80 cleavage assay with PreScission™ protease

The panning strategy with GST-TcdB-F80 was to utilize the protease cleavage site between GST and TcdB-F80 to release V_L-displaying phage bound to TcdB-F80. Before proceeding with panning, a test cleavage of GST-TcdB-F80 was performed with the PreScission™ protease at three temperatures (4°C, 21°C, and 37°C). Briefly, 3 μg of GST-TcdB-F80 in 5.5 μL was mixed with 1.5 μL of 10x PreScission™ cleavage buffer, 1 μL of PreScission™ protease (stock from GE Healthcare; 2 units/μL), and ddH_2O up to 15 μL. The

reactions were incubated at the various temperatures noted above for 4 h and analyzed by SDS-PAGE.

3.2.3 V_L library panning, phage ELISA, and V_L subcloning

V_L library panning was performed by pre-incubating V_L-displaying phages with GST followed by incubation with the GST-TcdB-F80 fusion protein. This process, referred to as subtractive panning, theoretically eliminates all GST-specific V_Ls from the pool before incubation with GST-TcdB-F80. Elution of the V_L-displaying phages, as noted above, was done with proteolytic separation of TcdB-F80 from GST and hence recovery of V_L-displaying phages specific to TcdB-F80.

To begin panning, two microwells were coated with GST or GST-TcdB-F80 (10 μg/well, 4°C, 20 h) diluted in PBS. The same day, exponentially growing TG1 *E. coli* cells were grown overnight in 2xYT medium containing no antibiotic (20 h, 37°C, 220 rpm). The next day, wells containing GST or GST-TcdB-F80 were blocked with 2% milk diluted in PBS-T (PBS + 0.05% (v/v) Tween 20) for 2 h at 37°C. The overnight TG1 culture was then diluted 100-fold in 2xYT (no antibiotics) and grown for 3 – 4 h (37C, 220 rpm) until OD_{600} = 0.5. Next, the V_L phage library stock was obtained and 100 μL of library (containing 2 x 10^{13} phages) was added to 100 μL of 5% BSA diluted in PBS-T. The 200 μL mixture was then added to the GST-coated microwell for 1 h at room temperature. Next, the unbound phages were removed from the GST-coated well, transferred to the GST-TcdB-F80 coated well, and incubated for 1 h at room temperature. After incubation the unbound phages were removed

and well was washed with 10 x 300 μL of PBS-T followed by 10 x 300 μL PBS. The bound phages were eluted by adding PreScission™ protease as follows: 1.5 μL of protease with 10 x PreScission™ protease digestion buffer and ddH_2O up to a final volume of 150 μL. All 150 μL were added to the well to elute the phages by incubating for 2 h at room temperature. After incubation, the eluted phages were removed by gentle pipetting.

To titer and amplify the eluted phages, the 150 μL elution was added to 30 mL of exponentially growing TG1 *E. coli* cells and incubated in a waterbath at 37°C for 30 min. To titer the phage, 100-fold dilutions (10^{-2} – 10^{-8}) of the infected cells were prepared in 2xYT media in a final volume of 500 μL (i.e., 5 μL of infected TG1 were added to 495 μL of 2xYT make the 10^{-2} dilution). Next, 100 μL of each dilution were spread on 2xYT plates containing tetracycline (5 μg/mL). The plates were incubated overnight at 37°C for counting and colony-PCR the next day. To amplify the eluted phages, the remaining 30 mL of infected TG1 cells were centrifuged at 3,000 *g* for 10 min, the resulting supernatant removed, and the pellet re-suspend in 1 mL of 2xYT media. Next, 250 μL was spread onto each of 4 large culture dishes containing 2xYT/Tet and incubate overnight at 37°C.

The next day, colony-PCR was performed on the titer plates and phages were purified from the large culture dishes for subsequent rounds of panning. To begin, 3 mL of exponentially growing TG1 cells were grown in 2xYT as above. Colony-PCR was performed under identical conditions reported above, with the exception of using the -96gIII and FdTet primer pair (Table 3.2), in order to estimate the number of colonies containing V_L inserts and for DNA sequencing of the V_Ls. To purify the phages, the cells were scraped from the large plates using 2 x 5 mL of 2xYT. The cells were combined, centrifuged for 10 min at

3,000 *g* and the supernatant removed containing the phages. The pellet, containing round 1 cells, was re-suspend in 2YT containing 15% (v/v) glycerol and stored at -80°C. The supernatant containing the phages was centrifuged at 10,000 *g* x 10 min. The phages were precipitated and purified using PEG/NaCl as described before. Purified phages were tittered by preparing serial dilutions in PBS and mixing these dilutions with exponentially growing TG1 cells. The remaining purified phages served as input phage for round 2 of panning.

The entire process was repeated for a total of 4 rounds. A total of 8, 8, 25, and 100 colonies were sequenced in rounds 1 – 4, respectively.

A total of 17 unique V_L sequences were identified and subsequently screened by phage ELISA for binding to GST, GST-TcdB-F80, or native TcdB. To begin the phage ELISA, GST, GST-TcdB-F80, and TcdB were coated at 5 μg/mL (100 μL/well) for 20 h at 4°C. The phage ELISA was performed essentially as described above for V_HHs.

V_LS that were shown to bind TcdB by phage ELISA were subcloned into the pSJF2H expression vector by PCR amplification using the HV_L24-BamHI and HV_L24-BbsI primer pair (Table 3.2) and digestion with *Bam*HI and *Bbs*I restriction endonucleases. The pSJF2H vectors containing V_LS were transformed into electrocompetent TG1 *E. coli* cells for protein expression.

3.2.4 Anti-TcdB V_L characterization

Before characterizing the anti-TcdB V_LS, the antibodies were expressed using the 5-day M9 media method (8) and purified using IMAC as described above for V_HHs. The purified V_LS were used directly for SEC and SPR analysis, or dialyzed into PBS for ELISA and neutralization assays.

SEC analysis on the purified V_LS was performed exactly as described above for V_HHs. SPR analysis was again carried out on a Biacore 3000 instrument. A total of 953 RUs of TcdB-GST-F80 and 882 RUs of GST were immobilized on CM5 dextran chips in 10 mM acetate buffer pH 4.0. The remaining immobilization conditions were the same as described above for TcdA. Monomeric V_LS collected from the SEC column were flowed over immobilized TcdB-GST-F80 and GST, at V_L concentrations ranging from 10 nM to 10 μM, and the response generated from binding to GST was subtracted from the response generated from binding to TcdB-GST-F80. Steady state analysis and the Biacore BIAevaluation 4.1 software were used to determine the affinity constants of each V_L.

To analyze V_L binding by ELISA, GST and GST-TcdB-F80 were immobilized in microtiter plate wells (0.5 μg/well, 4°C, 20 h). After blocking with 3% (w/v) milk diluted in PBS-T, serial dilutions of purified V_LS were incubated for 1 h at 37°C. Wells were washed with 5 x 300 μL of PBS-T and V_L binding was detected with a 1 h incubation at room temperature with rabbit anti-His_6 IgG conjugated to HRP (Cedarlane). A final PBS-T wash precluded the addition of HRP substrate and the absorbance was read at 450 nm.

The ability of purified V_LS to neutralize the cytotoxic effects of TcdB on fibroblast monolayers was also examined, essentially as described above for V_HHs. A range of V_L

concentrations, as high as 2.5 μM were incubated with TcdB and monolayers for 24 h after which the percentage of cells rounded was compared to control treatments not receiving antibodies.

3.3 Stability engineering of V_HHs

3.3.1 Cloning, expression, and purification of V_HH disulfide bond mutants

The nomenclature used throughout this work to distinguish between wild-type and mutant V_HHs is exemplified as follows: "A4.2" denotes a wild-type V_HH, "A4.2m" denotes a mutant V_HH. To construct mutant V_HHs with a second disulfide bond, splice-overlap extension-polymerase chain reaction (SOE-PCR) (71) was performed using 4 primers for each V_HH (Table 3.2) and two rounds of PCR essentially as described (9, 79). Ala or Gly and Ile codons at positions 54 and 78 (IMGT numbering system; http://imgt.cines.fr/), respectively, were changed to Cys codons through primer-forced mutation. In the first PCR, two mutagenized overlapping sub-fragments were generated for each V_HH. The primer pairs used for each V_HH were as follows: A4.2m (BbsI-V_HH and A4.2mR-Cys, A4.2mF-Cys and BamHI- V_HH); A5.1m (BbsI- V_HH and A5.1mRCys, A4.2mFCys and BamHI- V_HH); A19.2m (BbsI- V_HH and A19.2mR-Cys, A19.2mF-Cys and BamHI- V_HH); A20.1m (A20.1mSfiI-F and A20.1mR-Cys, A20.1mF-Cys and A20.1mSfiI-R); A24.1m (A20.1mSfiI-F and A24.1mR-Cys, A24.1mF-Cys and A20.1mSfiI-R); A26.8m (BbsI- V_HH and A26.8mR-Cys, A26.8mF-Cys and BamHI- V_HH). Each sub-fragment was gel purified and corresponding partner spliced in a second PCR. Briefly, 160 ng of each sub-fragment were added to a 50-μL

PCR mixture containing *Pfu* DNA polymerase, dNTPs and reaction buffer. The reaction was placed in a thermal cycler and the two fragments were spliced together using a program consisting of a preheating step at 94°C for 5 min and 10 cycles of 94°C for 30 s, 55°C for 30 s, and 72°C for 1 min. To amplify the spliced products, the reaction was heated to 94°C for 3 min, 5 pmol (0.5 μL) of each primer pair was added (BbsI-V_HH and BamHI-V_HH for A4.2m, A5.1m, A19.2m, and A26.8m; A20.1mSfiI-F and A20.1mSfiI-R for A20.1m and A24.1m), and 35 PCR cycles were performed exactly as described above. The resulting fragments were gel purified, digested with *Bbs*I and *Bam*HI (A4.2m, A5.1m, A19.2m, and A26.8m) or *Sfi*I (A20.1m and A24.1m) restriction enzymes, ligated into similarly digested expression vectors, and transformed into TG1 *E. coli* for V_HH expression. Positive colonies were identified by colony PCR and DNA sequencing, using the M13RP and M13RP primers.

Mutant V_HHs were expressed in the same vector as wild-type V_HHs (77). Expression and purification of wild-type and mutant V_HHs was performed as described (77), followed by dialysis into PBS, distilled, deionized water (ddH_2O) for mass spectrometry (MS) analysis, or 10 mM phosphate buffer pH 7.3 for circular dichroism (CD) experiments.

3.3.2 Mass spectrometry (MS) analysis

For mass determination, purified V_HHs (WT and mutant) were first buffer exchanged into ddH_2O. The V_HHs (15 pmol/μl in 50%/50% acetonitrile/H_2O + 0.1% formic acid) were then infused at 1 μL/min for electrospray ionization (ESI) mass spectrometric measurements using a Q-TOF 2™ mass spectrometer (Waters, Milford, MA). The mass

spectra of VHHs were deconvoluted using the MaxEnt 1 program under the MassLynx software (Waters).

Proteolytic peptide fragments of mutant VHHs were created by digestion with cyanogen bromide (CNBr) and trypsin. Briefly, 100 μL reactions containing 50 μg of mutant VHH (diluted in PBS), 10 μL of 1 M HCl and 40 μL of CNBr (10 mg/mL stock prepared in 1 M HCl) were digested for 14 h at ambient temperature in the dark. The next day, 100 μL of 1 M Tris-HCl (pH 8.6) and 60 uL of trypsin (100 μg/mL stock; sequencing grade, Roche, Mississauga, ON, Canada) were added directly to the CNBr reaction mixture and incubated for 2 h at 37°C. Samples were then analyzed by non-reducing SDS-PAGE to ensure digestion prior to MS analysis.

Nano-flow reversed-phase HPLC mass spectrometry (nanoRPLC-ESI-MS) with data dependent analysis (DDA) was performed to confirm disulfide bond formation in the mutant VHHs. An aliquot of the CNBr + trypsin digested VHHs was re-suspended in 0.1% formic acid (aq) and analyzed by nanoRPLC-ESI-MS using a nanoAcquity UPLC system coupled to a Q-TOF Ultima™ hybrid quadrupole/TOF mass spectrometer (Waters). The peptides were first loaded onto a 180 μm I.D. × 20 mm 5 μm symmetry®C18 trap (Waters), then eluted to a 100 μm I.D. × 10 cm 1.7 μm BEH130C18 column (Waters) using a linear gradient from 0% to 36% solvent B (acetonitrile + 0.1% formic acid) in 36 min, 36% - 90% solvent B for 2 min. Solvent A was 0.1% formic acid in water. The peptide MS^2 spectra were searched against mutant VHH protein sequences using the Mascot™ database searching algorithm (Matrix Science, London, UK). The MS^2 spectra of the disulphide-linked peptides

were deconvoluted using the MaxEnt 3 program (Waters) for de-novo sequencing to determine the exact disulfide-linked positions.

3.3.3 Determining mutant V_HH affinity by SPR

Mutant V_HHs were passed over a Superdex™ 75 (GE Healthcare) SEC column as described (*see* above and (77)) to determine their aggregation state and the collected fractions were used for SPR analysis. All kinetic rate and equilibrium constants were determined as described (77) using a Biacore 3000 instrument (GE Healthcare) and 10,287 RUs of immobilized TcdA. In addition, the dissociation rate constants (k_{off}s) of mutant V_HHs before and after digestion with pepsin were compared by SPR (*see* below).

3.3.4 Circular dichroism (CD) spectroscopy

Wild-type and mutant V_HHs were analyzed by CD spectroscopy using a Jasco J-815 spectropolarimeter (Jasco, Easton, MD) at pH 7.3 (10 mM phosphate buffer) and at pH 2.0 (10 mM phosphate buffer + 50 mM HCl). For all CD experiments performed at pH 2.0, proteins were equilibrated in the above buffer for a minimum of 2 h before scanning. For far-UV CD secondary structure scans, thermal refolding, and thermal unfolding experiments, a 5 mm cuvette containing 1.5 mL of V_HH at 50 μg/mL was used. In these experiments, 4 accumulations were collected for each sample between 200 nm – 260 nm with a 1 mm bandwidth, 20 nm/min scan speed and 0.5 nm data pitch. Raw ellipticity data, given in millidegrees (mdeg), was smoothed using the Jasco software, exported, and

converted to molar ellipticity, [θ]. To convert from mdeg to molar ellipticity ([θ]) in deg cm^2/dmol, Equation 1 (55) was used,

$[\theta] = (\text{mdeg} \times \text{MRW})/(\text{pathlength in mm} \times V_HH \text{ concentration in mg/mL})$ (Eq. 1)

where the mean residue weight, MRW = (molecular weight of the antibody in Da/number of backbone amino acids). Thermal unfolding was followed at 215 nm with CD measurements taken every 2°C from 30°C to 96°C with a temperature increase of 1°C/min. Molar ellipticity ([θ]) was used to calculate the fraction of protein folded (FF), which is shown in Equation 2 (54),

$FF = ([\theta] - [\theta_U])/([\theta_F] - [\theta_U])$ (Eq. 2)

where $[\theta_F]$ and $[\theta_U]$ is the molar ellipticity of the folded (30°C) and unfolded (96°C) states, respectively. The thermal unfolding midpoint temperature (T_m) was obtained by plotting FF against temperature (T) and fitting with a sigmoidal Boltzmann function in GraphPad Prism (GraphPad Software, La Jolla, CA).

For refolding experiments, V_HHs were first scanned (200 nm – 260 nm) at 25°C (folded), heated at 96°C for 20 min and scanned (unfolded) and equilibrated to 25°C for 3 h before a third scan (refolded). Raw data was converted as before and thermal refolding efficiencies (TRE) were calculated at 215 nm using Equation 3,

$$TRE = (([\theta_U] - [\theta_R])/([\theta_U] - [\theta_F])) \times 100 \quad \text{(Eq. 3)}$$

where $[\theta_F]$ is the molar ellipticity of the folded state acquired at 25°C, $[\theta_U]$ is the molar ellipticity of the unfolded state acquired at 96°C, and $[\theta_R]$ is the molar ellipticity of the refolded state acquired at 25°C .

To compare the tertiary structures of wild-type and mutant V_HHs at neutral and acidic pH, near-UV CD experiments were performed in the range of 250 nm – 340 nm using the conditions described above with the exception of a 10 mm cuvette containing 2 mL of protein at 250 μg/mL. In all cases, the ellipticity of buffer blanks were subtracted from experimental values and the reported data is the average of two independent experiments with 4 data accumulations in each.

3.3.5 Protease digestion assay

All reactions were performed in 20 μL volumes with 4.8 μg of V_HH diluted in PBS. For pepsin digestions, reactions contained 17 μL of V_HH, 2 μL of porcine stomach pepsin (460 U/mg; Sigma), and 1 μL of 1 M HCl (50 mM final). Final pepsin concentrations in each reaction ranged from 0.1 μg/mL to 100 μg/mL. Digestions were incubated at 37°C for 1 h and neutralized with 1 μL of 1 M NaOH. For trypsin and chymotrypsin digestions, reactions contained 18 μL of V_HH (diluted in PBS supplemented with 10 mM $CaCl_2$) and 2 μL of either trypsin or chymotrypsin (sequencing grade, Roche). Final trypsin/chymotrypsin concentrations ranged from 0.1 μg/mL to 100 μg/mL. Digestions were

incubated at 37°C for 1 h and neutralized with 1 μL of protease inhibitor cocktail (Sigma). All neutralized VHH-protease reactions and controls (VHHs with no protease) were separated by SDS-PAGE, stained with Coomassie and photographed using an AlphaImager3400 (Alpha Innotech Corporation, San Leandro, CA). To determine the percent of VHH retained after protease digestions, densitometry analysis was performed using the AlphaEaseFc software package (Version 7.0.1, Alpha Innotech Corporation) on control and digested VHHs. A total of three independent digestion reactions were performed on all of the VHHs at each protease concentration and each were run on separate SDS-PAGE gels. Digestions at the highest protease concentration (100 μg/mL) that were not analyzed by SDS-PAGE were buffer exchanged into water using Millipore Biomax 5K MWCO spin columns (Millipore, Billerica, MA) and subjected to mass spectrometry analysis to identify the cleavage products, or analyzed by Biacore for TcdA binding activity.

3.3.6 Toxin neutralization assay

In vitro TcdA neutralization assays were performed essentially as described above and in (77). Human lung fibroblast cell rounding was reported 24 h post addition of TcdA (100 ng/mL), TcdA + wild-type VHH (1000 nM) or TcdA + mutant VHH (1000 nM). Specifically, VHHs were added as pooled mixtures of A4.2, A5.1, A20.1, and A26.8 (250 nM each, 1000 nM total) or A4.2m, A5.1m, A20.1m, and A26.8m (250 nM each, 1000 nM total). The percentage of cell rounding was scored visually using light microscopy and the

reported values are the average of two independent experiments. In each experiment, each VHH mixture was tested in triplicate.

3.3.7 Homology modeling

The SWISS-MODEL online workspace (http://swissmodel.expasy.org/workspace/) (17) was used to construct homology models of A4.2 (WT) and A4.2m (mutant) VHHs. The 1qd0A (PDB) VHH was used as a template (171), sharing 73.4% and 71.8% homology, respectively. Images of the modeled sdAbs were generated using PyMOL (www.pymol.org).

4.0 RESULTS

In this chapter, the results of isolating and characterizing antitoxin llama V_HHs, antitoxin human V_LS, and engineering antitoxin V_HHs for improved stability are presented.

4.1 Isolation and characterization of *C. difficile* toxin A- and B-specific V_HHs

The first objective in this work was to isolate V_HHs capable of binding and neutralizing *C. difficile* TcdA and TcdB. It was hypothesized that V_HHs targeting the toxin's RBD region will block the toxin-receptor interaction, thereby preventing toxin entry into the host cell; a critical initial step in the TcdA/B mechanism of action (80). To do so, an immune, llama V_HH phage display library was constructed and panned with recombinant RBD fragments. The isolated V_HHs were then characterized for their ability to bind native toxins and recombinant RBD fragments, and the nature and relative positioning of epitopes. In addition, the ability of V_HHs to neutralize toxins in an *in vitro* cell cytotoxicity assay was assessed.

4.1.1 Llama immunization, serum response monitoring, and library construction

CDAD is caused by two high-molecular weight toxins composed of enzymatic, translocation, and cell receptor binding domains (Figure 4.1A, B). To isolate V_HHs which target the RBD of TcdA and TcdB, a llama was immunized with two recombinant RBD fragments, TcdA-RBD-f1 and TcdB-RBD-f1 (Figure 4.1A). An ELISA conducted on total serum from day 57 clearly showed a specific immune response for TcdA-RBD-f1 and TcdB-

RBD-f1 compared to pre-immune sera collected before immunization on day 0 (Figure 4.1C). A second ELISA performed on fractionated sera from day 84 indicated the HcAb and conventional IgG serum fractions recognized TcdA-RBD-f1 and TcdB-RBD-f1. For example, the G1 HcAb fraction was shown to specifically recognize both recombinant fragments and did not bind to two unrelated proteins PEB3 or CPS (Figure 4.1D). An immune, llama V_HH library was constructed in the pMED1 phagemid vector and its size was estimated at 5×10^7 individual transformants.

4.1.2 Library panning, phage ELISA, and subcloning

Colonies arising from four rounds of panning against TcdA-RBD-f1 and TcdB-RBD-f1 were screened by phage ELISA (Figure 4.1E) and the positive clones subjected to DNA sequencing. Seven unique TcdA-specific and 7 unique TcdB-specific binders, all determined to be V_HHs based on the presence of characteristic amino acids at positions 42, 49, 50, and 52 (Figure 4.2), were subcloned into expression plasmids, their expression targeted to the periplasm of TG1 *E. coli* and purified (Figure 4.3) with yields ranging from 1.2 – 105.9 mg/L bacterial culture (Table 4.1).

Figure 4.1. Isolation of anti-TcdA/B V_HHs.

(**A**) Schematic representation of native TcdA/B and recombinant fragments of the cell receptor binding domain (TcdA-RBD-f1 and TcdB-RBD-f1) used for llama immunization and library panning. Numbers represent the amino acid residues of each toxin, labelled from the N-termini (1) to C-termini (2710/2366 for TcdA and TcdB, respectively). Drawings are not to scale. GT: glucosyltransferase domain; CP: cysteine protease domain; HR: hydrophobic membrane insertion domain; RBD: cell receptor binding domain. (**B**) SDS-PAGE profile of purified *C. difficile* toxins (3 μg per lane; from strain 10463) used in this study. The upper arrow shows full-length TcdA (308 kDa) and TcdB (269 kDa). (**C**) ELISA demonstrating a total llama serum response for the recombinant RBD fragments. Serum was prepared from llama blood drawn 57 days after the initial immunization. Immune A: immune serum against TcdA-RBD-f1; Immune B: immune serum against TcdB-RBD-f1; Pre-Immune: pre-immune serum against TcdA-RBD-f1. (**D**) ELISA demonstrating the llama heavy-chain IgG (HcAb) G1 fraction response was specific for the recombinant RBD fragments. Serum was fractionated from llama blood drawn 84 days after the initial immunization and the G1 fraction shown did not recognize PEB3 or CPS, two unrelated antigens. (**E**) Phage ELISA evaluating the binding of phage-displayed V_HHs selected against TcdA-RBD. The specificity of several V_HH-displaying phages obtained by panning against rTcdA was evaluated by phage ELISA. Of 15 clones tested, 12 specifically recognized rTcdA, 2 did not show binding to either and 1 (clone 1) cross reacted to rTcdB. Molecular weight markers, M, are given in kDa. NR: non-reducing.

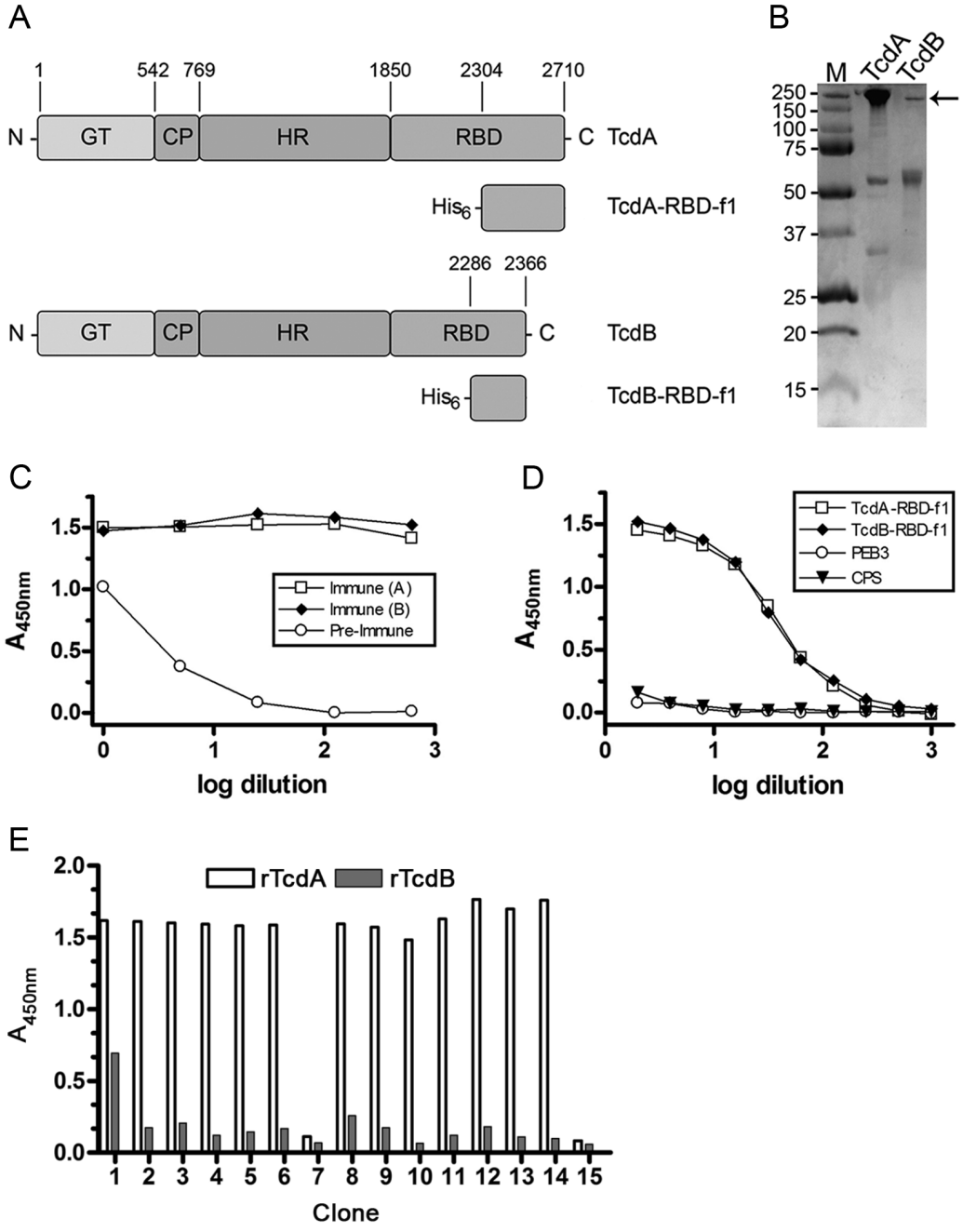
A
1
542
769
1850
2304
2710
N
GT
CP
HR
RBD
C
TcdA
His6
TcdA-RBD-f1
2286
2366
TcdB
TcdB-RBD-f1
B
M
TcdA
TcdB
250
150
100
75
50
37
25
20
15
C
Immune (A)
Immune (B)
Pre-Immune
A450nm
log dilution
D
TcdA-RBD-f1
TcdB-RBD-f1
PEB3
CPS
E
rTcdA
rTcdB
Clone

Figure 4.2. Anti-TcdA/B V_HH sequences.
Amino acid sequence alignment of V_HHs isolated in this study. Framework regions, FRs, and complementarity-determining regions, CDRs (shaded in grey), are grouped according to the IMGT numbering system (http://imgt.cines. Fr/). Hallmark positions, 42, 49, 50, and 52, where V_HHs can be distinguished from V_Hs based on amino acid identity are illustrated with asterisks. V_Hs almost invariantly have V, G, L and W at positions 42, 49, 50, and 52, respectively. In many V_HHs, the aforementioned residues are replaced with F/Y, E/Q/R, R and F/L, as shown.

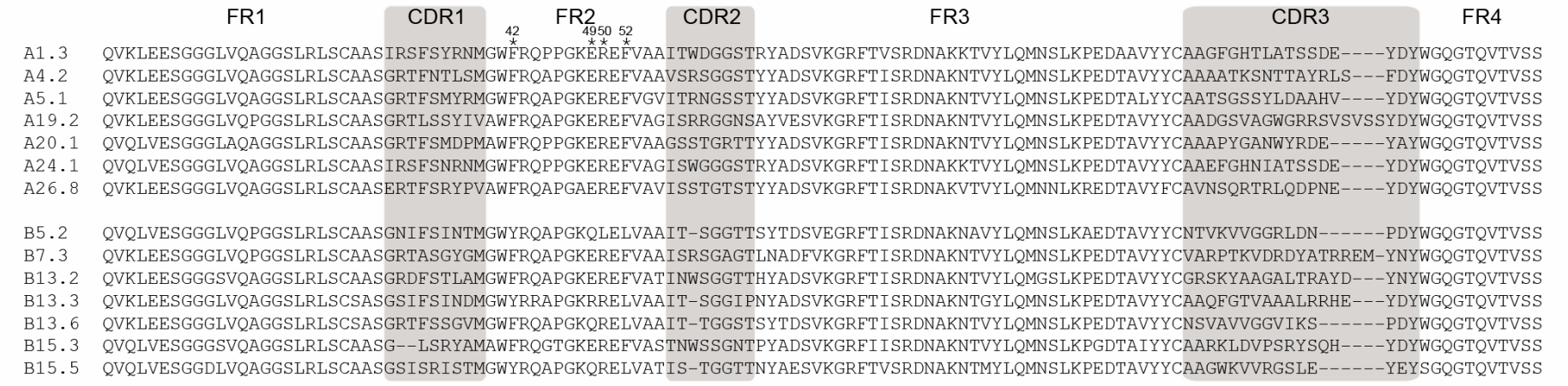
FR1
CDR1
FR2
CDR2
FR3
CDR3
FR4
42
49
50
52
A1.3 QVKLEESGGGLVQAGGSLRLSCAASIRSFSYRNMGWFRQPPGKEREFVAAITWDGGSTRYADSVKGRFTVSRDNAKKTVYLQMNSLKPEDAAVYYCAAGFGHTLATSSDE----YDYWGQGTQVTVSS
A4.2 QVKLEESGGGLVQAGGSLRLSCAASGRTFNTLSMGWFRQAPGKEREFVAAVSRSGGSTYYADSVKGRFTISRDNAKNTVYLQMNSLKPEDTAVYYCAAAATKSNTTAYRLS---FDYWGQGTQVTVSS
A5.1 QVKLEESGGGLVQAGGSLRLSCAASGRTFSMYRMGWFRQAPGKEREFVGVITRNGSSTYYADSVKGRFTISRDNAKNTVYLQMNSLKPEDTALYYCAATSGSSYLDAAHV----YDYWGQGTQVTVSS
A19.2 QVKLEESGGGLVQPGGSLRLSCAASGRTLSSYIVAWFRQAPGKEREFVAGISRRGGNSAYVESVKGRFTISRDNAKNTVYLQMNSLKPEDTAVYYCAADGSVAGWGRRSVSVSSYDYWGQGTQVTVSS
A20.1 QVQLVESGGGLAQAGGSLRLSCAASGRTFSMDPMAWFRQPPGKEREFVAAGSSTGRTTYYADSVKGRFTISRDNAKNTVYLQMNSLKPEDTAVYYCAAAPYGANWYRDE-----YAYWGQGTQVTVSS
A24.1 QVQLVESGGGLVQAGGSLRLSCAASIRSFSNRNMGWFRQPPGKEREFVAGISWGGGSTRYADSVKGRFTISRDNAKKTVYLQMNSLKPEDTAVYYCAAEFGHNIATSSDE----YDYWGQGTQVTVSS
A26.8 QVKLEESGGGLVQAGGSLRLSCAASERTFSRYPVAWFRQAPGAEREFVAVISSTGTSTYYADSVKGRFTISRDNAKVTVYLQMNNLKREDTAVYFCAVNSQRTRLQDPNE----YDYWGQGTQVTVSS
B5.2 QVQLVESGGGLVQPGGSLRLSCAASGNIFSINTMGWYRQAPGKQLELVAAIT-SGGTTSYTDSVEGRFTISRDNAKNAVYLQMNSLKAEDTAVYYCNTVKVVGGRLDN------PDYWGQGTQVTVSS
B7.3 QVKLEESGGGLVQPGGSLRLSCAASGRTASGYGMGWFRQAPGKEREFVAAISRSGAGTLNADFVKGRFTISRDNAKNTVYLQMNSLKPEDTAVYYCVARPTKVDRDYATRREM-YNYWGQGTQVTVSS
B13.2 QVKLEESGGGSVQAGGSLRLSCAASGRDFSTLAMGWFRQAPGKEREFVATINWSGGTTHYADSVKGRFTISRDNAKNTVYLQMGSLKPEDTAVYYCGRSKYAAGALTRAYD---YNYWGQGTQVTVSS
B13.3 QVKLEESGGGLVQAGGSLRLSCSASGSIFSINDMGWYRRAPGKRRELVAAIT-SGGIPNYADSVKGRFTISRDNAKNTGYLQMNSLKPEDTAVYYCAAQFGTVAAALRRHE---YDYWGQGTQVTVSS
B13.6 QVKLEESGGGLVQAGGSLRLSCSASGRTFSSGVMGWFRQAPGKQRELVAAIT-TGGSTSYTDSVKGRFTISRDNAKNTVYLQMNSLKPEDTAVYYCNSVAVVGGVIKS------PDYWGQGTQVTVSS
B15.3 QVQLVESGGGSVQAGGSLRLSCAASG--LSRYAMAWFRQGTGKEREFVASTNWSSGNTPYADSVKGRFIISRDNAKNTVYLQMNSLKPGDTAIYYCAARKLDVPSRYSQH----YDYWGQGTQVTVSS
B15.5 QVQLVESGGDLVQAGGSLRLSCAASGSISRISTMGWYRQAPGKQRELVATIS-TGGTTNYAESVKGRFTVSRDNAKNTMYLQMNSLKPEDTAVYYCAAGWKVVRGSLE------YEYSGQGTQVTVSS

Figure 4.3. SDS-PAGE profile of purified VHHs that were isolated from the immune llama phage display library and characterized in this study.
Although purified to homogeneity, some VHHs produce a doublet on non-reducing SDS-PAGE gels. Each lane contains 2 μg VHH per lane. Molecular weight markers, M, are given in kDa. NR: non-reducing.

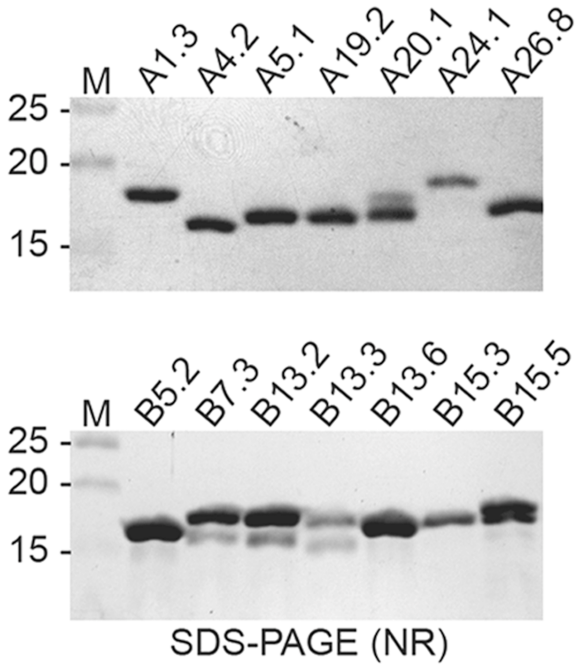
M
A1.3
A4.2
A5.1
A19.2
A20.1
A24.1
A26.8
25
20
15
M
B5.2
B7.3
B13.2
B13.3
B13.6
B15.3
B15.5
25
20
15
SDS-PAGE (NR)

Table 4.1. Properties of isolated anti-TcdA/B V_HHs and V_Ls.

V_HH / V_L	MW (Da)[1]	pI[2]	Yield (mg/L)	k_{on} ($M^{-1}s^{-1}$)	k_{off} (s^{-1})	K_D (nM)	Neutralizing?
A1.3	16.75	6.71	1.4	NB	NB	NB	No[3]
A4.2	15.73	8.59	31.3	6.7×10^5	1.6×10^{-2}	24	Yes
A5.1	15.80	6.71	55.5	1.6×10^6	5.0×10^{-3}	3	Yes
A19.2	16.01	8.61	3.8	1.4×10^4	3.9×10^{-3}	290	Yes
A20.1	16.81	6.64	105.9	8.2×10^5	1.6×10^{-3}	2	Yes
A24.1	16.91	6.71	8.5	6.0×10^4	1.6×10^{-2}	260	Yes
A26.8	16.02	6.65	64.9	1.4×10^6	1.6×10^{-2}	12	Yes
A4.2m	15.74	8.40	11.5	9.3×10^5	1.9×10^{-2}	20	Yes
A5.1m	15.83	7.20	3.6	9.5×10^6	1.6×10^{-2}	17	Yes
A19.2m	16.03	8.40	7.4	NB	NB	NB	NA
A20.1m	16.83	6.31	19.2	6.4×10^5	5.9×10^{-3}	9.2	Yes
A24.1m	16.92	6.71	0.6	NB	NB	NB	NA
A26.8m	16.03	6.65	2.2	1.0×10^6	2.8×10^{-2}	28	Yes
B5.2	15.11	6.04	6.7	2.0×10^3	2.0×10^{-4}	100	No[3]
B7.3	16.13	8.93	1.5	N/A	N/A	N/A	NA
B13.2	15.79	7.98	4.0	N/A	N/A	N/A	NA
B13.3	15.62	8.00	1.6	N/A	N/A	N/A	NA
B13.6	15.01	8.00	3.6	2.5×10^3	1.0×10^{-3}	400	No[3]
B15.3	15.58	8.59	1.2	N/A	N/A	N/A	NA
B15.5	15.23	7.18	4.6	2.8×10^3	1.0×10^{-3}	357	No[3]
B4.3 V_L	13.94	8.69	3.0	ND	ND	237	No[4]
B5.40 V_L	13.98	8.69	27.2	ND	ND	318	No[4]
B12.51 V_L	13.69	8.69	2.7	ND	ND	1800	No[4]
B17.62 V_L	13.76	9.07	5.9	ND	ND	1900	No[4]

1. Molecular weight includes c-Myc and His_6 tags.

2. Theoretical pI calculated using the ExPASy ProtParam tool [http://www.expasy.ch/tools/protparam.html].

3. Not neutralizing at a concentration as high as 1 μM.

4. Not neutralizing at a concentration as high as 2.5 μM.

NB: no binding detected by Biacore.

N/A: binding detected by Biacore (*see* Figure 4.6), but data not analyzable.

NA: not attempted.

ND: not determined.

4.1.3 SEC, soluble ELISA, and SPR analysis of isolated V_HHs

Purified V_HHs were analyzed by Superdex™ 75 SEC and as expected all were non-aggregating monomers (Figure 4.4). Soluble ELISA demonstrated that 6 of 7 anti-TcdA V_HHs recognized native TcdA and TcdA-RBD-f1 and that none of the V_HHs cross-reacted with TcdB or TcdB-RBD-f1 (Figure 4.5A, C). Of the 7 anti-TcdB V_HHs tested, 5 recognized TcdB and TcdB-RBD-f1 and one clone (B5.2) also recognized TcdA (Figure 4.5B, D). SPR analysis revealed 6 of 7 anti-TcdA V_HHs specifically bound TcdA with equilibrium dissociation constants ranging from 290 nM for A19.2 to 2 nM for A20.1 (Figure 4.6A – F, Table 4.1). Four of the clones had K_D values ranging from 2 to 24 nM (Table 4.1). All of the data collected fit a 1:1 binding model.

Analyzing the TcdB-binding V_HHs by SPR was more challenging. Initial attempts to immobilize TcdB onto the CM5 dextran biosensor chip were hindered, possibly, by the low pI of TcdB. An attempt to biotinylate TcdB for immobilization on a streptavidin-coated biosensor chip also as unsuccessful. To circumvent this problem, anti-TcdB V_HHs were immobilized directly onto the CM5 dextran chips and data collected using various concentrations of TcdB-RBD-f1. Analyzable data could only be collected for 3 of 7 anti-TcdB V_HHs, with affinity constants ranging from 100 nM to 400 nM (Figure 4.6G – I, Table 4.1). Specific binding was detected for the other 4 anti-TcdB V_HHs; however, the data were non-analyzable (Figure 4.6J – M).

Figure 4.4. Size exclusion chromatography (SEC) analysis of wild-type V_HHs.
The purified V_HHs were analyzed on a Superdex™ 75 column and all produced non-aggregating, monomeric peaks as expected.

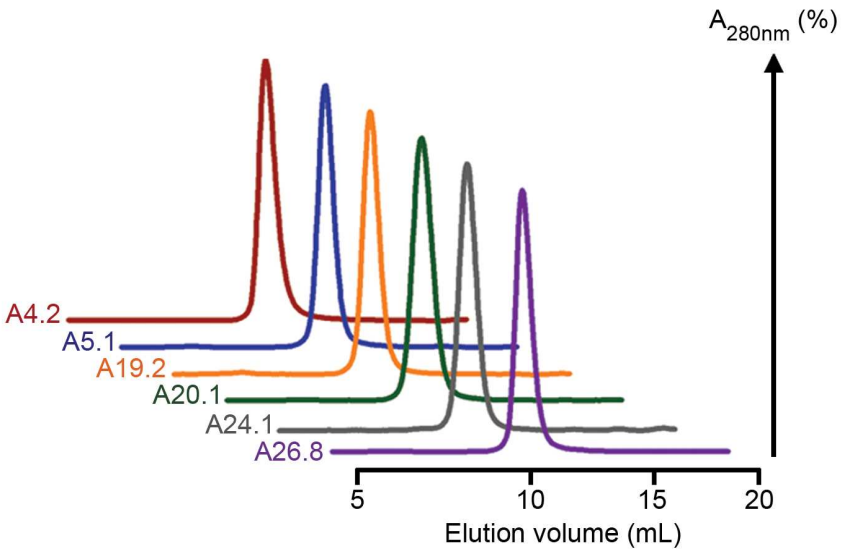
A280nm (%)
A4.2
A5.1
A19.2
A20.1
A24.1
A26.8
5
10
15
20
Elution volume (mL)

Figure 4.5. Characterization of anti-toxin VHH binding specificity and the nature of toxin epitopes.

ELISA demonstrating that purified anti-TcdA VHHs (**A**) and anti-TcdB VHHs (**B**) recognize both native toxins and recombinant RBD fragments. Wells were coated with equimolar concentrations of the proteins shown on the x-axis. VHHs were added at 2 μg/mL. The B5.2 VHH bound both TcdA and TcdB. (**C & D**) ELISA illustrating the binding of various concentrations of purified VHHs to immobilized TcdA or TcdB, respectively. (**E**) ELISA on TcdA treated with various temperatures for 30 min before probing with VHHs. The dotted line represents the TcdA midpoint unfolding temperature (T_m) of ≅55°C (162). At treatment temperatures above the TcdA T_m, binding of 4 out of 5 TcdA-specific VHHs was abolished. A19.2 bound TcdA exposed to temperatures above its T_m, confirming that denatured TcdA was coated in the wells and that A19.2 recognized a linear epitope. (**F**) Western blots (reducing/denaturing) probed with His-tagged anti-TcdA VHHs or control mouse anti-TcdA IgG (PCG4). Binding was detected with HisDetector™ Nickel-AP or goat anti-mouse IgG-AP secondary probes, respectively. Only A19.2 VHH and PCG4 IgG recognized denatured TcdA and the secondary probes did not bind denatured TcdA as expected. (**G**) Western blots (native-PAGE) probed with anti-TcdA VHHs or control PCG4. VHHs and PCG4 bound TcdA. The goat anti-mouse IgG-AP conjugates strongly cross-reacted with TcdA in the absence of PCG4. All molecular weight markers (numbers on the left side of images in **F** and **G**) are given in kDa.

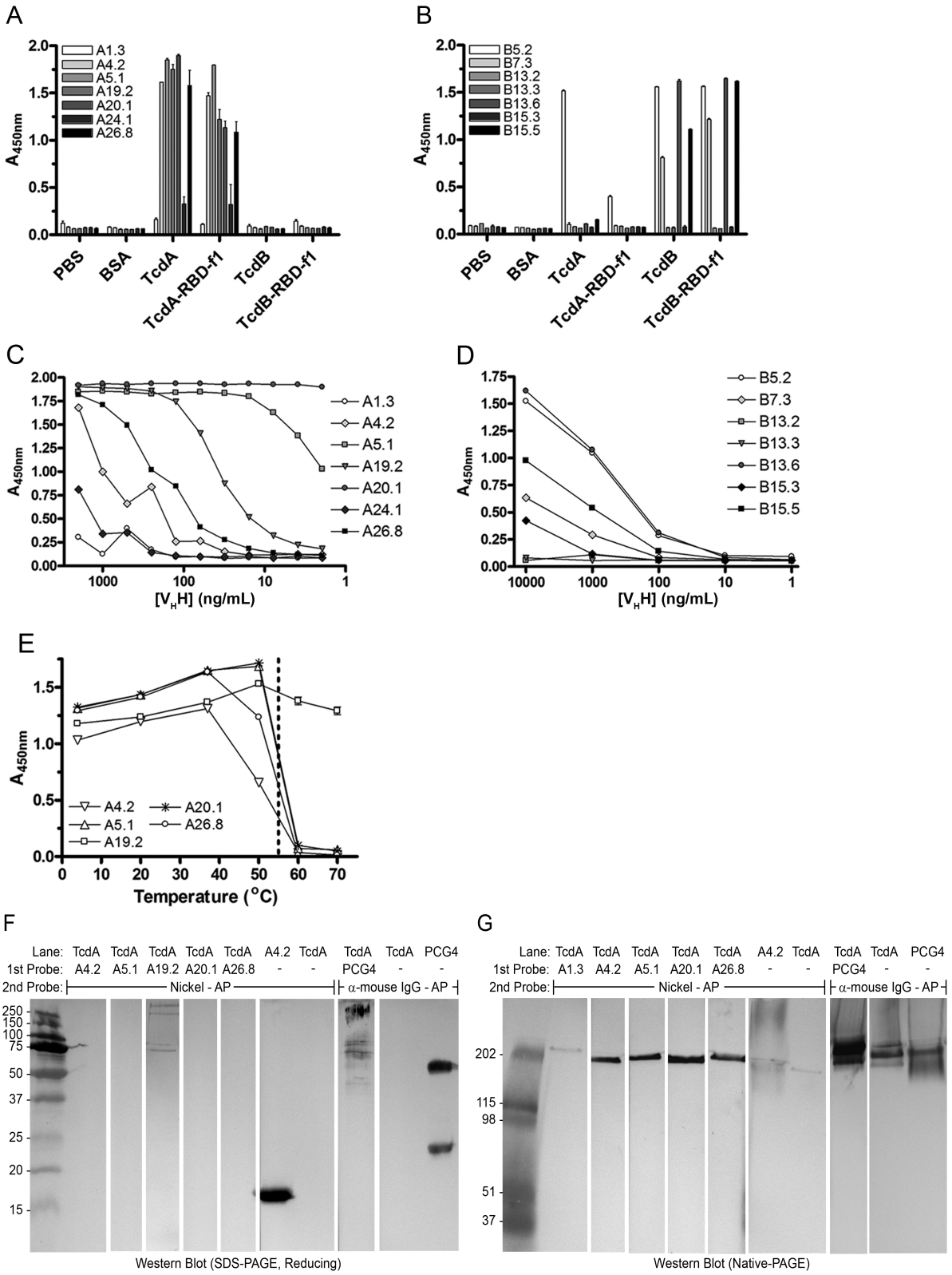
A
A1.3
A4.2
A5.1
A19.2
A20.1
A24.1
A26.8
A450nm
PBS
BSA
TcdA
TcdA-RBD-f1
TcdB
TcdB-RBD-f1
B
B5.2
B7.3
B13.2
B13.3
B13.6
B15.3
B15.5
C
[VHH] (ng/mL)
D
E
Temperature (°C)
F
Lane: TcdA TcdA TcdA TcdA TcdA A4.2 TcdA TcdA TcdA PCG4
1st Probe: A4.2 A5.1 A19.2 A20.1 A26.8 - - PCG4 - -
2nd Probe: Nickel - AP α-mouse IgG - AP
Western Blot (SDS-PAGE, Reducing)
G
Lane: TcdA TcdA TcdA TcdA TcdA A4.2 TcdA TcdA TcdA PCG4
1st Probe: A1.3 A4.2 A5.1 A20.1 A26.8 - - PCG4 - -
2nd Probe: Nickel - AP α-mouse IgG - AP
Western Blot (Native-PAGE)

Figure 4.6. VHHs bind TcdA and TcdB with high affinity.
SPR sensorgrams of TcdA-specific VHHs A4.2, A5.1, A19.2, A20.1, A24.1, and A26.8 binding to immobilized TcdA (**A - F**) and TcdB-RBD-f1 binding to immobilized TcdB-specific VHHs B5.2, B13.6, and B15.5 (**G - I**) are shown. The A19.2 sensorgrams were corrected for response differences between the active and reference flow cells. In experiments involving TcdA-specific VHHs, TcdA was immobilized on CM5-dextran chips and monomeric VHHs were passed over at concentration ranges noted on each sensorgram, giving affinity constants ranging from 2 nM to 290 nM. In experiments involving TcdB-specific VHHs, antibodies were immobilized on CM5-dextran chips and TcdB-RBD-f1 ranging in concentration from 2 μM to 200 nM was passed over, giving affinity constants ranging from 100 nM to 400 nM. (**J - M**) A subset of TcdB-specific VHHs showed complex binding to recombinant TcdB-RBD-f1. SPR sensorgrams for VHHs that showed binding to TcdB-RBD-f1, but whose data was non analyzable. The recombinant TcdB-RBD-f1 fragment (2 μM – 200 nM) was passed over immobilized VHHs (526 – 1209 RUs). For all sensorgrams, black lines represent raw data measurements and red lines represent fitted curves. Rate and affinity constants are given in Table 4.1.

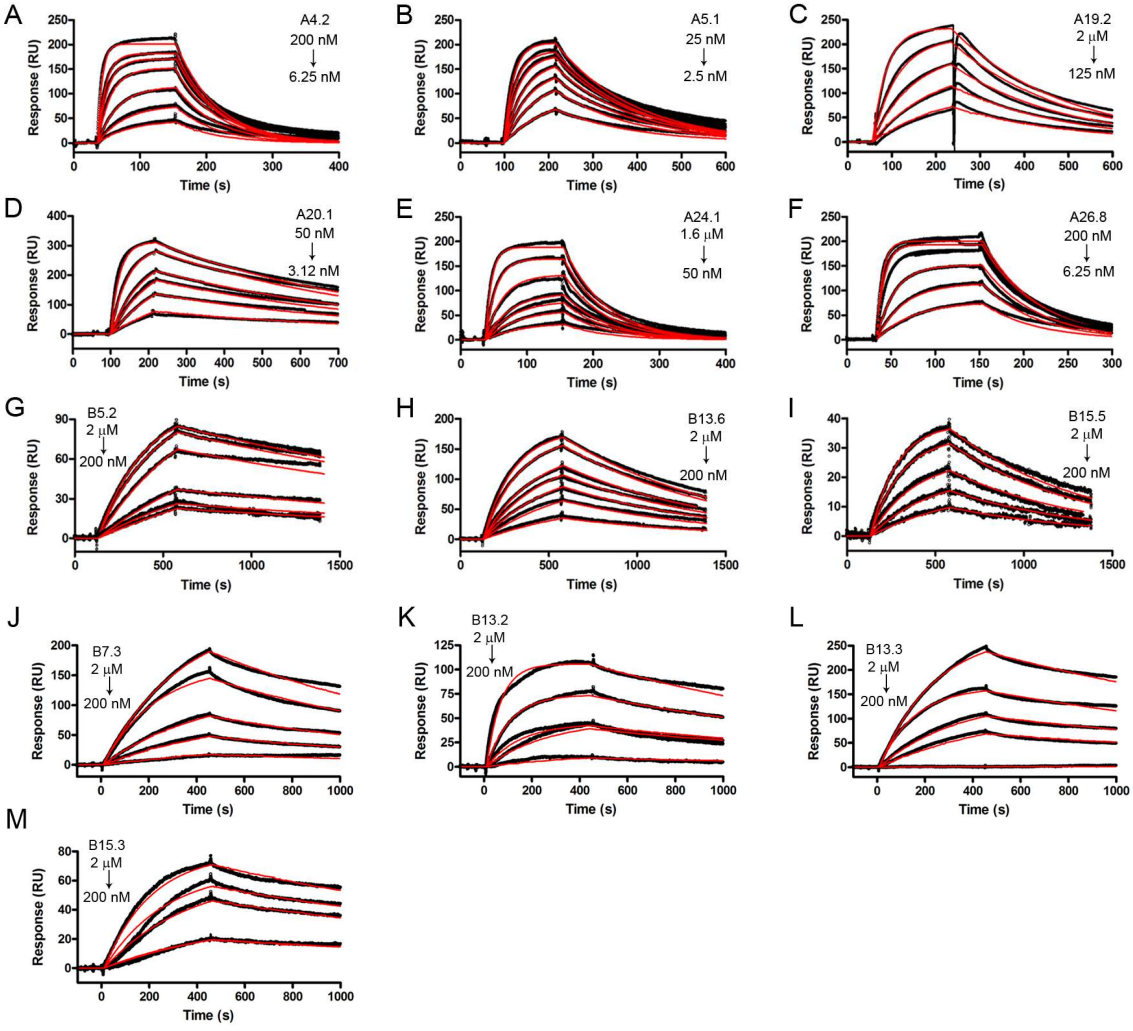
A
A4.2
200 nM
6.25 nM
B
A5.1
25 nM
2.5 nM
C
A19.2
2 μM
125 nM
D
A20.1
50 nM
3.12 nM
E
A24.1
1.6 μM
50 nM
F
A26.8
200 nM
6.25 nM
G
B5.2
2 μM
200 nM
H
B13.6
2 μM
200 nM
I
B15.5
2 μM
200 nM
J
B7.3
2 μM
200 nM
K
B13.2
2 μM
200 nM
L
B13.3
2 μM
200 nM
M
B15.3
2 μM
200 nM
Response (RU)
Time (s)

4.1.4 TcdA-specific V_HHs bind linear and conformational epitopes

To gain insight into whether the TcdA-specific V_HHs recognized linear or conformational epitopes on TcdA, Western blotting with both denaturing SDS-PAGE and native PAGE were performed. First, only A19.2 recognized TcdA run under denaturing and reducing conditions (Figure 4.5F). The anti-TcdA mAb PCG4 (122), which was previously shown to recognize TcdA in Western blots (142), confirmed that TcdA was transferred to the blot. The weak signal obtained from A19.2 relative to PCG4 is likely due to the low affinity (K_D = 290 nM) and/or lack of avidity of A19.2 for TcdA. In the absence of primary antibody, the secondary conjugates Nickel-AP and goat anti-mouse IgG-AP did not bind TcdA, as expected. The V_HH A4.2 and PCG4 were included to confirm the functionality of the secondary conjugates. Under non-denaturing conditions (native PAGE), V_HH binding to TcdA was originally probed with mouse anti-His_6 IgG-AP and found this secondary antibody cross-reacted with TcdA in the absence of V_HH (data not shown). To overcome this, the secondary antibody was replaced with Nickel-AP. Using this secondary conjugate, the V_HHs A4.2, A5.1, A20.1, and A26.8 recognized native TcdA while the non-binding A1.3 essentially did not react with TcdA (Figure 4.5G). The Nickel-AP secondary conjugate did not bind native TcdA in control blots. The diffuse signal and poor migration pattern of A4.2 V_HH control is likely due to its high pI (theoretical pI: 8.59). To confirm the presence of TcdA on native PAGE blots, PCG4 was used as a control. Just like anti-His_6 IgG-AP, the secondary antibody goat anti-mouse IgG-AP also bound TcdA in the absence of the primary probe, PCG4 in this case (Figure 4.5G).

To further validate the binding of the VHHs to conformational or linear TcdA epitopes, TcdA was exposed to various temperatures above and below its thermal unfolding midpoint temperature ($T_m \cong 55°C$; (162)) and probed with various VHHs in ELISA. For all antibodies except A19.2, VHH binding to TcdA was completely abolished when TcdA was heated above its T_m (Figure 4.5E). Collectively, these results suggest the anti-TcdA VHHs recognize a single or several conformational epitope(s) on TcdA, with the exception of A19.2, which recognizes denatured TcdA in ELISA (Figure 4.5E) and Western Blot (Figure 4.5F). These TcdA epitopes must be located in the RBD region of TcdA since llama immunization and library panning were both performed with TcdA-RBD-f1, and because the VHHs were shown to recognize this recombinant fragment by ELISA (Figure 4.5A).

4.1.5 TcdA-specific VHHs neutralize TcdA *in vitro*

Human lung fibroblast (HLF) cytotoxicity assays were used to determine whether VHHs could neutralize TcdA- or TcdB-induced HLF cell rounding. Dose-response experiments with TcdA and TcdB (Figure 4.7A) determined the minimum toxin concentrations capable of 100% cell rounding after 24 h to be 50 ng/mL (162 pM) and 5 ng/mL (18.6 pM), respectively. For all subsequent experiments, 2x this minimum concentration was used (i.e., 100 ng/mL (325 pM) of TcdA and 10 ng/mL (37 pM) of TcdB). VHHs had no effect on HLF cells when incubated in the absence of toxin A (Figure 4.7B). When VHHs (at 1000 nM concentration) and TcdA were added simultaneously to HLF cells, 6 of 7 anti-TcdA VHHs inhibited TcdA-induced cell rounding 24 h post TcdA addition

(Figure 4.7B – E), although the neutralization capacity of A19.2 was not significant (Table 4.2). The neutralizing capacity of the 4 strongest VHHs (A4.2, A5.1, A20.1, and A26.8) was similar, reflective of their close range of K_Ds (2 – 24 nM). The weakest neutralizers, A19.2 and A24.1, also possessed the weakest affinity constant of 290 nM and 260 nM, respectively. As expected, the non-binding A1.3 VHH did not inhibit cell rounding. At lower concentrations (10 nM), none of the VHHs significantly inhibited cell rounding with the exception of A26.8 ($P = 0.0095$).

Next, various combinations of VHHs were added to determine if VHH synergies would enhance toxin neutralizing efficacy. All possible doublet and triplet combinations were tested, with concentrations adjusted such that final VHH concentrations were the same as neutralizing experiments involving single VHHs. In general, doublet and triplet combinations improved toxin A inhibition significantly (Figure 4.7C – E, Table 4.2) (although it appears that at 1000 nM, the beneficial effect of combination is masked to some degree due to the high VHH concentration usage). For example, at 10 nM, all doublet and triplet VHH combinations significantly inhibited cell rounding, while only 1 of 6 singlets (A26.8) remained significant. At 10 nM and 0.1 nM concentrations, doublets involving A4.2 were weaker neutralizers compared to other pairs, likely a reflection of A4.2's poorer affinity (K_D = 24 nM) relative to the other VHHs. While all triplets remained significant inhibitors of cell rounding at 0.1 nM, only one combination (A4.2/A5.1/A26.8) showed improved efficacy relative to each of its 3 possible doublet components. However, two sets of doublets (A5.1/A20.1 and A20.1/A26.8) have neutralization potencies which are comparable to those of triplets. This is likely due to a combination of high affinity binding

and recognition of non-overlapping toxin A epitopes (*see* below and Discussion). At 0.1 nM, which is at least 20x lower than the VHHs' K_Ds, A5.1/A20.1 and A20.1/A26.8 doublets and all four triplet combinations (Figure 5E) inhibited at least 50% of cell rounding 24 h after TcdA addition. In particular, the A20.1/A26.8 pair and A4.2/A20.1/A26.8 triplet were capable of inhibiting nearly 75% of cell rounding.

Collectively, the above data demonstrate that VHHs binding the RBD region of TcdA provide an effective strategy for generating potent TcdA neutralizers. Furthermore, combinations of these VHHs increase toxin neutralizing efficacy.

Finally, the neutralizing capacity of the anti-TcdB VHHs was also tested. None of the 3 TcdB-specific VHHs examined were capable of TcdB neutralization, even at a concentration of 1 μM (data not shown).

Figure 4.7. Potent neutralization of TcdA-induced cell rounding *in vitro*.
(**A**) Dose-response curves of various concentrations of purified TcdA (top) and TcdB (bottom) on confluent monolayers of IMR-90 human lung fibroblast (HLF) cells. The percentage of cells rounded over time was visualized by light microscopy. (**B**) Representative photographs of HLF cells in the presence or absence of TcdA (325 pM) and/or VHHs (1000 nM), 24 h post addition of TcdA/VHH. The black bar represents 100 μm. (**C - E**) Summary of neutralization assays. The final concentrations of VHHs in each assay well were 1000 nM (**C**), 10 nM (**D**) and 0.1 nM (**E**) and VHHs were added as singles, pairs, or triplet combinations. White bars represent single VHHs or PBS control, grey bars represent paired combinations and black bars represent triplet combinations. Percent inhibition of cell rounding is relative to cells receiving TcdA only. Error bars represent standard error of the mean (n = 9). A total of 3 experimental replicates were peformed with 3 replicate wells in each experiment.

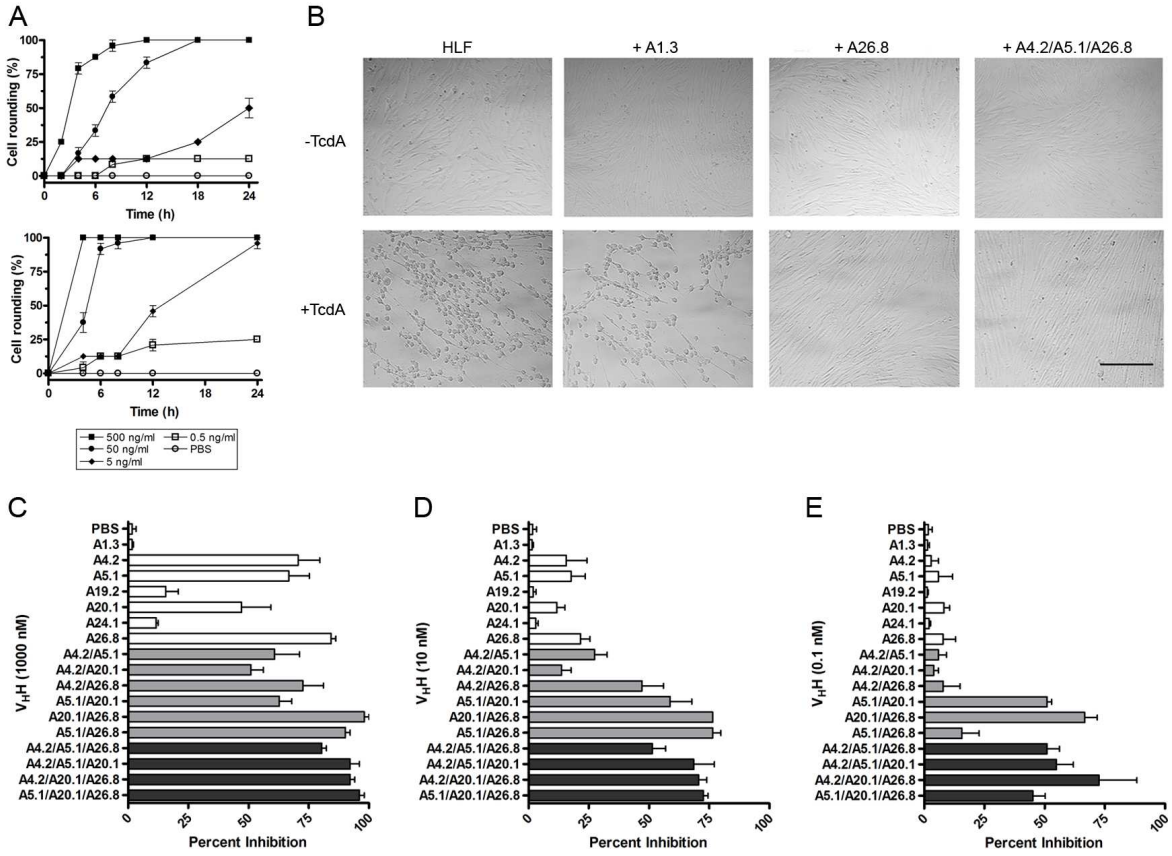
A
Cell rounding (%)
Time (h)
500 ng/ml
50 ng/ml
5 ng/ml
0.5 ng/ml
PBS
B
HLF
+ A1.3
+ A26.8
+ A4.2/A5.1/A26.8
-TcdA
+TcdA
C
D
E
PBS
A1.3
A4.2
A5.1
A19.2
A20.1
A24.1
A26.8
A4.2/A5.1
A4.2/A20.1
A4.2/A26.8
A5.1/A20.1
A20.1/A26.8
A5.1/A26.8
A4.2/A5.1/A26.8
A4.2/A5.1/A20.1
A4.2/A20.1/A26.8
A5.1/A20.1/A26.8
V_HH (1000 nM)
V_HH (10 nM)
V_HH (0.1 nM)
Percent Inhibition

Table 4.2. Neutralization assay statistical analysis.

Conc.	Format	Treatment	% Inhibition[1]	P value[2]
1000 nM	Singlet	A1.3	1.6 (±0.6)	ns
		A4.2	70.6 (±9.0)	0.0017
		A5.1	66.7 (±8.5)	0.0017
		A19.2	15.7 (±5.2)	ns
		A20.1	47.1 (±12.2)	0.0214
		A24.1	11.7 (±0.8)	0.0056
		A26.8	84.3 (±1.9)	<0.0001
	Doublet	A4.2/A5.1	60.8 (±10.4)	0.0049
		A4.2/A20.1	51.0 (±5.2)	0.0008
		A4.2/A26.8	72.6 (±8.5)	0.0012
		A5.1/A20.1	62.8 (±5.2)	0.0004
		A20.1/A26.8	98.0 (±1.9)	<0.0001
		A5.1/A26.8	90.2 (±1.9)	<0.0001
	Triplet	A4.2/A5.1/A26.8	80.4 (±2.0)	<0.0001
		A4.2/A5.1/A20.1	92.2 (±3.9)	<0.0001
		A4.2/A20.1/A26.8	92.2 (±1.9)	<0.0001
		A5.1/A20.1/A26.8	96.1 (±1.9)	<0.0001
10 nM	Singlet	A1.3	1.5 (±0.5)	ns
		A4.2	15.7 (±8.5)	ns
		A5.1	17.7 (±5.9)	ns
		A19.2	1.9 (±1.1)	ns
		A20.1	11.8 (±3.4)	ns
		A24.1	3.0 (±1.0)	ns
		A26.8	21.6 (±3.9)	0.0095
	Doublet	A4.2/A5.1	27.5 (±5.2)	0.0091
		A4.2/A20.1	13.7 (±3.9)	0.0477
		A4.2/A26.8	47.1 (±9.0)	0.0077
		A5.1/A20.1	58.8 (±9.0)	0.0033
		A20.1/A26.8	76.5 (±0.2)	<0.0001
		A5.1/A26.8	76.5 (±3.4)	<0.0001
	Triplet	A4.2/A5.1/A26.8	51.4 (±5.5)	0.0010
		A4.2/A5.1/A20.1	68.6 (±8.5)	0.0015
		A4.2/A20.1/A26.8	70.6 (±3.4)	<0.0001
		A5.1/A20.1/A26.8	72.6 (±1.9)	<0.0001
0.1 nM	Singlet	A1.3	1.3 (±0.8)	ns
		A4.2	2.9 (±2.9)	ns
		A5.1	5.8 (±5.8)	ns
		A19.2	1.2 (±0.4)	ns
		A20.1	8.2 (±2.4)	ns
		A24.1	2.1 (±0.5)	ns
		A26.8	7.8 (±5.2)	ns
	Doublet	A4.2/A5.1	5.9 (±3.4)	ns
		A4.2/A20.1	3.9 (±2.0)	ns
		A4.2/A26.8	9.8 (±5.2)	ns
		A5.1/A20.1	51.0 (±1.7)	<0.0001
		A20.1/A26.8	66.7 (±5.2)	0.0003
		A5.1/A26.8	15.7 (±7.1)	ns
	Triplet	A4.2/A5.1/A26.8	51.0 (±5.2)	0.0008
		A4.2/A5.1/A20.1	54.9 (±7.0)	0.0018
		A4.2/A20.1/A26.8	72.6 (±15.7)	0.0109
		A5.1/A20.1/A26.8	45.1 (±5.2)	0.0013

1. Mean percent inhibition of cell rounding (± SEM) (n = 9).

2. P values were obtained by comparing VHH treatments to PBS control. All P values were determined using the unpaired Student's *t* test (two tailed). P values less than 0.05 were considered significant. ns: not significant.

4.1.6 V_HHs recognize overlapping and non-overlapping epitopes on TcdA

The observation that combining anti-TcdA V_HHs increased TcdA neutralizing efficacy relative to single V_HHs at the same concentration (Figure 4.7C – E) suggested these antibodies recognized distinct, non-overlapping epitopes. We performed co-injection SPR experiments with pairs of V_HHs, in both orientations, to determine if antibodies could bind TcdA simultaneously (Figure 4.8A). Of the paired combinations, only those involving A20.1 V_HH showed a significant increase in response consistent with theoretical R_{max} values (≅160 – 180 RUs) upon co-injection. This suggests that A20.1 is free to bind TcdA when A4.2, A5.1 or A26.8 are bound at saturating concentrations and also indicates the A20.1 epitope is distinct and does not hinder binding of the other three V_HHs. For A4.2, A5.1 and A26.8 only minor changes in response were seen upon co-injection with theoretical R_{max} values not reached, an indication that the V_HHs were binding overlapping epitopes and hindering the binding of each other to TcdA (Figure 4.8A). This was confirmed by co-injection of all three of these V_HHs simultaneously (Figure 4.8B). Taken together, our SPR-based epitope mapping studies suggest A20.1 freely binds TcdA at a site which does not overlap with, or is sterically hindered by, A4.2, A5.1 or A26.8 binding. These V_HHs bind at sites on TcdA which hinder freely accessibly binding of the others, suggesting these antibodies share a single epitope, or bind epitopes in such close proximity to one another that it prevents unhindered interaction with sensor-chip immobilized TcdA.

Figure 4.8. Anti-TcdA V_HHs recognize overlapping and non-overlapping epitopes.
(**A**) SPR co-injection experiments were used to determine if pairs of V_HHs could bind TcdA simultaneously. The sensorgrams of all of the possible paired combinations of A4.2, A5.1, A20.1, and A26.8, in both orientations, are shown. Dashed lines represent injection of a single V_HH followed by injection of buffer. Solid lines represent co-injections of the first V_HH followed by injection of a second V_HH. For all experiments, 80 μL of each V_HH at a concentration 20x its K_D was injected over 10,287 RUs of immobilized TcdA at 40 μL/min. In general, A4.2, A5.1, and A26.8 appeared to share an overlapping epitope as no significant increase in response was found upon injection of the second species. Conversely, A20.1 appeared to bind a distinct, non-overlapping epitope. When A20.1 injections were followed by A4.2, A5.1, and A26.8 injections there was an approximate doubling of total signal with the second injection. However, this was not observed with the reverse injection combinations, particularly A4.2 followed by A20.1 and A26.8 followed by A20.1 because the relatively fast off-rates of A4.2 and A26.8 compared to A20.1 resulted in very significant dissociation of these V_HHs from the surface before equilibrium binding of A20.1 was reached. (**B**) Mixtures of A4.2, A5.1, and A26.8 V_HHs show binding at overlapping TcdA epitopes. The three V_HHs suspected of sharing an overlapping epitope (**A**, above) were further analyzed by surface plasmon resonance by injecting the V_HHs alone (A4.2, A5.1, or A26.8) or as a triplet mixture ("Mix") over immobilized TcdA. The sensorgram illustrates similar R_{max} (≅160 – 200 RUs) values for individual V_HHs with no increase in response upon injection of the mixed population, indicating these antibodies recognize an overlapping epitope on TcdA or at neighbouring epitopes that hinder the binding of subsequent species. If the mixture of V_HHs were free to bind at non-overlapping or non-hindering sites, one would expect an R_{max} value for the mixtures to reach the sum of all individual R_{max} values (i.e., ≅540 RUs). In all experiments, 80 μL of V_HHs were injected at 40 μL/min and used at 20x their K_D concentrations.

A

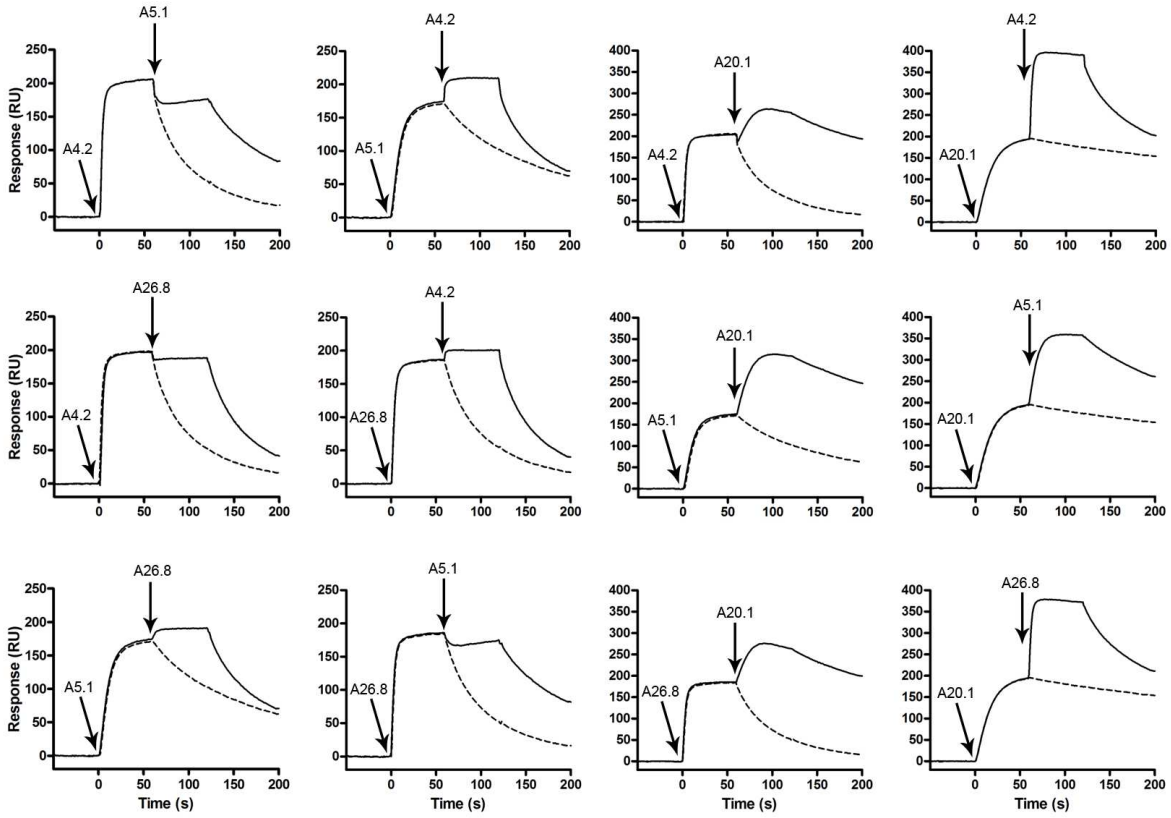
A5.1
A4.2
A4.2
A5.1
A20.1
A4.2
A4.2
A20.1
A26.8
A4.2
A4.2
A26.8
A20.1
A5.1
A5.1
A20.1
A26.8
A5.1
A5.1
A26.8
A20.1
A26.8
A26.8
A20.1
Response (RU)
Time (s)

B

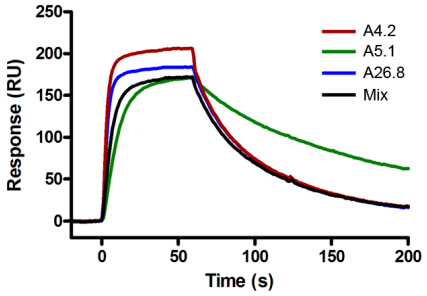
A4.2
A5.1
A26.8
Mix
Response (RU)
Time (s)

4.1.7 TcdA-specific VHHs do not bind at the carbohydrate binding pockets of TcdA

VHHs have long, flexible CDR3 loop regions that have been shown to form a convex paratope that can extend into clefts or active sites of protein antigens (29, 33). The recently solved crystal structure of TcdA-RBD was shown to contain seven carbohydrate binding pockets thought to be involved in cell receptor binding (53). We asked whether TcdA neutralization was due to VHH binding in the TcdA-RBD carbohydrate-binding pockets. Using SPR and two trisaccharides capable of binding TcdA-RBD within these pockets, we were unable to inhibit the binding of our neutralizing VHHs to TcdA in co-injection experiments (Figure 4.9, Figure 4.10). When both CD-grease and Le^X-AmHex trisaccharides were used at concentrations above the K_D values estimated from electrospray mass spectrometry ((34) and unpublished observations, C.C. Ling, J. Klassen and K-K. Ng), the trisaccharides bound to immobilized TcdA as detected by SPR, but carbohydrate-binding did not prevent the binding of VHH fragments to TcdA (Figure 4.9, Figure 4.10). In additional SPR experiments, we found that 10 mM concentrations of CD-grease trisaccharide (5x K_D concentration) were free to bind TcdA saturated with VHH (Figure 4.11). Furthermore, VHH binding to TcdA was not inhibited in ELISA with trisaccharide concentrations as high as 10 mM (data not shown). Taken together, these data indicate our VHHs do not inhibit free trisaccharides from accessing their binding sites on TcdA-RBD and that our VHHs are not binding at sites occupied by the trisaccharides.

Figure 4.9. TcdA-binding trisaccharides do not inhibit V_HH binding.
Using SPR, binding of V_HHs to immobilize TcdA was measured in the presence of trisaccharides CD-grease (**A**; CD) and Le^X-AmHex (**B**; Le^X). (**C**) Sensorgram illustrating the responses generated from A26.8 binding TcdA (red), CD-grease binding TcdA (black) and co-injection of A26.8 and CD-grease (light green). (**D**) Sensorgram illustrating the responses generated from A26.8 binding TcdA (red), Le^X-AmHex binding TcdA (black) and co-injection of A26.8 and Le^X-AmHex (light blue). (**E&F**) Subtraction of the responses generated by trisaccharide binding to TcdA from the response generated by co-injection experiments (**C**, green; **D**, teal blue) reveals a near identical response to that of A26.8 binding TcdA (red), an indication that V_HH binding to TcdA is not inhibited by the trisaccharides. In all experiments, V_HHs were used at their K_D concentrations and trisaccharides at their approximate K_D concentrations (2 mM).

A

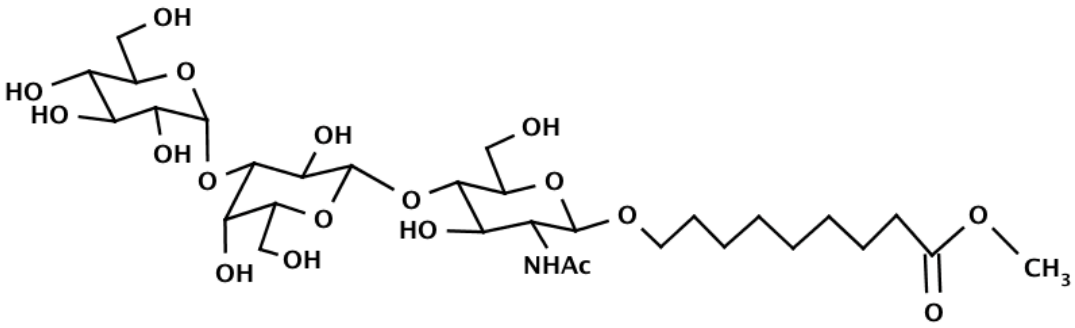
OH
HO
HO
O
OH
OH
O
O
OH
OH
O
OH
HO
NHAc
O
O
O
CH3

B

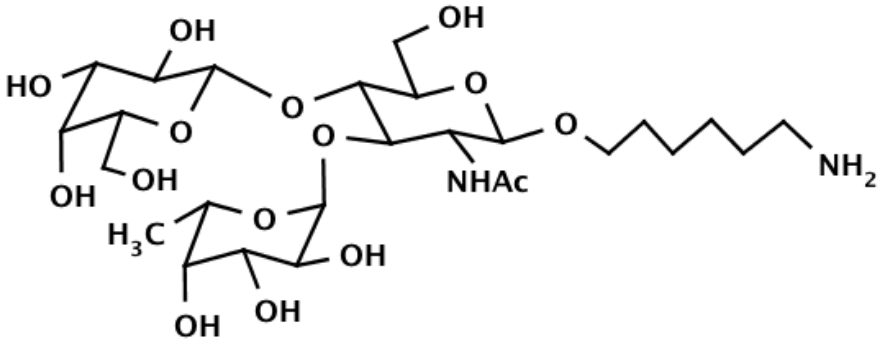
OH
HO
O
O
OH
OH
O
O
OH
NHAc
O
NH2
H3C
O
OH
OH
OH

C

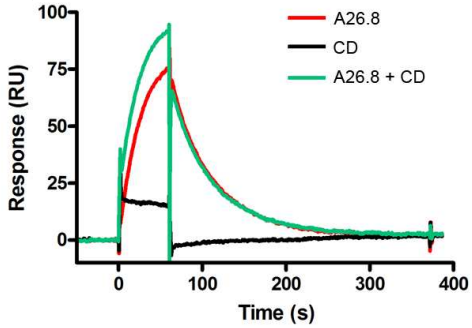
A26.8
CD
A26.8 + CD
Response (RU)
Time (s)
100
75
50
25
0
0
100
200
300
400

D

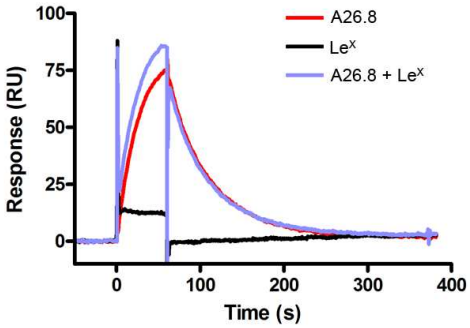
A26.8
Le^X
A26.8 + Le^X
Response (RU)
Time (s)
100
75
50
25
0
0
100
200
300
400

E

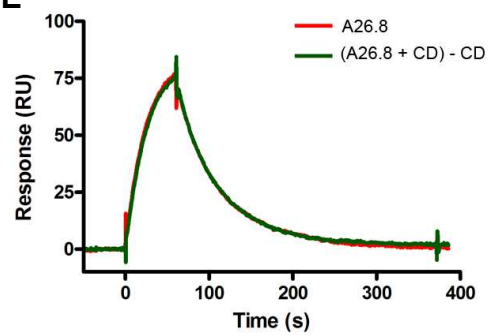
A26.8
(A26.8 + CD) - CD
Response (RU)
Time (s)
100
75
50
25
0
0
100
200
300
400

F

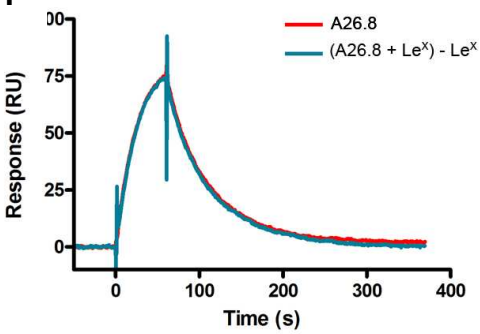
A26.8
(A26.8 + Le^X) - Le^X
Response (RU)
Time (s)
75
50
25
0
0
100
200
300
400

Figure 4.10. TcdA-binding trisaccharides do not inhibit V_HH binding.
SPR sensorgrams illustrating the subtraction of the response generated from either CD-grease (CD) or Le^X-AmHex (Le^X) trisaccharide binding to TcdA from co-injection (trisaccharide + V_HH) experiments is nearly identical to the response generated from V_HH to TcdA alone. In all experiments, V_HHs were used at their K_D concentrations and trisaccharides at their approximate K_D concentrations (2 mM). Control experiments illustrating CD-grease or LeX-AmHex binding are shown in Figure 4.9.

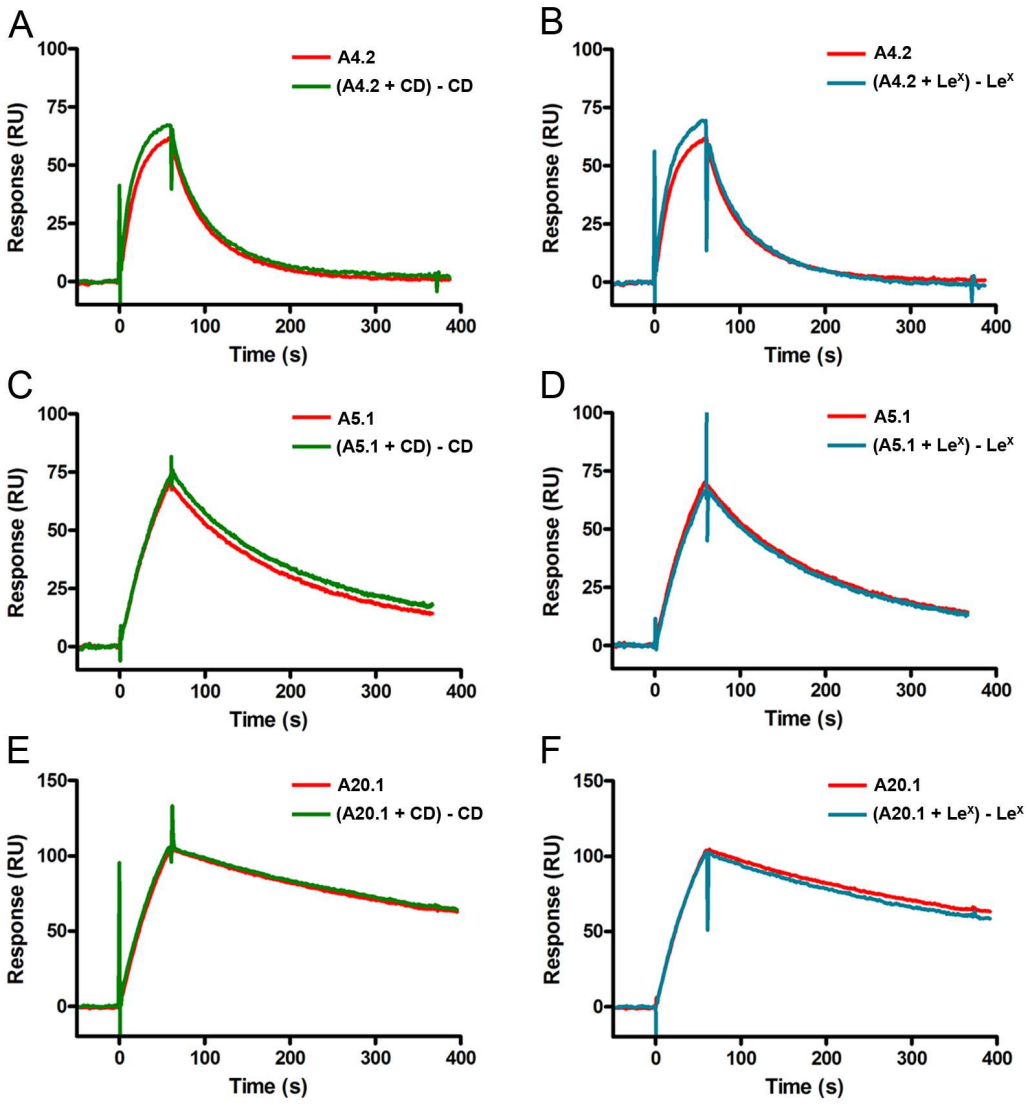
A
A4.2
(A4.2 + CD) - CD
Response (RU)
Time (s)
B
A4.2
(A4.2 + Le^x) - Le^x
Response (RU)
Time (s)
C
A5.1
(A5.1 + CD) - CD
Response (RU)
Time (s)
D
A5.1
(A5.1 + Le^x) - Le^x
Response (RU)
Time (s)
E
A20.1
(A20.1 + CD) - CD
Response (RU)
Time (s)
F
A20.1
(A20.1 + Le^x) - Le^x
Response (RU)
Time (s)

Figure 4.11. Pre-bound VHHs do not impair trisaccharide binding to TcdA.
At saturating concentrations (20x their [K_D]) of A20.1 and A26.8 bound to TcdA, CD-grease (10 mM) was not impaired from binding TcdA, confirming the VHHs do not interact with TcdA at or near the carbohydrate binding site. (**A**) SPR sensorgrams illustrate the injection of A20.1 ("A", solid and dashed lines), followed by injection of A20.1 ("B", dashed line) or A20.1 + CD-grease ("B", solid line), and finally injection of buffer ("C", solid and dashed lines). (**B**) SPR sensorgrams illustrate the injection of A26.8 ("A", solid and dashed lines), followed by injection of A26.8 ("B", dashed line) or co-injection of A26.8 + CD-grease ("B", solid line), and finally injection of buffer ("C", solid and dashed lines).

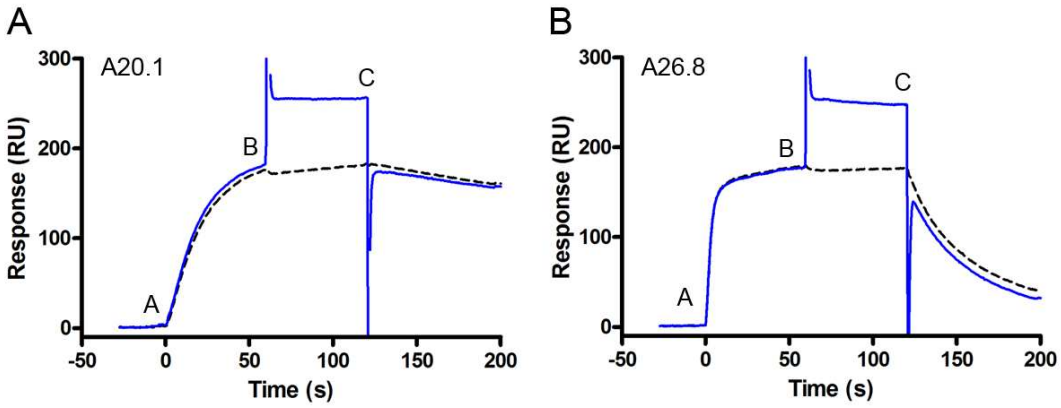
A
A20.1
300
200
100
0
Response (RU)
A
B
C
-50
0
50
100
150
200
Time (s)
B
A26.8
300
200
100
0
Response (RU)
A
B
C
-50
0
50
100
150
200
Time (s)

4.1.8 Production of V_HH variants for crystallography

Anti-TcdA V_HHs and anti-TcdB V_LS (*see* below) were expressed with a short N-terminal epitope tag to aid in co-crystal complex formation with either TcdA or TcdB. The short-tag variants expressed as well as their long-tag counterparts. At present, co-crystal structure determination is still underway at the University of Calgary. At least two complexes (A20.1:TcdA and A26.8:TcdA) have been solved by Dr. K-K. Ng and colleagues. The purpose of solving the structures of the V_HHs in complex with TcdA is to gain insight into the nature of the toxin:V_HH neutralization mechanism.

4.2 Isolation of *C. difficile* toxin B-specific V_LS

A synthetic human V_L phage display library was panned with a GST-stabilized fragment of recombinant TcdB to isolate TcdB-binding V_LS. The isolated V_LS were characterized with respect to aggregation state, affinity for TcdB, and ability to neutralize TcdB *in vitro*. The results of those experiments are presented in this section.

4.2.1 Synthetic V_L display library construction

The V_L library was constructed based on the previously identified HV_LP324 that showed robust biophysical properties, including resistance to aggregation, high expression, and high solubility (*J. Tanha, unpublished data*). The library was constructed by Dr. Jamshid Tanha's lab and characterized elsewhere (*J. Tanha, unpublished data*).

4.2.2 Assembly of GST-TcdB fusion protein

A fusion of *C. difficile* toxin B was constructed for the use as a panning reagent against the V_L library to isolate toxin B-specific V_L antibodies. Initially, expression of the C-terminal 80 amino acids of TcdB (TcdB-F80; Appendix 2) using the pET21b(+) expression vector was attempted. Two different expression protocols failed to yield any detectable amount of TcdB-F80 on a Western blot probed with anti-His_6 IgG (data not shown). To overcome this, we attempted to express TcdB-F80 as a C-terminal fusion to GST, using the pGEX-6P-2 expression vector that contains GST upstream of the multi-cloning site. The resulting protein contained an N-terminal GST tag fused to TcdB-F80, separated by a PreScission™ protease site harbored in the vector (Figure 4.12A). GST and GST-TcdB-F80 were easily expressed in *E. coli* and purified as described in Materials and Methods. SDS-PAGE analysis of the purified proteins (Figure 4.12B) showed GST and GST-TcdB-F80 running at their expected molecular weights of 26.65 kDa and 36.05 kDa, respectively.

To ensure the PreScission™ protease site was still accessible between the two fusion partners, a test cleavage was performed (Figure 4.12B) using PreScission™ protease and the GST-TcdB-F80 fusion protein. After 4 h, almost complete digestion of GST-TcdB-F80 into GST and TcdB-F80 was observed, at 3 different temperatures. This suggested that proteolytic elution of V_L-bound phages from surface-immobilized GST-TcdB-F80 was possible during panning (*see* below).

Figure 4.12. Isolation of TcdB-specific V_L human single-domain antibodies.
(**A**) Schematic of the two recombinant proteins expressed for panning of the V_L synthetic library. GST (*top*) was expressed as a control protein for panning experiments. GST-TcdB-F80 (*bottom*) is a fusion protein consisting of GST at the N-terminus and a recombinant 80 amino acid fragment of the TcdB cell receptor binding domain at the C-terminus. The PreScission™ protease site, denoted "P", separates the fusion proteins. (**B**) Non-reducing (NR) SDS-PAGE analysis of purified GST and GST-TcdB-F80, denoted "GST-F80", and subsequent proteolytic cleavage of the fusion protein with PreScission™ protease. The protease successfully cleaves GST-F80 into GST and F80, at all of the temperatures tested. Proteolytic cleavage of GST-F80 was used for dissociation of V_L-displaying phage during panning. (**C**) Overview of the V_L phage panning process. V_L library phages were incubated with surface-immobilized GST before incubation with surface-immobilized GST-F80 to remove GST-specific binders. V_L-displayed phages binding to immobilized GST-F80 were eluted by addition of PreScission™ protease and amplified for additional rounds of selection. (**D**) Phage ELISA on 17 unique V_L clones isolated after 4 rounds of panning. Phage displaying V_Ls were incubated with wells containing GST, GST-F80, and whole native TcdB. An anti-phage IgG conjugated to HRP was used for the detection of binding. Four of seventeen cones bound TcdB (*asterisks*) and were selected for subcloning, soluble expression, and functional characterization.

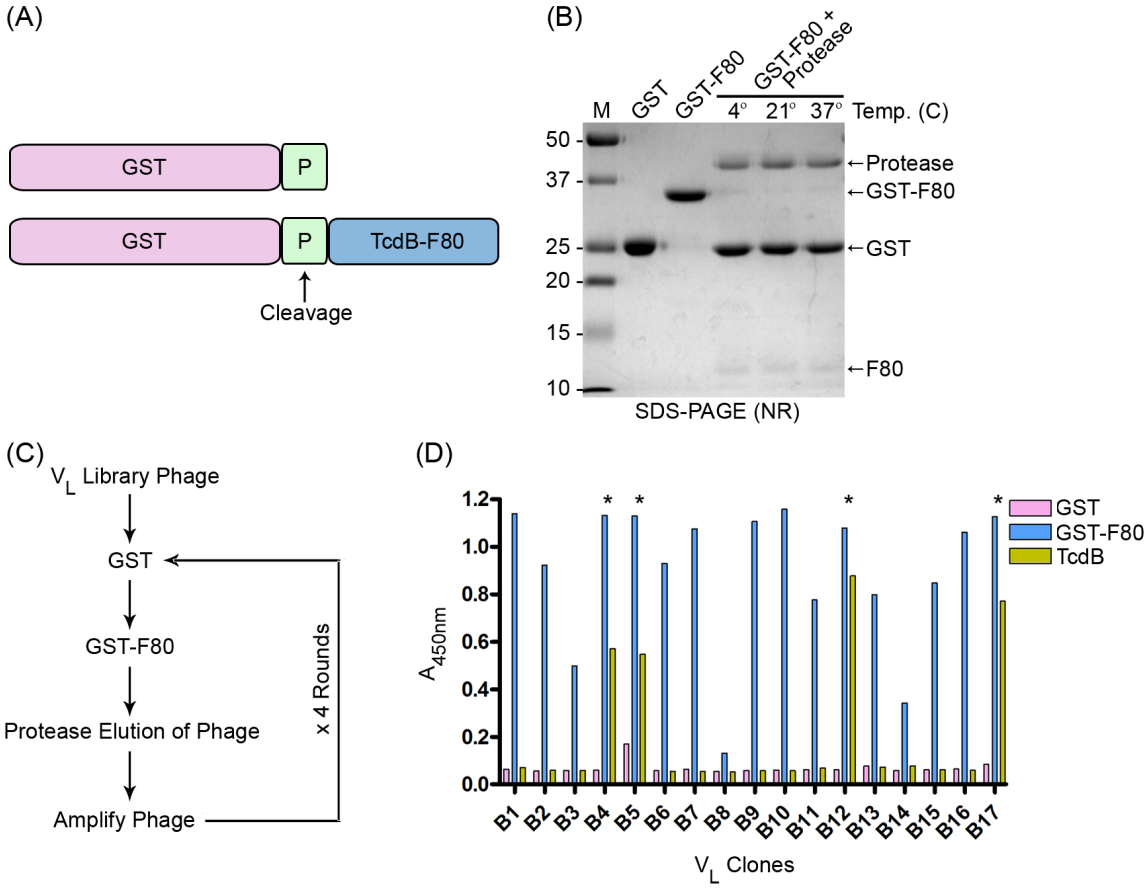
(A)
GST
P
GST
P
TcdB-F80
Cleavage
(B)
M
GST
GST-F80
GST-F80 + Protease
4°
21°
37°
Temp. (C)
50
37
25
20
15
10
←Protease
←GST-F80
←GST
←F80
SDS-PAGE (NR)
(C)
V_L Library Phage
GST
GST-F80
Protease Elution of Phage
Amplify Phage
x 4 Rounds
(D)
A450nm
1.2
1.0
0.8
0.6
0.4
0.2
0.0
B1
B2
B3
B4
B5
B6
B7
B8
B9
B10
B11
B12
B13
B14
B15
B16
B17
V_L Clones
GST
GST-F80
TcdB

4.2.3 V_L library screening, subcloning, and V_L expression

Four rounds of panning the V_L-phage display library (Figure 4.12C) and sequencing of 100 colonies after round 4 yielded 17 unique groups of V_{LS}. A phage ELISA (Figure 4.12D) revealed 16 of 17 V_{LS} (94%) recognized GST-TcdB-F80, the protein used for panning, while 4 of 17 V_{LS} (24%) recognized whole native TcdB from *C. difficile* strain 10463. The phage ELISA also showed none of the 17 V_{LS} bound GST, suggesting our subtractive panning strategy was a good one.

Only the 4 TcdB-binding V_{LS} were selected for soluble expression and further characterization. The 4 V_{LS}, whose sequences are shown in Figure 4.13A, were subcloned into the pSJF2H vector and TG1 *E. coli* cultures yielded 2.7 to 27.2 mg/L (Table 4.1).

4.2.4 Functional characterization of V_{LS}

Purified V_{LS} were subjected to SEC analysis (Figure 4.13B) which revealed that all were non-aggregating and monomeric, suggesting the biophysical properties of the library scaffold (HV_LP324) were maintained in the new antibodies (i.e., they we non-aggregating, soluble, and easily purified). A soluble ELISA on purified V_{LS} illustrated concentration dependent binding to immobilized GST-TcdB-F80 (Figure 4.13C).

SPR analysis and steady-state plots revealed 2 of 4 V_{LS} with mid-nM affinity constants (Figure 4.14, Table 4.1). The K_Ds of clones B4.3 and B5.40 were 237 nM and 318 nM, respectively, which are very strong affinities for human single-domain antibodies isolated from a synthetic library. Interestingly, the amino acid sequences of B4.3 and B5.40

were nearly identical with only 1 residue differing in CDR2, and 2 residues differing in CDR3. Of the 3 different residues, B5.40 acquired Pro/Ser and Pro/Val substitutions. All of the V_L sequences isolated contained a number of proline residues in their CDR regions, an amino acid known for its unordered, structure-breaking properties.

Finally, the V_{LS} were tested *in vitro* for their ability to neutralize TcdB. Just like their V_HH counterparts, the V_{LS} failed to neutralize TcdB-induced cell rounding at concentrations as high as 2.5 μM (data not shown).

Figure 4.13. Structural and functional characterization of TcdB-specific V_L antibodies.
(**A**) Amino acid sequences of the 4 V_LS selected for soluble expression and characterization. CDR regions were defined according to Kabat. (**B**) Size exclusion chromatography (SEC) analysis of purified V_LS revealed all were monomeric and non-aggregating. SEC analysis was performed using a Superdex™ 75 column under the control of an ÄKTA FPLC system. (**C**) ELISA demonstrating the concentration dependent binding of purified V_LS to surface-immobilized TcdB. V_L binding was detected with an anti-His_6 IgG labelled with HRP and the absorbance read at A_{450nm}.

A

	FR1	CDR1	FR2	CDR2	FR3	CDR3	FR4
B4.3	DIQMTQSPSSLSASVGDRVTITC	RASQSISTYLN	WYQQKPGKAPKLLIF	RASRRPS	GVPSRFSGSGSGTDFTLTISNLQPEDFATYYC	GQSEPGPPRT	FGHGTKVTVL
B5.40	DIQMTQSPSSLSASVGDRVTITC	RASQSISTYLN	WYQQKPGKAPKLLIF	RASRRVS	GVPSRFSGSGSGTDFTLTISNLQPEDFATYYC	TQSEPGPSRT	FGHGTKVTVL
B12.51	DIQMTQSPSSLSASVGDRVTITC	KASQGIASRLG	WYQQKPGKAPKLLIF	DASRRAS	GVPSRFSGSGSGTDFTLTISNLQPEDFATYYC	GQFSSI-PRT	FGHGTKVTVL
B17.62	DIQMTQSPSSLSASVGDRVTITC	VASQSIGMGLG	WYQQKPGKAPKLLIF	AASRRPS	GVPSRFSGSGSGTDFTLTISNLQPEDFATYYC	SQRKM-RPFT	FGHGTKVTVL

B

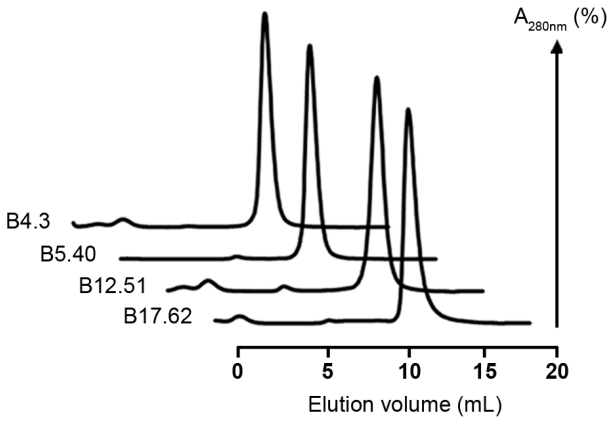

C

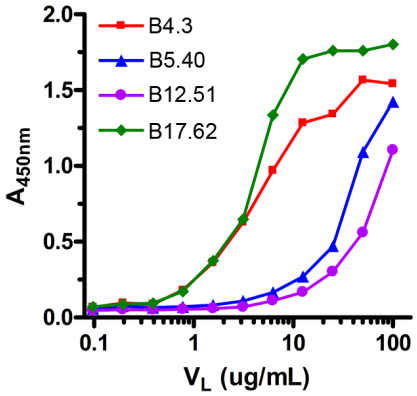

Figure 4.14. V_Ls bind TcdB-F80 with high affinity.
SPR was used to determine the affinity of V_Ls for TcdB-F80. Affinity constants (K_Ds) were determined by steady state analysis. SPR sensorgrams (*left*) and steady state plots (*right*) are shown for B4.3 (**A**), B5.40 (**B**), B12.51 (**C**), and B17.62 (**D**). The ranges of V_L concentrations injected over immobilized TcdB-F80 are shown on each sensorgram. The calculated K_D and R_{max} values are shown on each of the steady state plots.

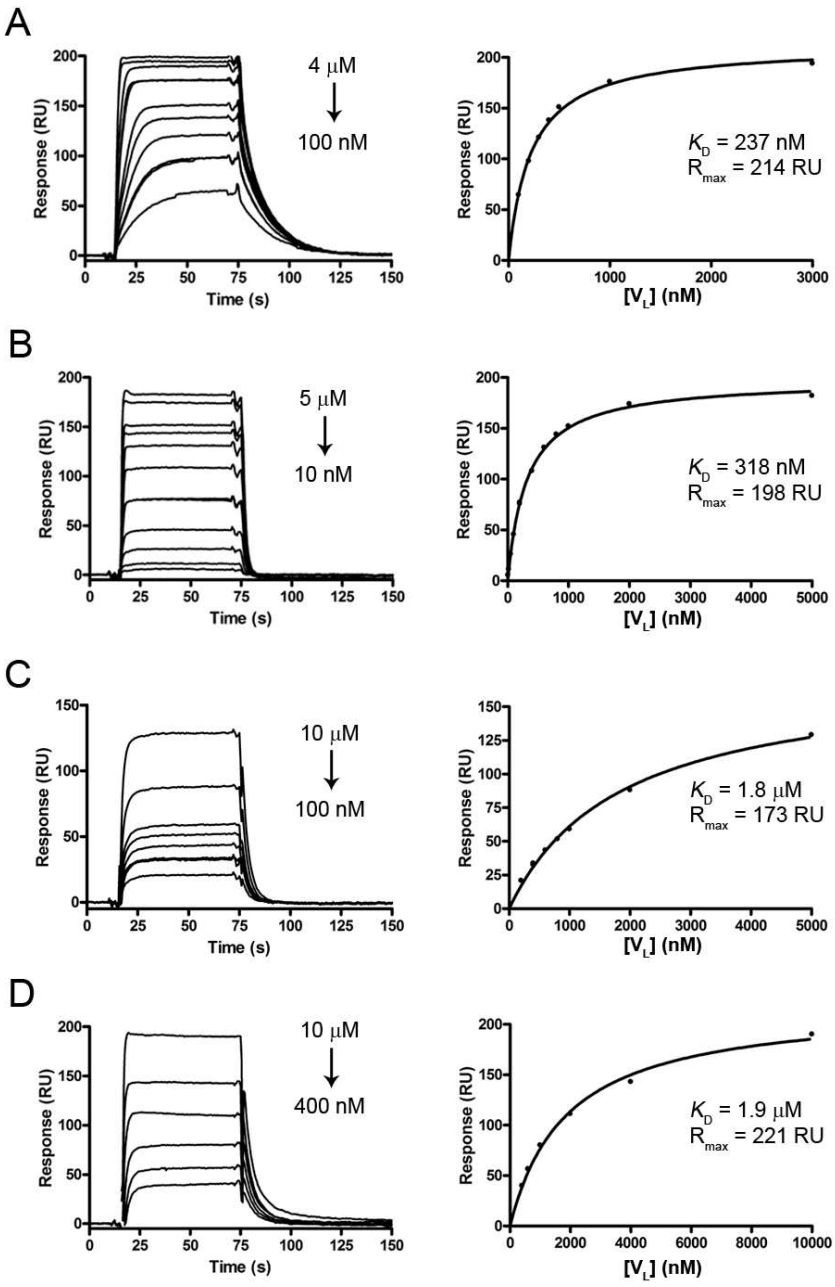
A
4 μM
100 nM
Response (RU)
Time (s)
K_D = 237 nM
R_{max} = 214 RU
[V_L] (nM)
B
5 μM
10 nM
Response (RU)
Time (s)
K_D = 318 nM
R_{max} = 198 RU
[V_L] (nM)
C
10 μM
100 nM
Response (RU)
Time (s)
K_D = 1.8 μM
R_{max} = 173 RU
[V_L] (nM)
D
10 μM
400 nM
Response (RU)
Time (s)
K_D = 1.9 μM
R_{max} = 221 RU
[V_L] (nM)

4.3 Stability engineering of V_HHs

In the following pages, the results from V_HH protein engineering experiments to improve V_HH thermal and proteolytic stability are presented. Specifically, two cysteine residues were introduced into the hydrophobic V_HH core, through mutagenesis of either Ala or Gly and Ile amino acids, and the resulting V_HH mutants were characterized.

4.3.1 Expression and purification of mutant V_HHs

To examine the stabilizing effects of an engineered disulfide bond on llama-derived V_HHs, two cysteine residues were introduced into the hydrophobic core of the six *C. difficile* TcdA-specific V_HHs isolated earlier in this thesis by incorporating $Ala/Gly^{54} \rightarrow Cys^{54}$ and $Ile^{78} \rightarrow Cys^{78}$ point mutations (Figure 4.15A, Figure 4.16). After mutagenesis, soluble V_HHs were extracted from the periplasm of TG1 *E. coli* and purified by IMAC with purified yields ranging from 3 – 12 mg/L of bacterial culture. Non-reducing SDS-PAGE and Western blot analysis of the purified products revealed the mutant V_HHs were of high purity and did not form interdomain disulfide bonds (Figure 4.15B). This is evident by a lack of higher order aggregates (i.e., dimers at ~32 kDa) on the SDS-PAGE gel. On non-reducing SDS-PAGE gels, mutant V_HHs consistently ran slower than their corresponding wild-type V_HHs (Figure 4.15C).

Figure 4.15. Design, purification, and SEC profiles of disulfide bond mutant V_HHs.
(**A**) Representative homology models of a wild-type V_HH A4.2 (*left*) and disulfide bond mutant V_HH A4.2m (*right*) were built on the PDB template 1qd0A (171), sharing 73.4% and 71.8% homology, respectively. Disulfide bonds are shown as red colored spheres in the hydrophobic core of the V_HH domains. (**B**) Non-reducing (NR) SDS-PAGE analysis (*top*) and Western blot (WB) probed with an anti-His_6 IgG (*bottom*) on IMAC-purified mutant V_HHs (top of image, mutant V_HHs A4.2m, A5.1m, A19.2m, A20.1m, A24.1m, and A26.8m). Molecular weight markers are given in kDa. (**C**) Representative SDS-PAGE analysis showing mutant V_HHs run slower than the corresponding wild-type V_HHs under non-reducing conditions. (**D, E**) SEC analysis of wild-type and mutant V_HHs revealed similar size exclusion profiles, indicating the second disulfide bond does not promote the formation of interdomain disulfide-bonds or multimers among mutant V_HHs.

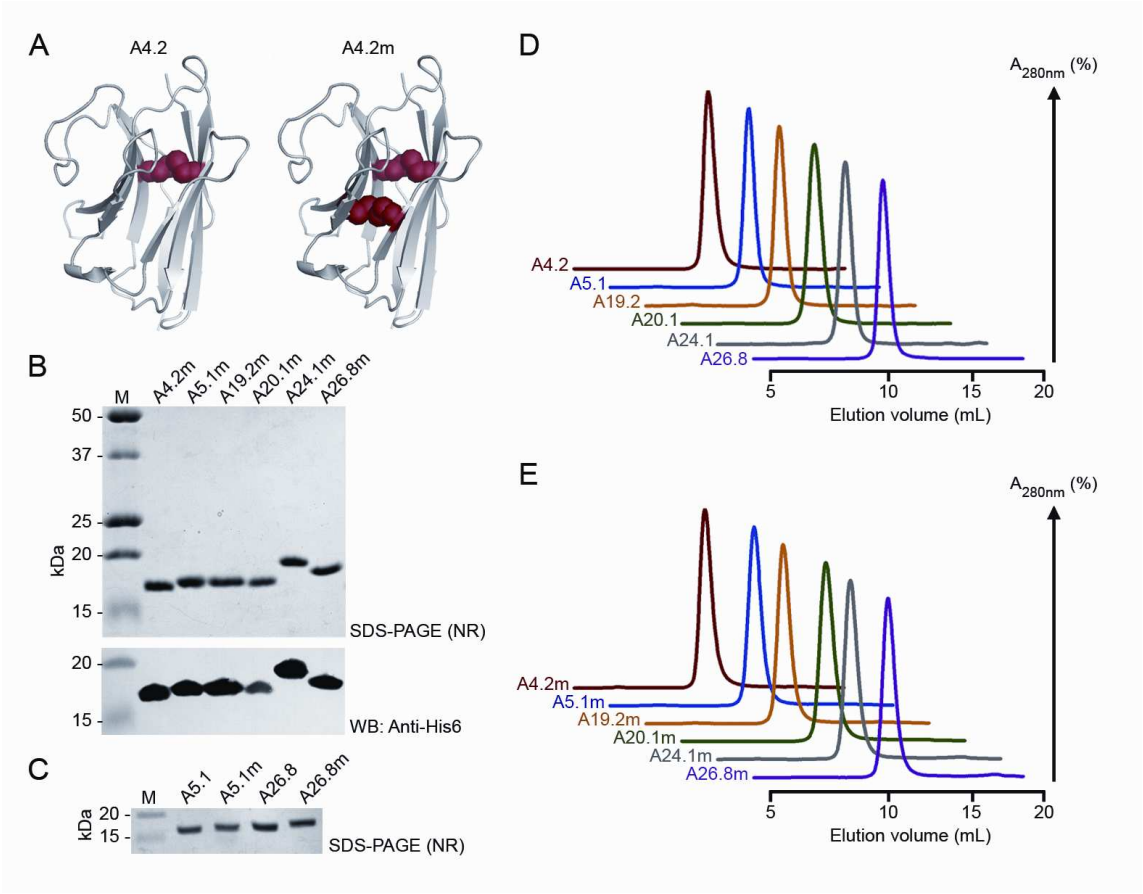
A
A4.2
A4.2m
B
M
A4.2m
A5.1m
A19.2m
A20.1m
A24.1m
A26.8m
50
37
25
20
15
kDa
SDS-PAGE (NR)
20
15
WB: Anti-His6
C
M
A5.1
A5.1m
A26.8
A26.8m
kDa
20
15
SDS-PAGE (NR)
D
A280nm (%)
A4.2
A5.1
A19.2
A20.1
A24.1
A26.8
5
10
15
20
Elution volume (mL)
E
A280nm (%)
A4.2m
A5.1m
A19.2m
A20.1m
A24.1m
A26.8m
5
10
15
20
Elution volume (mL)

Figure 4.16. Alignment and comparison of wild-type (WT) and mutant (Mut) V_HH amino acid sequences.

Wild-type V_HH sequences are shown with a single disulfide bond between Cys^{23} and Cys^{104}. A second disulfide bond was introduced through mutation of Ala^{54}/Gly^{54} and Ile^{78} to Cys^{54} and Cys^{78} in framework region 2 (FR2) and FR3, respectively. Disulfide bonds are shown as black lines. Residues coloured in blue illustrate the disulfide bond-linked peptides identified by nanoRPLC-ESI-MS analysis on CNBr and trypsin digested mutant V_HHs (Fig. 4.17). Amino acid numbering is based on the IMGT system (http://imgt.cines.fr/).

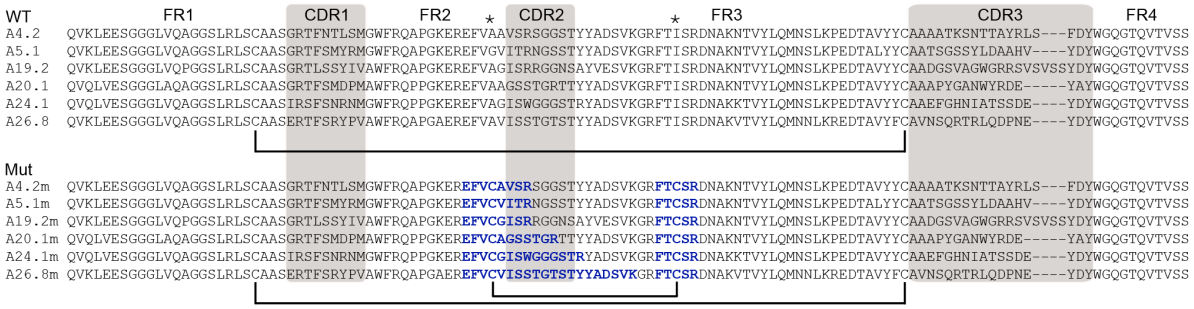
WT
FR1
CDR1
FR2
CDR2
FR3
CDR3
FR4
A4.2 QVKLEESGGGLVQAGGSLRLSCAASGRTFNTLSMGWFRQAPGKEREFVAAVSRSGGSTYYADSVKGRFTISRDNAKNTVYLQMNSLKPEDTAVYYCAAAATKSNTTAYRLS---FDYWGQGTQVTVSS
A5.1 QVKLEESGGGLVQAGGSLRLSCAASGRTFSMYRMGWFRQAPGKEREFVGVITRNGSSTYYADSVKGRFTISRDNAKNTVYLQMNSLKPEDTALYYCAATSGSSYLDAAHV----YDYWGQGTQVTVSS
A19.2 QVKLEESGGGLVQPGGSLRLSCAASGRTLSSYIVAWFRQAPGKEREFVAGISRRGGNSAYVESVKGRFTISRDNAKNTVYLQMNSLKPEDTAVYYCAADGSVAGWGRRSVSVSSYDYWGQGTQVTVSS
A20.1 QVQLVESGGGLAQAGGSLRLSCAASGRTFSMDPMAWFRQPPGKEREFVAAGSSTGRTTYYADSVKGRFTISRDNAKNTVYLQMNSLKPEDTAVYYCAAAPYGANWYRDE-----YAYWGQGTQVTVSS
A24.1 QVQLVESGGGLVQAGGSLRLSCAASIRSFSNRNMGWFRQPPGKEREFVAGISWGGGSTRYADSVKGRFTISRDNAKKTVYLQMNSLKPEDTAVYYCAAEFGHNIATSSDE----YDYWGQGTQVTVSS
A26.8 QVKLEESGGGLVQAGGSLRLSCAASERTFSRYPVAWFRQAPGAEREFVAVISSTGTSTYYADSVKGRFTISRDNAKVTVYLQMNNLKREDTAVYFCAVNSQRTRLQDPNE----YDYWGQGTQVTVSS
Mut
A4.2m QVKLEESGGGLVQAGGSLRLSCAASGRTFNTLSMGWFRQAPGKEREFVCAVSRSGGSTYYADSVKGRFTCSRDNAKNTVYLQMNSLKPEDTAVYYCAAAATKSNTTAYRLS---FDYWGQGTQVTVSS
A5.1m QVKLEESGGGLVQAGGSLRLSCAASGRTFSMYRMGWFRQAPGKEREFVCVITRNGSSTYYADSVKGRFTCSRDNAKNTVYLQMNSLKPEDTALYYCAATSGSSYLDAAHV----YDYWGQGTQVTVSS
A19.2m QVKLEESGGGLVQPGGSLRLSCAASGRTLSSYIVAWFRQAPGKEREFVCGISRRGGNSAYVESVKGRFTCSRDNAKNTVYLQMNSLKPEDTAVYYCAADGSVAGWGRRSVSVSSYDYWGQGTQVTVSS
A20.1m QVQLVESGGGLAQAGGSLRLSCAASGRTFSMDPMAWFRQPPGKEREFVCAGSSTGRTTYYADSVKGRFTCSRDNAKNTVYLQMNSLKPEDTAVYYCAAAPYGANWYRDE-----YAYWGQGTQVTVSS
A24.1m QVQLVESGGGLVQAGGSLRLSCAASIRSFSNRNMGWFRQPPGKEREFVCGISWGGGSTRYADSVKGRFTCSRDNAKKTVYLQMNSLKPEDTAVYYCAAEFGHNIATSSDE----YDYWGQGTQVTVSS
A26.8m QVKLEESGGGLVQAGGSLRLSCAASERTFSRYPVAWFRQAPGAEREFVCVISSTGTSTYYADSVKGRFTCSRDNAKVTVYLQMNNLKREDTAVYFCAVNSQRTRLQDPNE----YDYWGQGTQVTVSS

4.3.2 MS analysis to confirm the formation of the introduced disulfide bond

The molecular weights of all WT and mutant V_HHs were determined to be within 80 ppm mass accuracy using infusion ESI-MS (Table 4.3). Many V_HHs contained N-terminal pyro-glutamic acid (pyro-Q) residues, as shown previously for V_HHs (184). To precisely confirm the presence of the introduced disulfide bond, mutant V_HHs were digested with CNBr and trypsin (Figure 4.17A, B) and their digests subjected to MS^2 analysis. The identification coverage of the mutant V_HHs from the analysis of their CNBr/trypsin digests using nanoRPLC-ESI-MS with DDA was more than 30%. The disulfide-linked peptide ions appeared prominent in the survey scan of the DDA experiment when the proteins were digested with a combination of CNBr and trypsin (Figure 4.17 A, B). Peptide fragments linked by the engineered Cys^{54}-Cys^{78} disulfide bond (shown in blue text in Figure 4.16) were positively identified for all mutant V_HHs by manual de-novo sequencing (Table 4.4). For example, the protein sequence coverage of A5.1m was 43% and a prominent ion at m/z 526.25 (3+) was sequenced as a disulfide-linked peptide EFVCVITR (P1) and FTCSR (P2) as shown (Figure 4.16, Figure 4.17C, Table 4.4). An almost complete disulfide-linked y fragment ion series was observed from one peptide with the other peptide attached as a modification via a disulfide bond, which remains intact under collision induced dissociation (CID) (204).

Table 4.3. Mass determination of wild-type and mutant V_HHs by MS.

V_HH	MW_{for} (Da)[1]	MW_{exp} (Da)[2]	V_HH	MW_{for} (Da)[1]	MW_{exp} (Da)[2]
A4.2	15725.3	15708.0[3]	A4.2m	15745.3	15728.9[3]
A5.1	15800.4	14046.4[3, 4]	A5.1m	15834.5	15818.3[3]
A19.2	16005.6	15989.6[3]	A19.2m	16025.7	16009.5[3]
A20.1	16807.4	16791.1	A20.1m	16628.3	16627.1
A24.1	16904.5	16905.0	A24.1m	16725.4	16725.4
A26.8	16014.6	14261.4[3, 4]	A26.8m	16034.6	16017.2[3]

1. MW_{for}: formula (expected) molecular weight calculated with the Expasy ProtParam tool (http://www.expasy.ch/tools/protparam.html) assuming all cysteine residues were participating in disulfide bond formation.
2. MW_{exp}: experimental molecular weight, determined by infusion-ESI-MS analysis using a Q-TOF™ 2 mass spectrometer.
3. Protein may contain an N-terminal pyro-Q residue, giving an experimental MW 17.0 Da lower than predicted MW.
4. Proteins were detected with the loss of the C-terminal peptide tag LISEEDLNHHHHHH (Average MW: 1754.84 Da).

Table 4.4. Disulfide linkage determination of mutant V_HHs by MS^2 analysis.

V_HH	CNBr / tryptic peptides		MW_{for}	MW_{exp}	ΔMW
A4.2m	EFV**C**AVSR	FT**C**SR	1519.69	1519.70	-0.01
A5.1m	EFV**C**VITR	FT**C**SR	1575.75	1575.76	-0.01
A19.2m	EFV**C**GISR	FT**C**SR	1519.69	1519.64	0.05
A20.1m	EFV**C**AGSSTGR	FT**C**SR	1722.74	1722.84	-0.10
A24.1m	EFV**C**GISWGGGSTR	FT**C**SR	2064.91	2064.98	-0.07
A26.8m	EFV**C**VISSTGTSTYYADSVK	FT**C**SR	2766.25	2766.33	-0.08

Mutant V_HHs were digested with CNBr and trypsin and the peptides analyzed by MS^2. The peptides containing the Cys^{54}-Cys^{78} disulfide linkage are shown with connecting cysteines bolded. A nearly perfect match between MW_{for} and MW_{exp} equates to the presence of the Cys^{54}-Cys^{78} disulfide linkage. MW_{for}: formula (expected) molecular weight (Da); MW_{exp}: experimental molecular weight (Da); ΔMW is calculated: (MW_{for}-MW_{exp}).

Figure 4.17. Disulfide bond formation between residues Cys^{54} and Cys^{78} is confirmed by MS^2.

(**A**) Schematic diagram of mutant V_HH digestion with cyanogen bromide (CNBr) and trypsin before MS^2 analysis. (**B**) V_HHs (3 μg per lane) were subjected to SDS-PAGE under non-reducing (NR) conditions to illustrate near complete digestion with CNBr and trypsin. Untreated A5.1m was added as a control (Ctl). M: molecular weight marker in kDa. (**C**) MaxEnt 3 deconvoluted CID-MS^2 spectrum of the m/z 526.25 (3+) ion of the disulfide-linked peptide EFVCVITR (P1) – FTCSR (P2), encompassing the Cys^{54}-Cys^{78} disulfide bond, from CNBr/trypsin digested A5.1m. Amino acid positions are based on the IMGT numbering system.

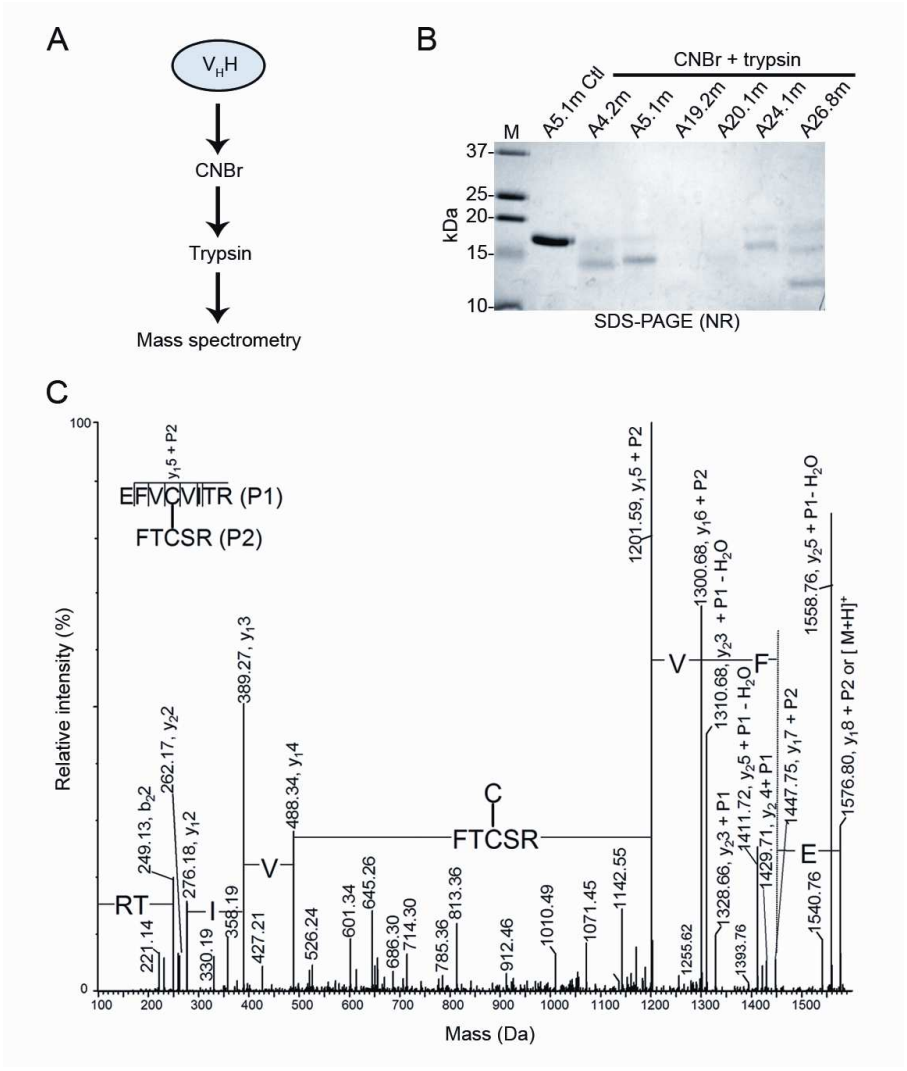
A
V_HH
CNBr
Trypsin
Mass spectrometry
B
CNBr + trypsin
M
A5.1m Ctl
A4.2m
A5.1m
A19.2m
A20.1m
A24.1m
A26.8m
kDa
37
25
20
15
10
SDS-PAGE (NR)
C
Relative intensity (%)
Mass (Da)
EFVCVITR (P1)
FTCSR (P2)
RT
I
V
C
FTCSR
V
F
E
249.13, $b_2$2
262.17, $y_2$2
276.18, $y_1$2
389.27, $y_1$3
488.34, $y_1$4
1201.59, $y_1$5 + P2
1300.68, $y_1$6 + P2
1310.68, $y_2$3 + P1 - H_2O
1328.66, $y_2$3 + P1
1411.72, $y_2$5 + P1 - H_2O
1429.71, $y_2$4+ P1
1447.75, $y_1$7 + P2
1540.76
1558.76, $y_2$5 + P1- H_2O
1576.80, $y_1$8 + P2 or [M+H]+

4.3.3 SEC and SPR analysis to determine V_HH aggregation state and affinity

Analysis of mutant V_HHs on a Superdex™ 75 SEC column produced a single, monomeric peak nearly identical to the profile for wild-type V_HHs (Figure 4.15D, E), confirming that the mutant V_HHs were non-aggregating. SPR analysis revealed specific and high-affinity binding of 4 of 6 mutant V_HHs to TcdA (Figure 4.18, Table 4.1). These four were also the strongest neutralizers (Figure 4.7). Two mutants (A19.2m and A24.1m) exhibited non-specific binding to control cell proteins and as a result specific interaction data could not be generated, even at antibody concentrations as high as 3.2 μM. When compared to their wild-type counterparts, the K_Ds of 3 TcdA-binding mutants were reduced approximately 2 – 6 fold (Table 4.1), while the affinity of one V_HH was relatively unchanged (K_Ds of 24 nM and 20 nM for A4.2 and A4.2m, respectively). The K_D reductions were largely a result of increased k_{off} values and to a much lesser extent influenced by decreased k_{on} values (Figure 4.18B). In general, these data suggest that the Cys^{54}-Cys^{78} disulfide bond may slightly distort the V_HH structure leading to decreases in target binding affinities.

Figure 4.18. Mutant V_HHs retain high affinity binding to TcdA.
(**A**) SPR sensorgrams demonstrating mutant V_HHs retained high affinity binding to immobilized *C. difficile* TcdA. The range of V_HH concentrations used in each experiment is shown. Red lines represent measured interaction data, and black lines represent fitted curves. The kinetic and affinity constants are reported in Table 4.1. Binding of A19.2m and A24.1m to TcdA was non-specific, and the kinetic and affinity constants could not be determined. (**B**) Rate plane plot with iso-affinity diagonals comparing wild-type (red) and mutant V_HHs (blue).

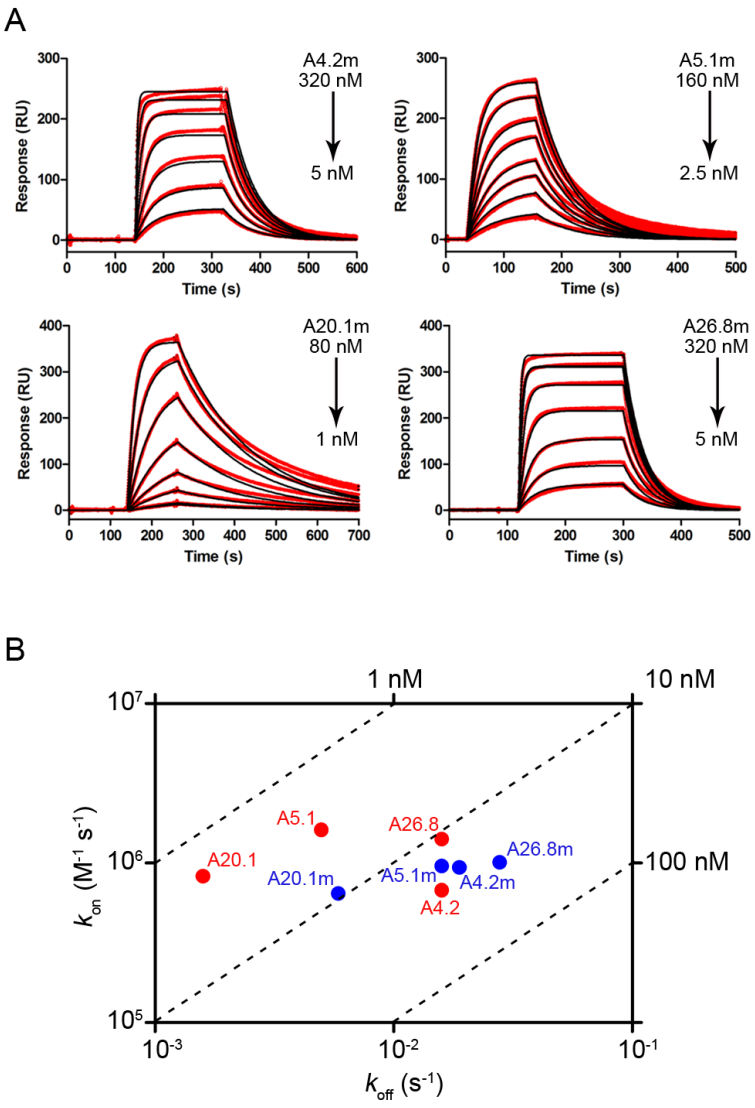
A
A4.2m
320 nM
5 nM
A5.1m
160 nM
2.5 nM
A20.1m
80 nM
1 nM
A26.8m
320 nM
5 nM
Response (RU)
Time (s)
B
1 nM
10 nM
100 nM
A5.1
A26.8
A20.1
A26.8m
A20.1m
A5.1m
A4.2m
A4.2
k_{on} (M^{-1} s^{-1})
k_{off} (s^{-1})

4.3.4 V_HH structural and thermal stability characterization

CD experiments were used to examine V_HH secondary structure, tertiary structure, thermal refolding efficiency, and thermal stability at both neutral and acidic pH. We first examined V_HH secondary structure by far-UV CD (Figure 4.19). Although the overall shape of the far-UV CD spectra from wild-type and mutant V_HH pairs was similar at a given pH, spectra intensity shifts were observed for all wild-type/mutant pairs. In general, peak minima were seen at 216 nm – 218 nm and at 230 nm – 235 nm wavelengths, but in almost all cases, the intensity of the peak at 216 nm – 218 nm was lower (decreased negative ellipticity) for mutant V_HHs. Another prominent feature in the far-UV CD spectra was that mutant V_HHs exhibited a near-UV shift in the peak range of 230 nm – 235 nm. Wild-type V_HHs possessed peak minima around 230 nm – 232 nm whereas mutants displayed peak minima in this region around 232 nm – 235 nm. Interestingly, A4.2/A4.2m, which of all the wild-type/mutant pairs had the most similar CD spectra at neutral pH, also had the same binding affinity for TcdA.

We next examined V_HH tertiary structures with near-UV CD spectroscopy (Figure 4.20). The CD spectra generated in the 250 nm – 340 nm come primarily from aromatic residues within the V_HH, with Phe contributing in the range of 250 nm – 270 nm, Tyr contributing in the range of 270 nm – 290 nm, and Trp contributing in the range of 280 nm – 300 nm. Overall, the near-UV spectra profiles were similar between wild-type and mutant V_HH pairs. Spectra from wild-type and mutant pairs shared nearly identical peak wavelengths, however, between 250 nm to 295 nm, the ellipticity of mutant V_HHs was consistently more negative than wild-type V_HHs. There were also subtle differences in

peaks occurring around 297 nm, with mutant VHHs exhibiting a minor but consistent shift to the right. Three of the four wild-type/mutant pairs (A4.2/A4.2m, A5.1/A5.1m, and A20.1m/A20.1m) produced predominantly negative ellipticity, whereas the A26.8/A26.8m pair remained positive. The contributions of the second disulfide bond cannot be ruled out as a factor which may augment the contribution of aromatic residues to ellipticity (increasing negatively) of the mutants.

We also used far-UV CD to determine the thermal refolding efficiencies (TREs) of wild-type and mutant VHHs at neutral and acid pH. CD scans were performed on 50 μg/mL concentrations of VHHs (3.1 μM) at 25°C (folded), after heating to 96°C (unfolded), and after cooling for 3 h to 25°C (refolded). Thermal refolding efficiencies were determined as the extent to which the CD spectrum of the heated-and-cooled VHH approached that of the folded one. At pH 7.3, the TRE of wild-type VHHs was essentially 100% and significantly higher than mutants (Figure 4.21, $p = 0.018$, unpaired two-tailed *t*-test). Specifically, wild-type VHHs possessed a mean TRE of 99.7% ± 0.2% compared to mutant VHHs with a mean TRE of 90.0% ± 3.4 % (Figure 4.21). The ability of VHHs to refold in acidic conditions was also examined and in general mutants showed higher TREs at pH 2.0 (Figure 4.21, Table 4.5). For example, the mean TRE of wild-type VHHs in acid was 68.2% ± 9.4% compared to 80.6% ± 4.8% for mutant TREs in acid (Figure 4.21). However, these mutant TREs were not significantly higher ($p = 0.268$, unpaired two-tailed *t*-test). It should be noted the TRE of 5 of 6 mutant VHHs increased in acidic conditions, with the TRE of A26.8m reaching 64.7% compared to only 25.8% for A26.8.

Figure 4.19. Far-UV CD analysis of VHHs at neutral and acidic pH.
CD scans (210 nm – 260 nm) were performed at 25°C on VHHs (50 μg/mL) equilibrated for 2 h in 10 mM phosphate buffer (pH 7.3) or 10 mM phosphate buffer + 50 mM HCl (pH 2.0). The spectra represent the mean residue ellipticity of 8 data accumulations collected from 2 independent experiments. Raw data were smoothed using the Jasco software and converted to mean residue ellipticity as described in *Materials and Methods*. Red lines: wild-type VHH at pH 7.3; blue lines: mutant VHH at pH 7.3; green lines: wild-type VHH at pH 2.0; orange lines: mutant VHH at pH 2.0.

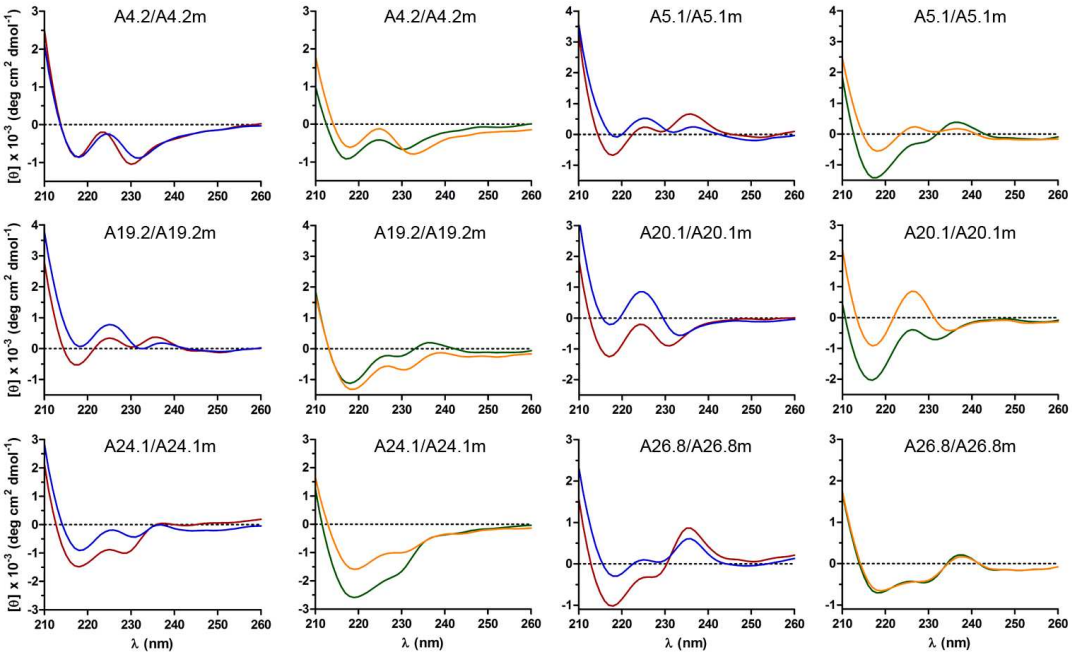
A4.2/A4.2m
A4.2/A4.2m
A5.1/A5.1m
A5.1/A5.1m
A19.2/A19.2m
A19.2/A19.2m
A20.1/A20.1m
A20.1/A20.1m
A24.1/A24.1m
A24.1/A24.1m
A26.8/A26.8m
A26.8/A26.8m
[θ] x 10^-3 (deg cm^2 dmol^-1)
λ (nm)

Figure 4.20. Near-UV CD analysis of V_HHs at neutral and acidic pH.
CD scans (250 nm – 340 nm) were performed at 25°C on V_HHs (250 μg/mL) equilibrated for 2 h in 10 mM phosphate buffer (pH 7.3) or 10 mM phosphate buffer + 50 mM HCl (pH 2.0). The spectra represent the mean residue ellipticity from 8 data accumulations collected from 2 independent experiments. Raw data were smoothed using the Jasco software and converted to mean residue ellipticity as described in *Materials and Methods*. Red lines: wild-type V_HH at pH 7.3; blue lines: mutant V_HH at pH 7.3; green lines: wild-type V_HH at pH 2.0; orange lines: mutant V_HH at pH 2.0.

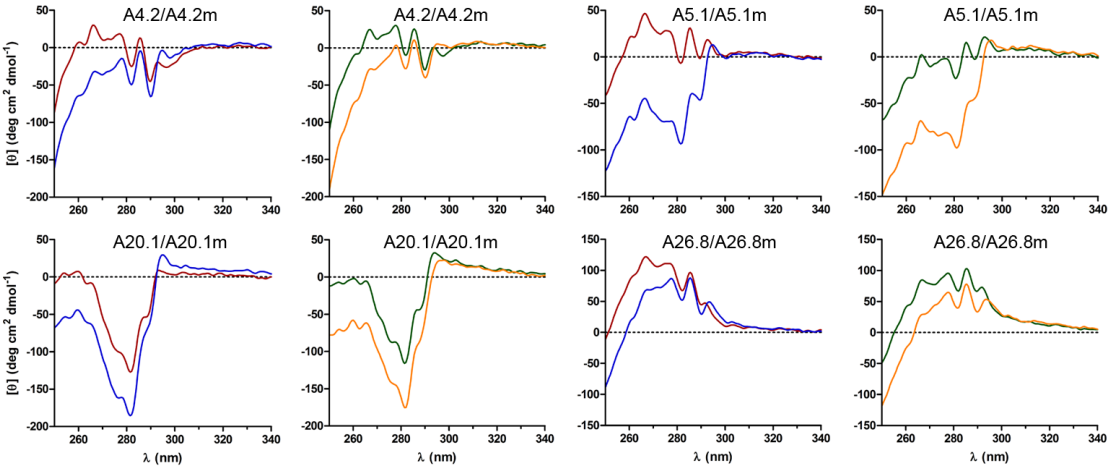
A4.2/A4.2m
A4.2/A4.2m
A5.1/A5.1m
A5.1/A5.1m
A20.1/A20.1m
A20.1/A20.1m
A26.8/A26.8m
A26.8/A26.8m
[θ] (deg cm2 dmol-1)
λ (nm)

Figure 4.21. Analyzing V_HH thermal refolding efficiencies (TREs).
(**A**) Far-UV CD scans were used to determine V_HH TREs under neutral and acidic pH conditions. A5.1 is shown as a representative example. CD spectra were collected on equilibrated V_HHs (50 μg/mL) at 25°C before heat treatment (scan 1, *solid lines*), after exposure to 96°C for 20 min (scan 2, *dotted lines*), and after cooling to 25°C for 3 h (scan 3, *dashed lines*). The scans that are shown are an average of 4 data accumulations. (**B**) Summary of TREs at pH 7.3 and pH 2.0, calculated using Equation 3 in *Materials and Methods* and following the changes in ellipticity at 215 nm. Dots represent the mean TRE of individual V_HHs from two independent experiments with 4 data accumulations in each experiment. Bars represent the mean TRE of each group of V_HHs.

A

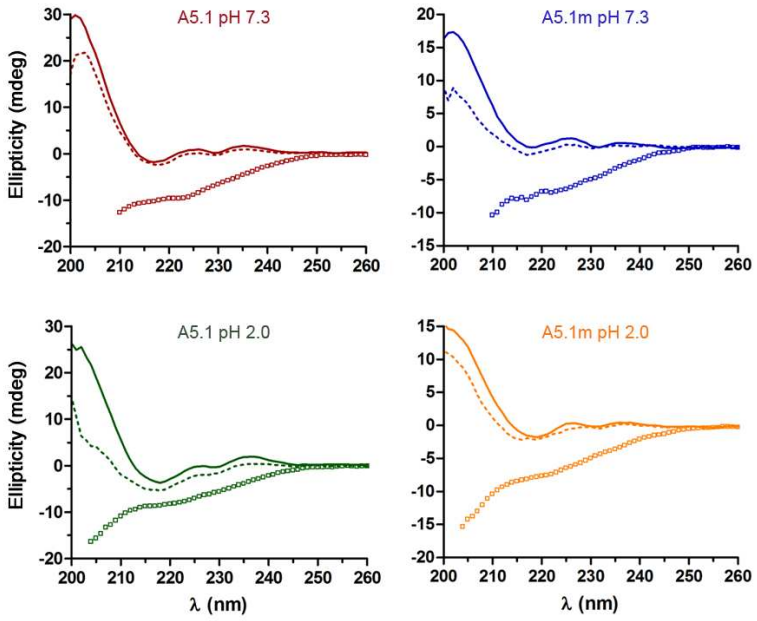
A5.1 pH 7.3
A5.1m pH 7.3
A5.1 pH 2.0
A5.1m pH 2.0
Ellipticity (mdeg)
λ (nm)

B

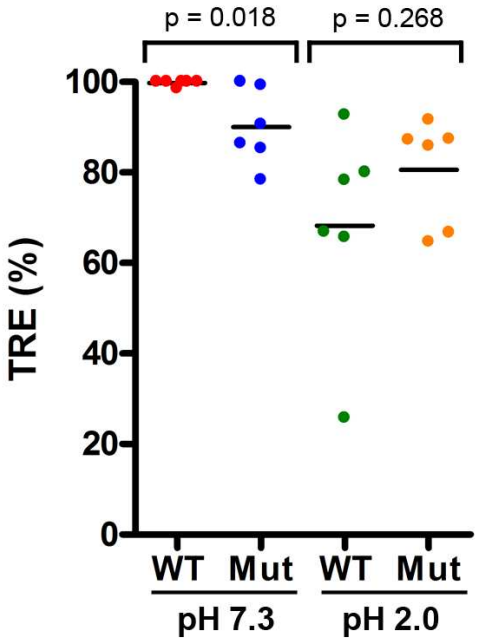
p = 0.018
p = 0.268
TRE (%)
WT
Mut
WT
Mut
pH 7.3
pH 2.0

Table 4.5. Thermal refolding efficiencies (TREs) of wild-type and mutant V_HHs at pH 2.0.

V_HH	TRE (%)	V_HH	TRE (%)
A4.2	80.0 ± 3.8	A4.2m	87.4 ± 1.6
A5.1	66.9 ± 4.2	A5.1m	87.2 ± 3.1
A19.2	78.3 ± 4.9	A19.2m	91.6 ± 1.4
A20.1	65.7 ± 2.5	A20.1m	85.9 ± 2.2
A24.1	92.7 ± 0.6	A24.1m	66.7 ± 0.3
A26.8	25.8 ± 17.6	A26.8m	64.7 ± 2.2

TRE (%) ± SEM (n = 8).

Finally, temperature-induced unfolding experiments were conducted in order to determine V_HH T_ms and T_{onset}s by following changes in V_HH ellipticity at 215 nm (Figure 4.22, Figure 4.23, Table 4.6, Table 4.7). The T_{onset} termperature is defined as the temperature at which 5% of the V_HH domain is unfolded. All V_HHs exhibited sigmoidal melting curves, indicative of cooperative unfolding of a protein that exists in either a folded or unfolded state. The wild-type V_HHs already have high T_ms (as high as 84.7°C) - significantly higher than those reported for other V_HHs (37). At neutral pH, all mutant V_HHs had significantly higher thermal unfolding midpoint temperatures ($p = 0.031$, unpaired two-tailed *t*-test) than their wild-type V_HH counterparts. The T_m values of mutants ranged from 78.8°C to 93.6°C, with one mutant, A5.1m, having a T_m 11.6°C higher than wild-type (A5.1). The increase in mutant V_HH T_ms relative to wild-type ranged from 3.7°C to 11.6°C. Overall, at neutral pH, the mean T_m ± SEM was 76.2°C ± 1.8°C and 83.6°C ± 2.3°C for wild-type and mutant V_HHs, respectively (Figure 4.23A). These findings are in agreement with previous reports that showed significant increases in the T_ms of disulfide bond engineered V_HHs (20, 57, 159). In a second series of experiments, temperature-induced unfolding was conducted at pH 2.0 by

once again following VHH ellipticity changes at 215 nm (Figure 4.22, Figure 4.23A, Table 4.6). At acidic pH a considerable reduction in T_m was observed for both wild-type (22.1°C to 32.4°C) and mutant (23.7°C to 31.2°C) VHHs when compared to the T_m values recorded at pH 7.3. However, in acidic pH the T_m of all six mutants was still significantly higher than wild-type VHHs ($p = 0.002$, unpaired two-tailed *t*-test). In acid, the increase in mutant VHH T_ms relative to wild-type ranged from 2.1°C to 11.6°C, which is a nearly identical spread in temperature increases to that seen at neutral pH. Overall, at pH 2.0, the mean T_m ± SEM was 49.3°C ± 1.2°C and 56.6°C ± 1.2°C for wild-type and mutant VHHs, respectively (Figure 4.23A). Interestingly, the highest T_m gains at both pHs were seen in the case of the four strongest neutralizers. The T_m differences between wild-type/mutant pairs are more significant at acidic pH than neutral pH. Taken together, these results (Table 4.6, Figure 4.22, Figure 4.23) suggest the Cys^{54}-Cys^{78} disulfide bond may stabilize the VHHs from acid-induced denaturation. Using our thermal unfolding curves, we also identified VHH T_{onset} temperatures, the temperature at which 5% of the VHH was unfolded (Figure 4.22, Table 4.7). The T_{onset} of mutant VHHs was significantly higher than wild-type VHHs at both neutral and acidic pH ($p = 0.027$ and $p = 0.006$, respectively, unpaired two-tailed *t*-test). The T_{onset} differences between wild-type/mutant pairs were more significant at acidic pH than neutral pH. At pH 7.3, the mean T_{onset} ± SEM was 68.9°C ± 1.8°C and 74.9°C ± 1.5°C for wild-type and mutant VHHs, respectively. At pH 2.0, the mean T_{onset} ± SEM was 41.2°C ± 1.3°C and 47.3°C ± 1.3°C for wild-type and mutant VHHs, respectively. Therefore, the lowest T_{onset} for the mutants was 45.0°C, whereas two of the wild-type VHHs (A5.1, A20.1) already had T_{onset}s of ~37°C at pH 2.0 (physiological stomach conditions).

Figure 4.22. V_HH thermal unfolding curves.
Thermal unfolding of wild-type and mutant V_HHs (50 μg/mL) at pH 7.3 (10 mM sodium phosphate buffer) and pH 2.0 (10 mM sodium phosphate buffer + 50 mM HCl) were followed at 215 nm to identify the thermal unfolding midpoint temperature (T_m). The T_m was determined for each curve by Boltzmann non-linear curve fitting analysis in GraphPad Prism and reported in Table 4.6. Red lines: wild-type V_HH at pH 7.3; blue lines: mutant V_HH at pH 7.3; green lines: wild-type V_HH at pH 2.0; orange lines: mutant V_HH at pH 2.0.

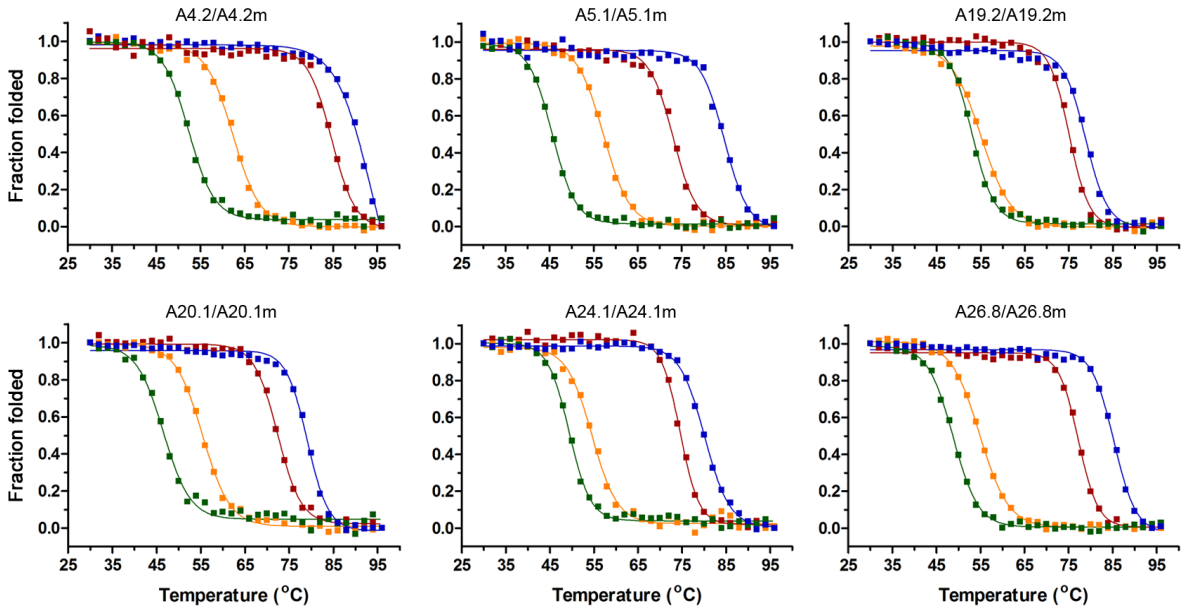
A4.2/A4.2m
A5.1/A5.1m
A19.2/A19.2m
A20.1/A20.1m
A24.1/A24.1m
A26.8/A26.8m
Fraction folded
Temperature (°C)
1.0
0.8
0.6
0.4
0.2
0.0
25 35 45 55 65 75 85 95

Figure 4.23. Mutant (Mut) V_HH T_ms and T_{onset}s are significantly greater than wild-type (WT) T_ms and T_{onset}s.

V_HH thermal unfolding midpoint temperatures (T_ms) were determined using CD spectrometry by following antibody unfolding (50 μg/mL) at 215 nm in 10 mM phosphate buffer +/- 50 mM HCl. Dots represent individual V_HHs and the black bars represent the mean T_m. (**A**) Summary of V_HH T_ms. (**B**) Summary of V_HH T_{onset} temperatures. The T_{onset} is defined as the temperature at which 5% of the V_HH is unfolded. P-values were determined using the unpaired two-tailed *t*-test.

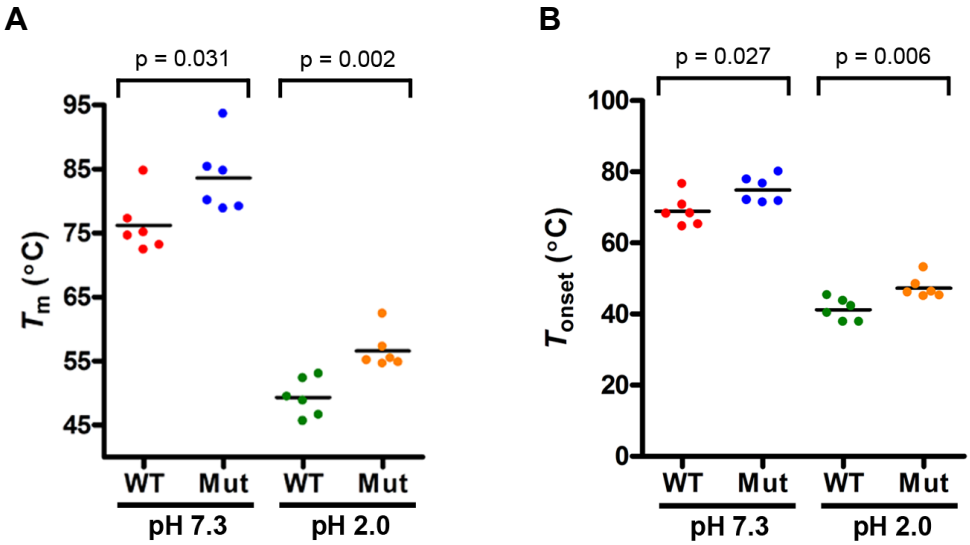
A
p = 0.031
p = 0.002
95
85
75
65
55
45
T_m (°C)
WT
Mut
WT
Mut
pH 7.3
pH 2.0
B
p = 0.027
p = 0.006
100
80
60
40
20
0
T_{onset} (°C)
WT
Mut
WT
Mut
pH 7.3
pH 2.0

Table 4.6. Thermal unfolding midpoint temperatures (T_ms) of wild-type and mutant V_HHs.

V_HH	T_m (°C) at pH 7.3			T_m (°C) at pH 2.0		
	Wild-type	**Mutant**	**ΔT_m**	**Wild-type**	**Mutant**	**ΔT_m**
A4.2/ A4.2m	84.7	93.6	8.9	52.3	62.4	10.1
A5.1/ A5.1m	73.1	84.7	11.6	45.6	57.2	11.6
A19.2/ A19.2m	75.1	78.8	3.7	53.0	55.1	2.1
A20.1/ A20.1m	72.4	79.1	6.7	46.6	55.4	8.8
A24.1/ A24.1m	74.6	80.1	5.5	49.4	54.6	5.2
A26.8/ A26.8m	77.2	85.3	8.1	48.8	54.8	6.0

Table 4.7. Onset temperatures (T_{onset}s) of wild-type and mutant V_HHs.

V_HH	T_{onset} (°C) at pH 7.3		T_{onset} (°C) at pH 2.0	
	Wild-type	**Mutant**	**Wild-type**	**Mutant**
A4.2/ A4.2m	76.5	80.0	43.7	53.1
A5.1/ A5.1m	65.2	76.6	37.8	48.4
A19.2/ A19.2m	68.3	71.4	45.3	45.0
A20.1/ A20.1m	64.6	72.0	37.8	46.3
A24.1/ A24.1m	68.2	71.7	42.2	46.0
A26.8/ A26.8m	70.7	77.8	40.3	45.2

4.3.5 Protease digestion assays

Proteins traveling through the GI tract encounter low pH and digestive enzymes in the stomach. We therefore asked if the Cys^{54}-Cys^{78} disulfide bond improved V_HH resistance to proteolytic degradation. We compared the effects of the major GI proteases pepsin, trypsin, and chymotrypsin on wild-type and mutant V_HHs through SDS-PAGE and MS analysis. Proteases were used individually, in all cases. Initially, protease concentrations of 0.1 μg/mL, 1 μg/mL, 10 μg/mL, and 100 μg/mL were explored. When the lowest concentrations of proteases (0.1 μg/mL and 1 μg/mL) were used in digestion reactions, wild-

type and mutant V_HHs appeared similar to undigested controls on SDS-PAGE (data not shown). Similarly, V_HHs were only moderately susceptible to protease degradation at 10 μg/mL (data not shown). In order to see clear differences in the proteolytic susceptibility of wild-type and mutant V_HHs, all remaining digestions were performed at protease concentrations of 100 μg/mL. SDS-PAGE analysis of pepsin-digested wild-type and mutant V_HHs showed a reduction in V_HH size from ~16 kDa (control) to either ~14 kDa (for A5.1m mutant V_HH), or complete digestion (for A5.1 wild-type) to smaller fragments (Figure 4.24A). The band at ~14 kDa routinely appeared in digestions with each of the proteases. Similar to V_H protease digestion studies (184), MS mass analysis on the ~14 kDa products revealed cleavage at various positions within the V_HH C-terminal c-Myc epitope tag. Loss of the epitope tag corresponded to reductions of 1641.7 Da, 1754.8 Da, and 1641.7 Da for pepsin, trypsin, and chymotrypsin digested V_HHs, respectively (data not shown).

Overall, significant increases in pepsin resistance were found for all mutant V_HHs compared to wild-type V_HHs as determined by Mann-Whitney U test ($p = 0.026$) (Figure 4.24B, Figure 4.25, Table 4.8). The increase in mutant V_HH pepsin resistance relative to wild-type ranged from almost 4.5% to 63% (Table 4.8). For example, A5.1 was completely degraded after incubation with pepsin, while nearly 50% of A5.1m remained intact (Figure 4.24A, B). The biggest increase in pepsin resistance was found for A4.2m, where an almost 63% increase in intact V_HH structure was found relative to A4.2. Interestingly, A4.2m also had the highest T_m and T_{onset} at pH 2.0 (Table 4.6, Table 4.7), the same pH at which the pepsin digestions were undertaken. Increases in mutant V_HH resistance to chymotrypsin were not as universal (Figure 4.25, Figure 4.26, Table 4.8), but nonetheless, 4 of 6 mutant

VHHs showed increased resistance to chymotrypsin, with significant increases found in clones A5.1m, A24.1m, and A26.8m ($p < 0.05$) compared to their wild-type counterparts. No statistical differences were found between trypsin digested wild-type and mutant VHHs (Figure 4.25, Figure 4.26, Table 4.8), except for A4.2m, where trypsin resistance was actually reduced from almost 36% in the wild-type VHH to almost 5% in the mutant. Both the wild-type and mutant versions of A19.2 and A26.8 were very susceptible to trypsin degradation.

Table 4.8. Protease resistance profiles of wild-type and mutant VHHs to the major GI proteases.

VHH	Pepsin resistance (%)		Trypsin resistance (%)		Chymotrypsin resistance (%)	
	Wild-type	Mutant	Wild-type	Mutant	Wild-type	Mutant
A4.2	11.08 ± 1.88	73.87 ± 7.23	35.72 ± 7.08	4.80 ± 0.61	13.60 ± 6.50	3.18 ± 1.10
A5.1	0.53 ± 0.15	46.63 ± 1.99	96.23 ± 7.09	83.30 ± 4.96	14.03 ± 3.15	27.00 ± 4.05
A19.2	30.37 ± 3.16	52.27 ± 0.32	0.73 ± 0.73	0.27 ± 0.27	8.30 ± 1.14	0.18 ± 0.10
A20.1	0.68 ± 0.68	5.04 ± 0.76	72.77 ± 4.85	82.80 ± 1.97	10.17 ± 1.85	16.17 ± 5.26
A24.1	10.45 ± 2.39	36.02 ± 1.11	75.03 ± 9.63	66.50 ± 3.58	22.03 ± 5.01	43.80 ± 2.08
A26.8	3.17 ± 1.24	24.56 ± 1.45	2.03 ± 2.03	4.10 ± 1.27	8.40 ± 1.23	40.83 ± 8.81

All VHH digestions were performed at 37°C for 1 h in the presence of 100 μg/mL protease. Resistance values were obtained by comparing the intensity of protease-digested VHHs relative to untreated controls using SDS-PAGE and imaging software. *See* Figure 4.24A as an example. Values represent the mean ± SEM of three independent experiments.

Table 4.9. Theoretical number of protease cleavable sites[1].

VHH	Pepsin[2]	Chymotrypsin[3]	Trypsin
A4.2/ A4.2m	41-3-0-6-(9)	32-2-0-4-(6)	14-1-1-2-(4)
A5.1/ A5.1m	43-3-0-7-(10)	34-2-0-5-(7)	13-2-1-0-(3)
A19.2/ A19.2m	39-3-0-6-(9)	29-2-0-3-(5)	15-1-2-2-(5)
A20.1/ A20.1m	40-1-0-8-(9)	34-2-0-5-(7)	12-1-1-1-(3)
A24.1/ A24.1m	37-1-2-6-(9)	32-1-1-4-(6)	13-2-0-0-(2)
A26.8/ A26.8m	40-2-0-5-(7)	29-1-0-3-(4)	15-2-0-2-(4)

Table notation: VHH Total-CDR1-CDR2-CDR3-(CDR sum).

1. Expasy PeptideCutter (http://www.expasy.ch/tools/peptidecutter/) program was used.
2. Selected for "pH > 1.3".
3. Selected for "low specificity".

Figure 4.24. Mutant VHHs are resistant to pepsin degradation.
(**A**) Representative SDS-PAGE analysis showing the separation of A5.1 and A5.1m VHHs after digestion with various concentrations of pepsin (increasing from left to right: 1 μg/mL, 10 μg/mL and 100 μg/mL) at pH 2.0 and 37°C for 1 h. Control VHHs (Ctl) were incubated under the same conditions without pepsin. Three micrograms of protein was loaded per lane. Bands appearing ~2 kDa below the full-length VHH ("VHH + tag") were identified by MS (data not shown) as VHHs cleaved within the C-terminal c-Myc tag ("VHH – tag"), as shown before with protease-digested human VHs (184). (**B**) Summary of VHH resistance profiles to 100 μg/mL pepsin treatment. Resistance values were obtained by densitometric measurements of pepsin-treated VHHs relative to controls (as in **A**). Error bars represent the SEM obtained from 3 independent digestions for each VHH. (**C**) SPR analysis (*bottom*) on mutant VHHs digested with pepsin (100 μg/mL, 1 h, 37°C). The pepsin-treated VHHs retained their ability to bind surface-immobilized TcdA. SDS-PAGE (*top*) showing untreated (lanes 1, 3, 5, 7) and pepsin-digested (lanes 2, 4, 6, 8) VHHs used for SPR. The contents of lanes 1 thru 8 are described in the box in *C*. Normalized k_{off}s for pepsin treated VHHs were similar to the k_{off} of untreated controls (*box* and *see* Table 4.1). M: molecular weight markers in kDa; WT: wild-type VHH; Mut: mutant VHH; P: pepsin; R: reducing SDS-PAGE conditions.

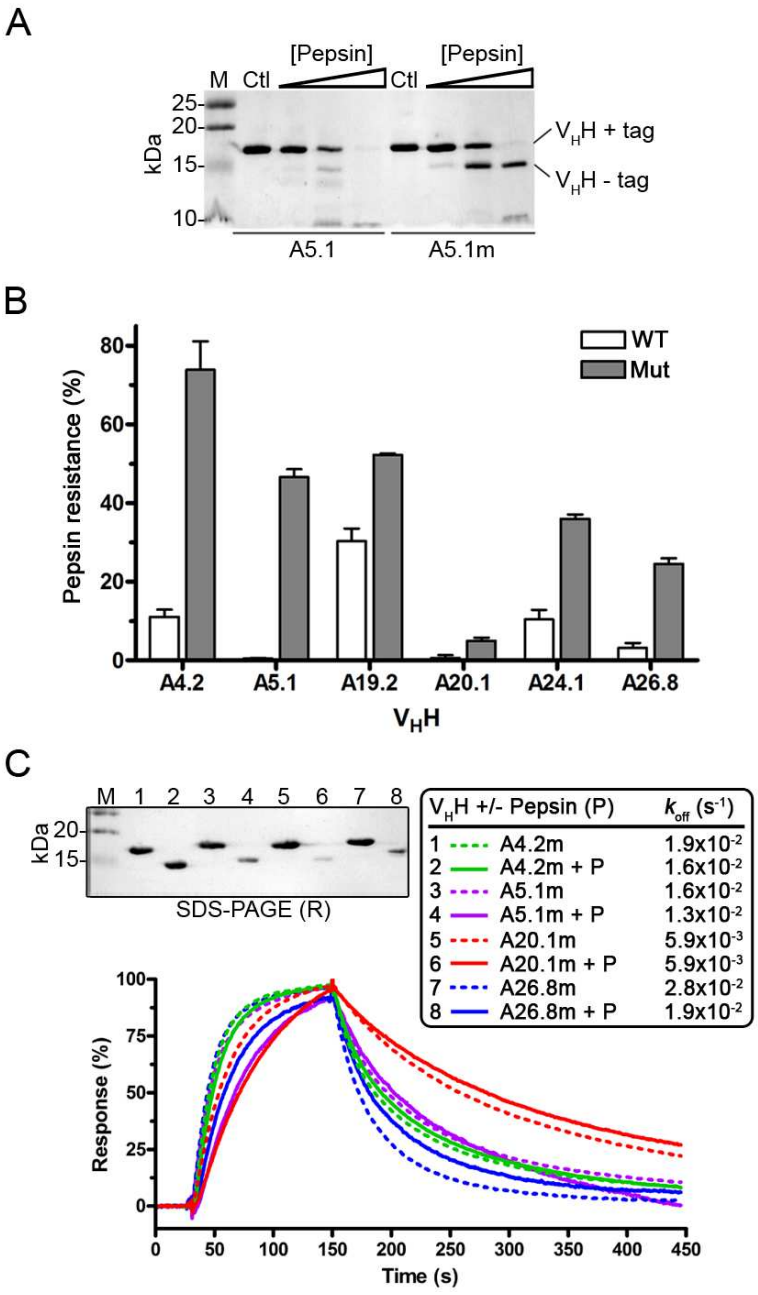
A
[Pepsin]
[Pepsin]
M
Ctl
Ctl
25
20
15
10
kDa
V_HH + tag
V_HH - tag
A5.1
A5.1m
B
WT
Mut
Pepsin resistance (%)
80
60
40
20
0
A4.2
A5.1
A19.2
A20.1
A24.1
A26.8
V_HH
C
M 1 2 3 4 5 6 7 8
kDa
20
15
SDS-PAGE (R)
V_HH +/- Pepsin (P)
k_{off} (s^{-1})
1 A4.2m 1.9x10-2
2 A4.2m + P 1.6x10-2
3 A5.1m 1.6x10-2
4 A5.1m + P 1.3x10-2
5 A20.1m 5.9x10-3
6 A20.1m + P 5.9x10-3
7 A26.8m 2.8x10-2
8 A26.8m + P 1.9x10-2
Response (%)
100
75
50
25
0
0
50
100
150
200
250
300
350
400
450
Time (s)

Figure 4.25. Summary of V_HH resistance profiles to pepsin, trypsin, and chymotrypsin. V_HH resistance to the major GI proteases was determined by proteolytic digestion (100 μg/mL protease, 37°C, 1 h) and SDS-PAGE densitometry analysis. Dots represent the mean (n = 3) protease resistance profile of each V_HH relative to undigested controls and the black bars represent the median resistance of each group. P-values were determined using the unpaired two-tailed Mann-Whitney *U* test. Chymo: chymotrypsin.

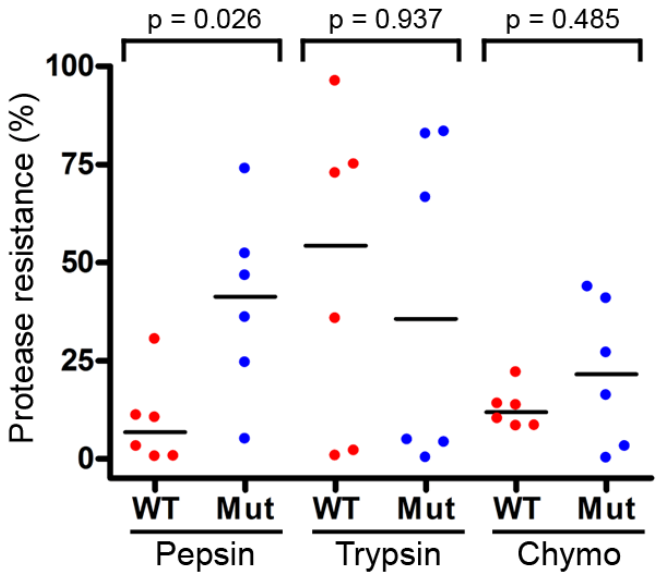
p = 0.026
p = 0.937
p = 0.485
Protease resistance (%)
100
75
50
25
0
WT
Mut
WT
Mut
WT
Mut
Pepsin
Trypsin
Chymo

Figure 4.26. V_HH resistance profiles to trypsin and chymotrypsin.
Wild-type (WT) and mutant (Mut) V_HHs were digested with 100 μg/mL of trypsin (**A**) or chymotrypsin (**B**) for 1 h at 37°C and separated by SDS-PAGE. Resistance values were calculated as in Figure 4.24.

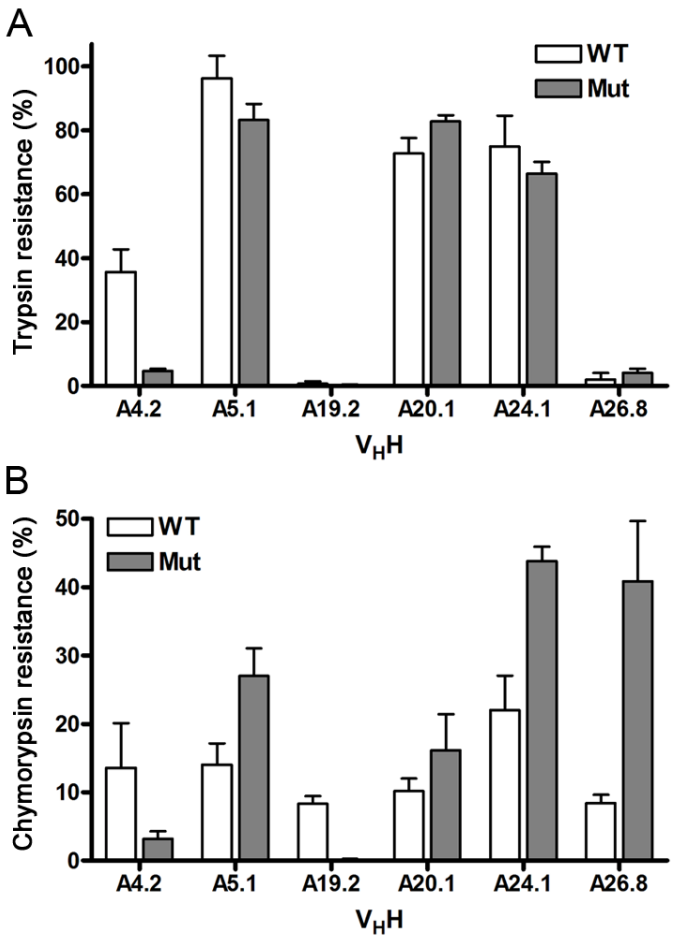
A
WT
Mut
Trypsin resistance (%)
100
80
60
40
20
0
A4.2
A5.1
A19.2
A20.1
A24.1
A26.8
V_HH
B
WT
Mut
Chymorypsin resistance (%)
50
40
30
20
10
0
A4.2
A5.1
A19.2
A20.1
A24.1
A26.8
V_HH

A correlation was observed between V_HH pepsin resistance and T_ms at pH 2.0 (r^2 = 0.735, Figure 4.27A). Thus, while wild type V_HHs with lower T_ms occupied the low protease resistance region of the graph, the mutants with higher T_ms occupied the high protease resistance region of the graph. There was also a moderate correlation between V_HH pepsin resistance and T_ms at pH 7.3 (r^2 = 0.500, data not shown). No correlation was evident between V_HH trypsin resistance and T_ms at pH 7.3 or pH 2.0 (r^2 = 0.138 and r^2 = 0.138, respectively) or between V_HH chymotrypsin resistance and T_ms at pH 7.3 or pH 2.0 (r^2 = 0.012 and r^2 = 0.004, respectively). In addition, a strong correlation between wild-type V_HH pepsin resistance and wild-type V_HH T_{onset} at pH 2.0 was noted (r^2 = 0.975, Figure 4.27B, Table 4.7). No correlation was evident between mutant V_HH pepsin resistance and mutant V_HH T_{onset} at pH 2.0 (r^2 = 0.191), presumably because mutant V_HH T_{onset} temperatures were much higher than the temperature in which pepsin digestions were performed (37°C). Interestingly, we also noted a correlation between V_HH trypsin resistance and the theoretical number of trypsin cleavage sites located within the whole V_HH (r^2 = 0.822) or located within the V_HH CDR (r^2 = 0.681) regions (Table 4.9, Figure 4.28). No correlation was found between V_HH pepsin or chymotrypsin resistance and the theoretical number of pepsin or chymotrypsin cleavage sites, respectively.

The ability of pepsin-treated mutants (A4.2m, A5.1m, A20.1m, and A26.8m) to bind TcdA was evaluated by SPR. SPR confirmed the mutants ("V_HH – tag") retained TcdA binding as their k_{off} values (Figure 4.24C) were essentially the same as those of untreated controls (Table 4.1, Figure 4.24C). SPR analysis on pepsin-digested wild-type V_HHs could not be performed since these V_HHs were significantly degraded by pepsin. These

experiments highlight the profound impact a second disulfide bond in the hydrophobic core has on VHH conformational stability at low pH and resistance to proteolytic degradation by pepsin.

4.3.6 Toxin neutralization assay

Mutant VHHs retained their ability to neutralize the cytotoxic effects of TcdA on monolayers of fibroblast cells. Comparison of the neutralization capacity of pooled mixtures (1000 nM total) of wild-type and mutant VHHs revealed mutants performed nearly as well as wild-type at reducing TcdA-mediated cell rounding (Figure 4.29). Given that 3 of 4 mutants showed weaker affinity for TcdA the reduction in neutralizing capacity relative to wild-type VHHs is not unexpected.

Figure 4.27. Correlation between V_HH pepsin resistance and thermal stability at acidic pH.

(**A**) Linear regression between V_HH pepsin resistance and V_HH T_m at pH 2.0. Red and blue boxes show the wild-type and mutant V_HHs, respectively. Linear regression analysis gave a correlation coefficient of $r^2 = 0.735$ and a significantly non-zero slope of the line ($p = 0.0004$). (**B**) Linear regression between wild-type V_HH pepsin resistance and wild-type V_HH T_{onset} at pH 2.0. The T_{onset} is defined as the temperature at which 5% of the V_HH is unfolded. Linear regression analysis gave a correlation coefficient of $r^2 = 0.975$ and a significantly non-zero slope of the line ($p = 0.0002$).

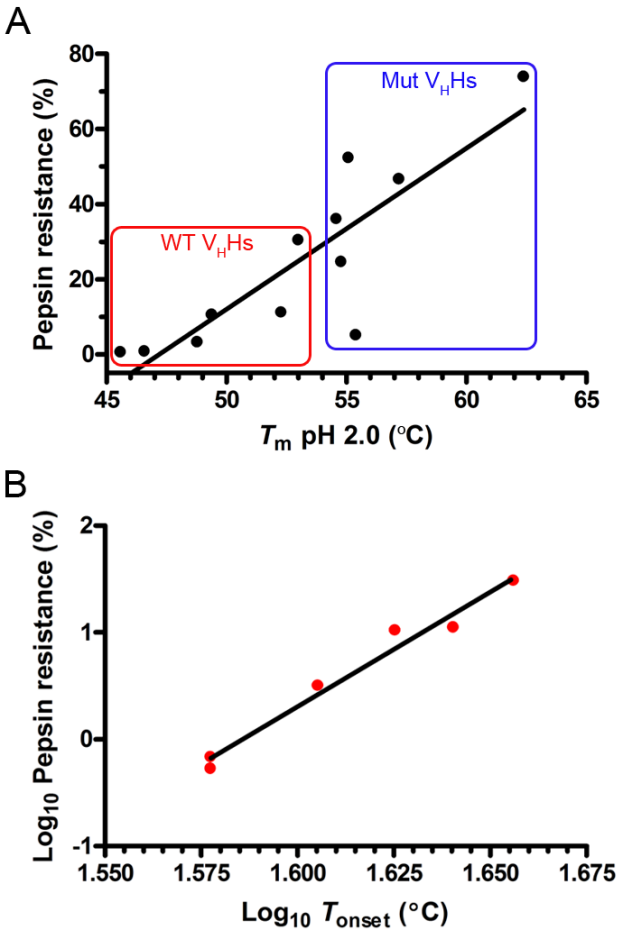
A
Pepsin resistance (%)
80
60
40
20
0
45
50
55
60
65
T_m pH 2.0 (°C)
Mut V_HHs
WT V_HHs
B
Log_{10} Pepsin resistance (%)
2
1
0
-1
1.550
1.575
1.600
1.625
1.650
1.675
Log_{10} T_{onset} (°C)

Figure 4.28. Correlation between V_HH protease resistance and the number of theoretical proteolytic cleavage sites.

Linear regression between V_HH protease resistance and the number of theoretical cleavage sites within the whole V_HH ("Total sites") or within the IMGT-defined CDR regions ("CDR sites") is shown. Wild-type and mutant V_HH protease resistance values were combined for each protease. The number of protease cleavage sites was determined as in Table 4.9. Linear regression analysis was used to analyze the correlation coefficient (r^2) and significantly non-zero slope of the line (p) in each graph.

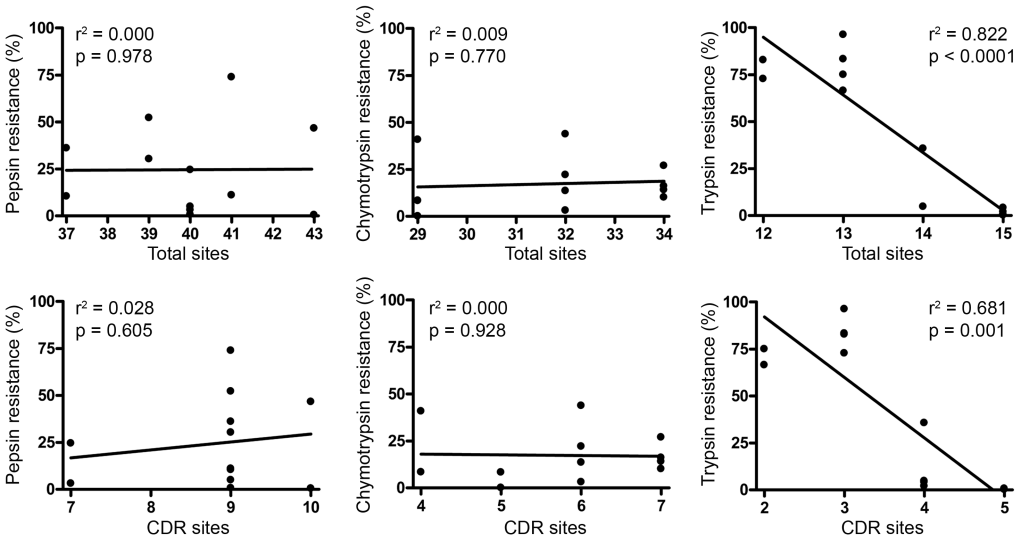
Pepsin resistance (%)
r² = 0.000
p = 0.978
Total sites
Chymotrypsin resistance (%)
r² = 0.009
p = 0.770
Total sites
Trypsin resistance (%)
r² = 0.822
p < 0.0001
Total sites
Pepsin resistance (%)
r² = 0.028
p = 0.605
CDR sites
Chymotrypsin resistance (%)
r² = 0.000
p = 0.928
CDR sites
Trypsin resistance (%)
r² = 0.681
p = 0.001
CDR sites

Figure 4.29. Mutant V_HHs retain TcdA-neutralizing capacity.
Confluent monolayers of IMR-90 human lung fibroblasts were incubated with TcdA (100 ng/mL) or TcdA + V_HHs (1000 nM) for 24 h, and the percentage of cells rounded was scored using a light microscope from 0% to 100%. V_HHs (wild-type (WT) or mutant (Mut)) were added as pooled mixtures of A4.2, A5.1, A20.1, and A26.8 (250 nM each) or A4.2m, A5.1m, A20.1m, and A26.8m (250 nM each). Neutralization experiments were replicated 3 times with 3 identical wells in each experiment. Bars represent the standard error of the mean (n = 9).

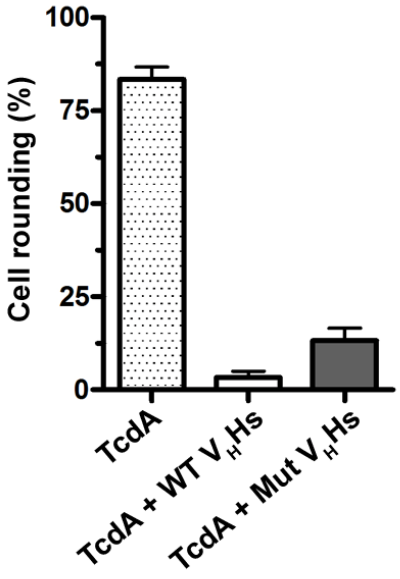
Cell rounding (%)
100
75
50
25
0
TcdA
TcdA + WT V$_H$Hs
TcdA + Mut V$_H$Hs

5.0 DISCUSSION

5.1 Isolation of *C. difficile* toxin A- and B-specific VHHs

C. difficile is a gastrointestinal pathogen which causes CDAD with symptoms ranging from mild diarrhea to fatal pseudomembrane colitis. Patients infected with the Gram-positive bacterium are routinely treated with oral antibiotic therapy. However, hypervirulent *C. difficile* strains which express elevated levels of TcdA and TcdB are now common hospital isolates (112) and are making treatment more challenging. The increasing number of patients who relapse with *C. difficile* symptoms after antibiotic treatment is also of considerable concern. Due to the heavy antibiotic load, relapsing patients cannot repopulate their gastrointestinal tract with the normal complement of commensal microbiota. Relapsing patients also mount poor anti-TcdA immune responses, specifically low serum IgG and possibly secretory IgA titers. It has been shown that patients who do not relapse after antibiotic treatment, or are asymptomatic carriers of *C. difficile*, possess higher antitoxin A antibody titers. Collectively, this suggests the introduction of toxin-neutralizing antibodies may be an effective therapy to treat recurrent CDAD.

In this work, we set out to isolate a panel of llama single domain antibodies (VHHs) which target TcdA or TcdB. We hypothesized that VHHs which bind the C-terminal RBD of TcdA and TcdB will block toxin binding to host-cell receptors or prevent cellular uptake of the toxins. The experimental design was based on previous studies that illustrated successful neutralization of *C. difficile* toxins using antibodies targeting TcdA, or through RBD-based vaccines (11, 46, 99, 121, 195).

We generated a V_HH phage display library by immunizing a llama with recombinant RBD fragments and isolated V_HH binders by panning this library with these same fragments. The isolated antibodies were well expressed in *E. coli* periplasm, yielding up to 105 mg/L of culture all in monomeric, non-aggregating form, as expected, and recognized native TcdA/B isolated from *C. difficile* strain 10463 as well as recombinant RBD fragments. Given the high degree of TcdA-RBD sequence identity among different *C. difficile* strains, it is very likely that these current V_HHs will also recognize TcdA from hypervirulent isolates. For example, a comparison between the TcdA-RBD from the 10463 strain and the hypervirulent 027 ribotype strains (i.e., 196, B11, SM and 855) revealed 96% sequence identity. The observed V_HH affinities for TcdA were strong, with four having K_Ds in the range of 2 – 24 nM, which is typical for *Camelidae* single-domain antibodies isolated from immune libraries against protein targets (7, 51, 52, 68, 115, 174). The anti-TcdA V_HHs isolated here are among the highest affinity proteinaceous toxin-binding single-domain antibodies characterized to date (7, 51, 52, 68, 115, 174).

In characterizing the V_HH – toxin interaction, we determined that most V_HHs recognized a conformational epitope on TcdA. Under denaturing Western blot conditions, only A19.2 V_HH and control PCG4 IgG bound to TcdA. Conversely, in native PAGE blot analysis, all specific V_HHs tested bound to TcdA. However, when the V_HH or PCG4 primary antibodies were omitted from the native blots, the secondary mouse anti-His_6 IgG-AP or goat anti-mouse IgG-AP antibodies bound to TcdA. This was not the case with the denaturing Western blots, indicating a genuine binding interaction between native (non-denatured) TcdA and secondary IgG antibody. Interestingly, the rabbit anti-His_6 IgG-HRP

conjugate used in our ELISA assays did not recognize TcdA when the primary antibody was omitted. Binding of TcdA to mouse mAbs has been reported (120) and found to occur through the Fab component (24) with TcdA possibly interacting a carbohydrate on C_H1. Binding of our V_HHs was specific to TcdA, as shown by Biacore and ELISA, and could not possibly occur from glycosylation of the V_HH since these domains do not contain putative glycosylation sites and were expressed in *E. coli*. The cross-reactivity of secondary mAbs encountered here reinforces the need to perform proper controls during immunoassays. When the cross-reacting secondary antibody was replaced with a Nickel-AP conjugate, V_HH binding to TcdA was detected in native PAGE Western blots, but not in denaturing SDS-PAGE Western blots.

To further validate V_HH binding to linear and conformational TcdA epitopes, TcdA was exposed to various heat treatments and probed by anti-TcdA V_HHs in ELISA. Most of the V_HHs did not recognize TcdA samples heated above its thermal unfolding midpoint temperature (T_m) of ≅55°C. However, A19.2 bound denatured TcdA in this ELISA and by Western blotting. Furthermore, we were unsuccessful at identifying peptide binders, i.e., V_HHs recognizing linear epitopes, in A4.2 and A5.1 V_HHs through panning of a New England Biolabs 12-mer peptide library (data not shown). Taken together, we conclude most of our V_HHs recognize a conformational epitope(s) on TcdA that is destroyed upon exposure of the toxin to denaturants. At this point, it is not known whether multiple epitopes are being recognized.

We evaluated the ability of V_HHs to neutralize *C. difficil*e toxins in a standard cytotoxicity assay. Six of the seven TcdA-specific V_HHs evaluated were neutralizing, with

four being potent neutralizers, demonstrating that our llama immunization strategy involving the use of TcdA-RBD as an immunogen is an effective one for generating toxin neutralizing antibodies. As shown by binding assays, neutralization was achieved by binding of V_HHs to sites other than the toxin's carbohydrate binding pocket. Clones A19.2 (K_D = 290 nM) and A24.1 (K_D = 260 nM) were the poorest neutralizers and also possessed the lowest affinities for TcdA. The potent neutralizers (A4.2, A5.1, A20.1, and A26.8) possessed much higher affinity for TcdA than A24.1 and A19.2, and all showed comparable efficacy. As such, efficacious toxin neutralization is dependent on high affinity binding to TcdA epitopes that are important in toxin-cell receptor contacts.

The structure of TcdA-RBD contains 7 putative carbohydrate binding sites (53, 70), which are thought to interact with epithelial cell surface receptors to mediate endocytosis (42). The binding sites are spaced between 3 and 5 nm away from each other, and due to geometric constraints, all 7 sites likely cannot access the cell-surface receptors simultaneously. Rather, 4 or 5 sites appear to be suitably presented for binding cell surface carbohydrates simultaneously, depending on the rotational orientation of the RBD relative to the cell surface (53, 70). The structure of the RBD thus strongly suggests that avidity is crucial to the strength of toxin binding to its cellular receptors.

To deduce the molecular mechanism of toxin neutralization, a competition experiment was performed to test whether V_HHs directly interfered with the binding of small carbohydrate ligands capable of interacting with individual binding sites. Since these small ligands did not compete directly with the binding of V_HHs to the toxin, the neutralization activity of the V_HHs does not derive from a disruption of the portion of the

receptor binding sites interacting with two synthetic trisaccharide ligands believed to bind to the central portion of the RBD's carbohydrate-binding sites. These experiments do not rule out the possibility that VHH binding may occlude the binding of larger ligands occupying a more extended binding site. It is also possible that VHH binding may sterically interfere with the binding of multiple RBD binding sites to ligands presented on a cell surface.

If an indirect, steric interference mechanism is operating, we hypothesized that the addition of more than one neutralizing VHH, each of which recognizes distinct epitopes on the TcdA-RBD may provide an enhanced neutralizing potency through greater hindrance of toxin-cell receptor contacts. In fact, when various combinations of A4.2, A5.1, A20.1 and A26.8 were tested, their TcdA neutralizing efficacy was greater than any of the VHHs alone. These findings are similar to Nowakowski et al (138) and Demarest et al (31) who showed increased BoNT/A and TcdA neutralizing capacity, respectively, with a mixture of mAbs. These observations suggested the VHHs recognized distinct epitopes on TcdA, which was subsequently confirmed for one VHH (A20.1) by co-injection SPR epitope mapping experiments (Figure 4.8). In contrast, the other potent neutralizers appeared to bind to overlapping epitopes on TcdA. These data explain the increased neutralizing capacity seen for pairs and triplet combinations containing A20.1, but do not explain why some pairs (i.e., A5.1/A26.8) or triplet combinations (i.e., A4.2/A5.1/A26.8) show greater efficacy than these VHHs on their own. The Biacore data indicated a 1:1 binding stoichiometry which is difficult to reconcile with the observation of enhanced neutralizing efficacy with mixed VHHs binding to overlapping epitopes. The binding stoichiometry determination assumes a

mainly active toxin surface (i.e., immobilized toxin that is not degraded or conformationally altered) which may not be the case since our toxin preparations showed a significant amount of breakdown products (Figure 4.1B, Figure 4.5F, G). It is clear that the neutralization and Biacore experiments are not related methodologies and were employed to assess for two different effects. However, together they do not completely agree with the conclusion of "distinct epitopes". For example, one may have expected to see additive effects with the A4.2/A20.1 doublet in neutralization assays and not with A4.2/A26.8 or A5.1/A26.8 doublets based on the epitope mapping results. The observed neutralization effect may be the net result of interplay of many factors including K_D, association and dissociation rate constants, k_{on} and k_{off}, the identity and overlapping nature of epitopes, stability of the VHHs under the neutralization assay condition and limitations of the assay. These factors may also explain why in several instances triplets were not better neutralizers than doublets. We are currently performing electrospray ionization mass spectrometry (ES-MS) assays (34) and solving co-crystal structures to determine the VHH:TcdA binding stoichiometry and TcdA epitopes, respectively. If the VHH to toxin binding stoichiometry is in fact greater than 1:1, the synergistic effect observed with VHHs recognizing overlapping epitopes may be due to binding orientation effects.

Compared to other studies involving *C. difficile* toxin-neutralization (Table 1.2), our VHHs performed well. First, TcdA and VHH were not pre-incubated together, which is routinely done in *in vitro* experiments involving neutralizing antibodies and toxins (11, 56, 63). We felt the simultaneous addition of VHH and toxin to fibroblast cells was more representative of *in vivo* scenarios and did not bias our *in vitro* results by pre-incubating.

Second, we used several fold more TcdA (325 pM or 100 ng/mL) compared to the study of Babcock *et al* (11). However, different sources of TcdA, length of storage, storage conditions and minor breakdown products may affect the concentrations of a given stock of TcdA which cause cytotoxic responses in cell culture, making reliable comparisons between the two studies difficult. Babcock *et al* (11) reported the most potent TcdA neutralizer (mAb 1B11) inhibited 50% TcdA-induced rounding at a concentration of 0.1 nM after 18 hours. While our individual VHHs did not perform as well as mAb 1B11 after 24 hours, A5.1/A20.1 and A20.1/A26.8 pairs and most triplet VHH combinations prevented at least 50% cell rounding at a concentration of 0.1 nM, 24 hours after toxin addition. Thus, our pooled VHHs should serve as a very effective therapeutic cocktail as they possess comparable efficacy to anti-TcdA mAbs currently in clinical trials. In addition, a range of structure-based and random mutagenesis approaches are available for further improving the binding affinities and neutralization efficacies of VHHs.

Furthermore, the isolated TcdB-specific VHHs were not capable of neutralizing TcdB. Their apparent affinities for the TcdB-RDB-f1 fragment ranged from 100 nM to 400 nM and it is not clear whether this affinity is insufficient for neutralization, or if the epitopes these VHHs were raised against are not involved with the binding of TcdB to cell surface receptors. While the anti-TcdB VHHs recognized TcdB-RBD-f1 and native TcdB in ELISA (Figure 4.5B), we did not collect reliable SPR data for the VHH-TcdB interaction; rather, data were only collected against TcdB-RBD-f1 which may show significant structural differences when presented in the context of the whole toxin (152). As such, the VHH affinities for TcdB may even be lower than the reported values above and this could account for poor

neutralization. There is also the possibility that the lack of neutralization of toxin B binding VHHs is due to the fact that regions of TcdB other than the RBD are involved in host cell surface binding and cellular entry, as previously suggested (13, 34). B5.2, in particular, cross reacted with toxin A and it would be interesting to determine its K_D as well as its neutralization potential towards toxin A. Although epitope mapping experiments were not carried out in the case of toxin B binders, the amino acid sequence data indicate that B5.2 probably uses the same D gene (KVVGGRL) as B13.6 (AVVGGVI) and B15.5 (KVVRGSL), suggesting that all 3 VHHs may interact with the same epitope.

5.2 Isolation of *C. difficile* toxin B-specific VLs

Of 17 unique VLs isolated which bound the GST-TcdB fusion, only 4 recognized native TcdB, suggesting our GST fusion may be distorting the conformation of TcdB such that TcdB is different from its native state. This could be the case, since none of the 17 VLs bound to GST, and 16 showed specific binding the GST-TcdB fusion protein. Another possibility is that the VLs are recognizing an epitope which is shared between GST and TcdB. Regardless, 4 VLs were characterized and found to all be monomeric, non-aggregating antibodies with 2 possessing affinities in the low nM range.

Despite not neutralizing TcdB, the 4 VLs are currently being used for co-crystal structure determination of the TcdB carbohydrate binding domain. The structure of this region of TcdB has so far remained elusive, but it is hoped that stabilization with a small

binding domain such as a V_L may aid in crystallization and ultimately structure determination.

5.3 Stability engineering of V_HHs

The GI tract is the site of numerous microbial infections caused by a range of pathogens, including, *Helicobacter pylori*, *Salmonella typhi*, *Vibrio cholerae*, *Escherichia coli* and *C. difficile*. The current approach for treating most of these infections involves administration of antibiotics, which places selection pressure on the organism, can lead to antibiotic resistance and suppresses or eliminates beneficial commensal microbes. Disease-causing pathogens of the GI tract rely on a myriad of virulence factors for colonization, adherence, motility, cellular entry and pathogenesis. These include, but are not limited to: surface-layer proteins, adhesions, invasions, flagella, high-molecular weight toxins, and quorum sensing molecules. Inhibition of bacterial virulence factors that are essential for disease pathogenesis therefore represents a novel, non-antibiotic based strategy to treat infectious disease, while reducing the risk of microbial resistance and maintaining commensal gut populations (19, 23, 124).

Several approaches are being explored for antivirulence microbial therapy. Inhibition of *E. coli* pilus assembly (179), *B. anthracis* lethal factor (144, 167), Type III secretion systems (76, 133), *S. aureus* quorum sensing pathways (125), Cholera toxin (182), and *C. difficile* toxins A and B (67, 107) with small molecules and peptides, are examples currently under development. One of the most pursued antivirulence strategies is targeting

bacterial toxins with antibodies. Neutralizing antibodies against anthrax (166), shiga toxin (177), cholera toxin (149), botulinum toxin (138), and *C. difficile* toxins (11, 99, 118) have all been successfully isolated. This is evident by the number of clinical trials currently underway involving antibodies to bacterial targets (16). For human pathogens that secrete toxins into the lumen before cellular entry, such as *C. difficile* (80), it may be advantageous to neutralize the toxins within the GI tract. Several studies indicate that oral administration of immunoglobulins (i.e., bovine Ig, human IgA, chicken IgY) may be successful at controlling various gastrointestinal pathogens, including *C. difficile* (183), rotavirus (27), shigella (180), and enterotoxigenic *E. coli* in humans (181) and neonatal pigs (205). However, there are major limitations facing orally administered immunotherapeutics, including the susceptibility of antibodies to proteolytic degradation, instability at low pH, high dosing requirements, and cost (155).

Recombinant antibody fragments, such as single-domain antibodies (sdAbs) (10, 58) isolated from (Fv) regions of conventional IgGs (i.e., V_{HS}, V_{LS}), from the heavy-chain IgG of *Camelidae* species (i.e., V_HHs or Nanobodies) and from cartiligous sharks (i.e., VNARs), are ideal agents to explore for oral immunotherapy because of their small size (12-15 kDa), high intrinsic protease and thermal stability, amenability to library selection under denaturing conditions, ease of genetic manipulation, and lack of immunogenicity. Many sdAbs have been isolated relevant to infection and immunity (200). However, sdAbs isolated without selection pressure or engineered or formulated for stability were degraded in the low pH, pepsin-rich environment of the stomach and by digestive enzymes in the duodenum when administered orally (63, 105, 189). Several engineering and selection-based approaches have

been taken to improve the thermal stability and protease resistance of sdAbs and other recombinant antibody fragments (i.e., scFvs and Fabs). Engineered disulfide bonds (57, 159, 207) and other stabilizing mutations (203) have increased the thermal stability of various recombinant fragments. Library selection of antibodies in the presence of proteases, denaturants, extreme pH and elevated temperatures has lead to the isolation of antibody fragments with favourable characteristics such as improved stability, increased protease resistance and resistance to aggregation (22, 39, 40, 82, 83, 88, 127, 168). Elsewhere, random mutagenesis approaches have been used to increase the proteolytic stability of VHHs (64). There have been few universal strategies to increase recombinant antibody thermal and protease stability simultaneously.

Here, through protein engineering, we increased the protease, acid and thermal stability of llama-derived VHHs which target and neutralize *C. difficile* toxin A without dramatically affecting biological function. Our stabilization strategy involved the substitutions of two amino acid residues at positions 54 and 78 for cysteine, allowing for the formation of a second, non-native disulfide bond between FR2 and FR3 in the VHH hydrophobic core. Incorporation of a disulfide bond at these positions has been previously reported in dromedary- and llama-derived VHHs (20, 57, 159) and was found to increase VHH chemical and thermal stability. We hypothesized that the additional disulfide bond may also enhance VHH resistance to proteases, especially in denaturing acidic conditions.

To test this hypothesis, we generated the disulfide bond mutants and compared them to their wild-type counterparts containing only the native disulfide bond between residues 23 and 104. Mutant VHHs were well expressed in *E. coli* when targeted to the

periplasmic space, although with lower yields compared to the wild type VHHs, and all were non-aggregating monomers as determined by size exclusion chromatography. To confirm disulfide bond formation, we used a combination of proteolytic and chemical digestion coupled with MS^2 to precisely identify VHH peptide fragments harboring the introduced disulfide bond. This approach is preferred over the Ellman's assay approach for the determination of disulfide linkage formation, as it requires less quantities of protein and reveals the positional identity of Cys pairs in a given disulfide bond. The latter information is important, as there is also the possibility that the two engineered Cys residues, besides forming the desired disulfide bond between themselves, may form undesired disulfide bonds with the two conserved Cys residues at positions 23 and 104. After confirming disulfide bond formation in our mutants, SPR binding experiments revealed most mutant VHHs possessed 1- to 5-fold weaker affinity constants relative to wild-type, which is consistent with others that showed up to 3-fold reductions in the affinities of VHHs containing the same introduced disulfide bond (20, 159). However, for the two weak neutralizing VHHs, A19.2m and A24.1m, the non-canonical disulfide linkage compromised specificity.

We used CD spectroscopy to compare wild-type and mutant VHH secondary structure, tertiary structure, thermal stability (T_m and T_{onset}), and thermal refolding efficiency (TRE). Comparisons of VHH secondary and tertiary structures with far-UV and near-UV CD spectroscopy strongly suggested structural differences between wild-type and mutants, at both neutral and acidic pH. For all mutants, peak intensity and selective peak minima shifts were observed, although the overall spectral profiles remained very similar in all wild

type/mutant pairs. More specifically, mutants consistently showed rightward peak shifts in the peak range of 230 nm – 235 nm (far-UV CD spectra) and around 297 nm (near-UV CD spectra) compared to wild type V_HHs. Such patterns may be used as signatures to quickly identify V_HHs containing a properly formed non-canonical disulfide bond, as could SDS-PAGE motility values, since compared to wild type V_HHs, mutants consistently moved slower in SDS-PAGE gels. Thus, the far- and near-UV CD spectral data suggest the introduced disulfide bond changes the structure of V_HHs. This is consistent with the observed perturbations in affinities and specificities and increased GI protease resistance of the mutant V_HHs compared to the wild types (*see* below). We used CD spectroscopy thermal denaturation experiments to show a profound and significant increase in the T_ms and T_{onset}s of mutant V_HHs at both neutral and acidic pH. These mutants are more thermostable than previously reported V_HHs, which were affinity selected from a V_H phage display library under stability pressure (39). The beneficial effect of the non-canonical disulfide linkage on T_ms varies widely, with T_m increases ranging from ≈4°C to ≈12°C. This suggests that for the mutant V_HHs with a higher thermostability gain, the non-canonical disulfide linkage may have been a better fit to their overall fold. A19.2m and A24.1m showed the lowest thermostability gains, and if it is true that this is because of them acquiring an unfit disulfide linkage, it would explain why they were transformed into non-specific binders upon mutation. For A4.2m on the other hand, the non-canonical disulfide linkage seems to be a natural fit, as it increased its T_m the most (by almost 12°C) and significantly improved GI protease resistance (with the highest increase in pepsin resistance; *see* below), all without adversely affecting the K_D. We also observed a correlation

between pepsin resistance and T_m, and this has implications in terms of using heat as the selective pressure for selecting pepsin resistant antibody fragments by *in vitro* evolutionary approaches. Finally, V_HH refolding was also examined using CD spectroscopy. With respect to TRE, while wild-type refolding was better than mutant V_HH refolding at neutral pH, the reverse was true under stringent conditions (acidic pH). At acidic pH, 5 of 6 mutant V_HHs possessed greater refolding efficiency than wild-type after complete thermal denaturation with the majority essentially showing reversible thermal unfolding. It should be noted that we did not determine antigen binding after performing refolding experiments. Dumoulin et al (37) found that despite high refolding efficiencies from CD experiments, target antigen affinities were reduced by up to 50% for some V_HHs. This was attributed to the improper refolding of the antigen-binding CDR loops.

We also examined the resistance profiles of the disulfide bond mutants to the major GI proteases. Mutant V_HHs were universally more resistant to pepsin and many were more resistance to chymotrypsin when compared to their wild-type counterparts. Protease sensitivity is a function of many variables including the location of proteolytic sites (e.g., loops *vs* protein core in antibodies), the theoretical number of proteolytic sites, and protein compactness and thermodynamic stability (44, 75). Since each wild-type and mutant V_HH pair possessed the identical number of theoretical protease cleavage sites, we speculate that the second disulfide bond presents a more compact and thermodynamically stable V_HH structure, preventing pepsin and chymotrypsin from accessing proteolytic cleavage sites. This view is consistent with the increased T_ms in mutants (an indicator of mutants' increased thermostability), the positive correlation between pepsin resistance and T_m

(Figure 4.27), and the lack of correlation between pepsin/chymotrypsin resistance and the number of theoretical protease cleavage sites (Figure 4.28). The pepsin resistance *vs* T_m/T_{onset} correlation curves also point to the fact that structural compactness and thermodynamic stability plays a more prominent role in pepsin resistance which is understandable given that pepsin requires protein unfolding for efficient digestion. This benefit is not realized for mutants against trypsin, possibly because their cleavage sites are at hydrophilic residues (Lys or Arg) which must be in more exposed regions of the V_HH. The positive correlation between V_HH trypsin resistance and the number of theoretical trypsin cleavage sites is a testament to this (Figure 4.28). Harmsen *et al* (64) have suggested the CDR regions of V_HHs to be the most sensitive sites to proteolysis due to their flexibility and exposed position relative to the V_HH core. Indeed, there are more predicted trypsin-cleavage sites in the CDR regions (Table 4.9, Figure 4.28) of trypsin-sensitive V_HHs (A4.2, A19.2, and A26.8) compared to trypsin-resistant V_HHs (A5.1, A20.1, and A24.1). This is not the case for pepsin and chymotrypsin sensitivities (Table 4.9, Figure 4.28).

Importantly, we also observed an increase in T_{onset} temperatures for mutants at the physiological condition representative of the stomach (pH 2.0 and 37°C) to values significantly above 37°C (T_{onset}s from 45°C – 53°C). This suggests that the mutants should remain fully folded at 37°C in the stomach, hence resisting pepsin degradation (and denaturation) to a higher extent than wild type V_HHs, a statement supported by our *in vitro* pepsin digestion experiments. Contrary to the mutants, 3 wild type V_HHs, for example, have low T_{onset} values of 37.8°C (A5.1 and A20.1) and 40.3°C (A26.8) which suggests partial unfolding in the stomach (pH 2.0, 37°C), increasing their proteolytic susceptibility. This

indeed is the case in an *in vitro* setting as A5.1 and A20.1, V_HHs with T_{onset} temperatures overlapping the physiological temperature, are completely pepsin sensitive, and A26.8 with the T_{onset} slightly above the physiological temperature, although somewhat better than the former two, is barely resistant to pepsin (pepsin resistance: ≈3%). In the corresponding pepsin resistant mutants, acquiring resistance parallels an increase in T_{onset}. In line with these findings, we observe a strong positive correlation between pepsin resistance and T_{onset} (Figure 4.27B), and depending on the melting curve profile, T_{onset}s may be a better predictor of a pepsin resistance status of proteins than T_ms.

Compared to other studies involving *in vitro* V_HH proteolysis, our mutant V_HHs performed remarkably well; withstanding near physiological concentrations of pepsin and chymotrypsin and retaining functionality thereafter. Additionally, half of the mutants were trypsin resistant and for those which were not, identification and removal of their cleavage site(s) should be straight forward, e.g., by MS analysis and site-directed mutagenesis. Balan *et al* (12) note the human stomach contains pepsin concentrations ranging from 500 μg/mL to 1 mg/mL, while Schmidt *et al* (165) found the average pepsin concentration in the stomach of piglets to be 155 U/mL. Our pepsin digestion assays were performed at 100 μg/mL concentrations, which correspond to 46 U/mL. The most stable V_HH mutant produced by Harmsen *et al* (64) using a DNA shuffling approach showed only 21% residual V_HH remaining after digestion with 100 μg/mL of pepsin. In contrast, our most stable V_HH (A4.2m) showed 74% residual V_HH remaining after digestion, while 4 others had residual pepsin resistance values of 24% or higher. In addition, all 4 disulfide bond mutant V_HHs retained binding to TcdA after pepsin treatment, confirming their resistance to the protease

and retention of functionality. SPR binding studies of VHHs to TcdA at pH 2.0 was not attempted.

We also examined the toxin A neutralizing efficacy of our disulfide bond mutant VHHs. Compared to the wild-type VHHs, the mutants were 3 – 4 fold poorer neutralizers of toxin A in cell-based assays, presumably a reflection in the reduced affinities of 3 of 4 VHHs for the toxin. If a more thorough analysis was performed on individual VHHs, it is possible that clone A4.2m, which showed the same affinity as A4.2 for toxin A, be a more potent neutralizer due to its higher stability. Under stringent conditions *in vivo*, the lower affinity mutants may actually be more efficacious than the higher affinity wild-type VHHs due to their greater stability, as shown elsewhere (20). Besides, a number of methods are available to increase the affinity of the disulfide-stabilized domains, allowing for the creation of superpotent toxin A neutralizing antibodies capable of withstanding a wide range of harsh conditions.

6.0 CONCLUSIONS AND RECOMMENDATIONS

6.1 Conclusions

In conclusion, *C. difficile* toxin A and B specific V_HHs and V_LS were isolated from an immune llama phage display library and characterized. Several TcdA-specific V_HHs were found to be capable of neutralizing TcdA *in vitro* through high-affinity interactions with TcdA- RBD. V_HHs are extremely stable antigen-binding domains that are expressed at high yields in recombinant organisms and are capable of neutralizing infectious disease-related targets (200). With respect to CDAD therapy, V_HHs could be administered systemically to target TcdA and TcdB, as they share high sequence homology with human V_H domains and are thus well tolerated in humans (193; www.Ablynx.com), or formulated for oral administration to the gastrointestinal tract. Enhanced toxin neutralizing efficacy should be obtainable by increasing their intrinsic affinity, blood circulation half lives, size, and avidity through chimeric formats of anti-TcdA V_HHs linked to an Fc domain or through the generation of bi- or tri-specific antibody fusions with two or three anti-TcdA V_HHs recognizing unique epitopes. Although not neutralizing, the present toxin B-specific V_HHs/V_LS could, nonetheless, enhance the neutralization efficacy of other toxin B neutralizing V_HHs/V_LS by a chelating effect when fused to them. By targeting *C. difficile* virulence factors such as TcdA/B, selection pressure is removed from the organism, decreasing the chance of antibiotic resistance. A mutation in the RBD, which is well conserved among *C. difficile* isolates including the hypervirulent 027 ribotype strains, is unlikely to benefit the organism and in the event it does occur, the toxin may lose its ability

to enter host cells. As such, anti-TcdA/B VHHs are logical agents to explore for CDAD therapy.

Furthermore, we have shown that the introduction of a second disulfide bond into the hydrophobic core of a panel of llama VHHs increased thermal stability and GI protease resistance; the approach is both effective and general. The approach does not come without some drawbacks, including reduced affinity, specificity, and expression yield. However, the mutants outperformed the wild-type VHHs under more stringent physiological conditions, which outweigh the reductions in affinity, as noted above. Whether the mutant VHHs are more efficacious than the wild-type VHHs *in vivo* remains to be determined. Based on our results and that of others, we suggest incorporating the non-canonical disulfide bond between position 54 and 78 at the library construction phase and not after the selection/screening phase to avoid adverse side effects on affinity and specificity seen here and in other studies. Our mutant VHHs are ideal building blocks for oral therapeutic agents that must survive the harsh GI tract, and provide promising alternatives to antibiotics. The oral administration of therapeutic proteins is of interest to the pharmaceutical and biotechnological industries (6, 75, 155, 199). Protein-based oral therapeutics have several conceived advantages over systemic administration: convenience, patience compliance, lower cost, pain-free administration, drug purity, flexibility in production source (i.e., bacterial, plant, etc.), and lower concerns over immunogenicity. Despite the many advantages of oral administering protein therapeutics, few successes have been realized due to the destabilizing environment of the GI tract. Of the major GI proteases, pepsin is considered the primary cause of antibody degradation (64, 155, 189) and hence a major

obstacle facing orally delivered antibody therapeutics. Regarding the mutant V_HHs generated in this study, the therapeutic efficacy can be further enhanced by improving their affinity (through selection of affinity maturation display libraries) and by formulation. The affinity maturation libraries could yield V_HHs which are hyper-stabilized (e.g., high GI protease resistance) in addition to being of ultra-high affinity, if selection pressures (acid, proteases, heat) are applied during the panning stage (39, 82). Indeed, the correlation between V_HH pepsin resistance and T_m suggests that selection under heat should produce pepsin-resistant V_HHs. Other applications for our stabilized domains include: (i) use as delivery agents for mucosal vaccines (114) or (ii) use as robust affinity purification reagents resistant to acidic and heat elution steps. Furthermore, the recent incorporation of these engineered disulfide bonds into human V_H sdAbs not only resulted in increased thermal stability, but also markedly reduced V_H aggregation (96), suggesting that the introduced disulfide bond imparts a universal stabilizing effect in all immunoglobulin variable domains.

6.2 Recommendations

The following are a series of recommendations and possible directions for future work on this project, based on the experiences gained here and from recent advances in the literature.

1. On the isolation of TcdB-neutralizing VHHs

To isolate high affinity TcdB-neutralizing VHHs, a llama may need to be immunized with the entire TcdB RBD region. The recombinant antigen used for immunization in this study was a very short segment of the carbohydrate binding domain that only encompassed one of the 5 repeat domains.

Recent work by Pruitt *et al* (152) has suggested portions of the N-terminal glycosyltransferase domain of TcdB may be involved in host cell receptor contacts. As such, VHHs targeting both the glycosyltransferase domain and RBD regions may be needed for effective TcdB neutralization.

2. On enhancing the efficacy of antitoxin A VHHs

Conceivably, the efficacy of TcdA-neutralizing VHHs could be improved through several means. For example, the VHHs could be engineered for higher affinity binding to TcdA using affinity maturation, or site-directed mutagenesis if the exact amino acids known to interact with TcdA are revealed in the crystal structures.

Efficacy could also be enhanced by creating bi-specific VHHs in which two VHHs that target unique TcdA epitopes are covalently linked as a single polypeptide. Further, bi-specific VHHs consisting of the same VHH may also show efficacy improvements. There also exists the option of fusing the isolated VHH domains to Fc regions for enhanced potency if the antibodies were to be used systemically. Fusion to the Fc region would greatly enhance their serum half lives, making the antibody more efficacious. Of course the scope of this

work was to develop the groundwork for an oral antibody-based therapy, so fusion to an Fc would have been beyond the scope of this study.

Finally, neutralizing antibody efficacy could be enhanced by creating bi-specific VHHs with one antibody targeting TcdA and the other antibody targeting TcdB.

3. On determining the mechanism of VHH-based TcdA neutralizing

From the biochemical and *in vitro* data, it was not clear why some VHHs, when used in combinations, enhanced neutralizing efficacy. Through current collaborations with Dr. Ken Ng at the University of Calgary, VHH co-crystal structures are being solved in complex with fragments of TcdA. It is hoped these data will give a better idea behind the neutralization mechanism of action, especially with respect to the VHH:TcdA stoichiometry and the nature and location of the epitope.

4. On *in vivo* animal studies using antitoxin A/B VHHs

If TcdB neutralizing VHHs could be isolated, *in vivo* animal studies should be performed using the Syrian hamster model or mouse model. The well established hamster model involves administration of antibiotics 5-days before administration of *C. difficile* spores. This would be followed by the oral administration of TcdA and/or TcdB neutralizing VHHs. The primary endpoint would be hamster survival.

5. On formatting VHHs for oral immunotherapy

Mutant VHHs isolated in this study with an introduced disulfide bond showed remarkable resistance to heat, extreme pH, and proteolytic degradation. In addition to the mutational strategy developed in this work, there exists several other options, or formulation "add-ons", that may enhance the survival and efficacy of orally administered VHHs (i.e., encapsulation, PEGylation, etc.).

Probiotic bacteria expressing and secreting toxin-neutralizing VHHs could be one avenue to explore for orally administering the toxin-neutralizing payload. Probiotic bacterial expression would not only circumvent VHH degradation by the digestive enzymes of the upper GI tract, but the strategy would also alleviate the need to purify large quantities of VHHs for administration and provide an omnipresent amount of antitoxin VHH payload in the lower GI tract. Concerns over the release of genetically modified probiotics into the environment could be reduced or eliminated by using bacterial strains deficient in the thymidylate synthase gene (*thyA*) (173).

6. On additional targets for VHH-based CDAD immunotherapy

The following *C. difficile* virulence factors and cell-associated proteins may be interesting targets for VHH-based CDAD immunotherapy, in addition to the toxins:

(i) High and low molecular weight surface layer proteins (SLPs)

(ii) Flagellin (i.e., FliC) and flagellin cap proteins (i.e., FliD)

(iii) *C. difficile* spore coat proteins

(iv) *C. difficile* binary toxin

7.0 REFERENCES

1. **Aas, J., C. E. Gessert, and J. S. Bakken.** 2003. Recurrent *Clostridium difficile* colitis: case series involving 18 patients treated with donor stool administered via a nasogastric tube. Clin Infect Dis **36:**580-5.

2. **Abderrazek, R. B., I. Hmila, C. Vincke, Z. Benlasfar, M. Pellis, H. Dabbek, D. Saerens, M. El Ayeb, S. Muyldermans, and B. Bouhaouala-Zahar.** 2009. Identification of potent nanobodies to neutralize the most poisonous polypeptide from scorpion venom. Biochem J **424:**263-72.

3. **Abougergi, M. S., A. Broor, W. Cui, and B. G. Jaar.** 2010. Intravenous immunoglobulin for the treatment of severe *Clostridium difficile* colitis: an observational study and review of the literature. J Hosp Med **5:**E1-9.

4. **Albesa-Jove, D., T. Bertrand, E. P. Carpenter, G. V. Swain, J. Lim, J. Zhang, L. F. Haire, N. Vasisht, V. Braun, A. Lange, C. von Eichel-Streiber, D. I. Svergun, N. F. Fairweather, and K. A. Brown.** 2010. Four distinct structural domains in *Clostridium difficile* toxin B visualized using SAXS. J Mol Biol **396:**1260-70.

5. **Allo, M., J. Silva, Jr., R. Fekety, G. D. Rifkin, and H. Waskin.** 1979. Prevention of clindamycin-induced colitis in hamsters by *Clostridium sordellii* antitoxin. Gastroenterology **76:**351-5.

6. **Amorij, J. P., W. Hinrichs, H. W. Frijlink, J. C. Wilschut, and A. Huckriede.** 2010. Needle-free influenza vaccination. Lancet Infect Dis **10:**699-711.

7. **Anderson, G. P., J. L. Liu, M. L. Hale, R. D. Bernstein, M. Moore, M. D. Swain, and E. R. Goldman.** 2008. Development of antiricin single domain antibodies toward detection and therapeutic reagents. Anal Chem **80:**9604-11.

8. **Arbabi-Ghahroudi, M., R. MacKenzie, and J. Tanha.** 2009. Selection of non-aggregating VH binders from synthetic VH phage-display libraries. Methods Mol Biol **525:**187-216, xiii.

9. **Arbabi-Ghahroudi, M., R. Mackenzie, and J. Tanha.** 2010. Site-directed mutagenesis for improving biophysical properties of VH domains. Methods Mol Biol **634:**309-30.

10. **Arbabi Ghahroudi, M., A. Desmyter, L. Wyns, R. Hamers, and S. Muyldermans.** 1997. Selection and identification of single domain antibody fragments from camel heavy-chain antibodies. FEBS Lett **414:**521-6.

11. **Babcock, G. J., T. J. Broering, H. J. Hernandez, R. B. Mandell, K. Donahue, N. Boatright, A. M. Stack, I. Lowy, R. Graziano, D. Molrine, D. M. Ambrosino, and W. D. Thomas, Jr.** 2006. Human monoclonal antibodies directed against toxins A and B prevent *Clostridium difficile*-induced mortality in hamsters. Infect Immun **74:**6339-47.

12. **Balan, K. K., A. T. Jones, N. B. Roberts, J. P. Pearson, M. Critchley, and S. A. Jenkins.** 1996. The effects of *Helicobacter pylori* colonization on gastric function and the incidence of portal hypertensive gastropathy in patients with cirrhosis of the liver. Am J Gastroenterol **91:**1400-6.

13. **Barroso, L. A., J. S. Moncrief, D. M. Lyerly, and T. D. Wilkins.** 1994. Mutagenesis of the *Clostridium difficile* toxin B gene and effect on cytotoxic activity. Microb Pathog **16:**297-303.

14. **Bauer, M. P., J. T. van Dissel, and E. J. Kuijper.** 2009. *Clostridium difficile*: controversies and approaches to management. Curr Opin Infect Dis **22:**517-24.

15. **Beales, I. L.** 2002. Intravenous immunoglobulin for recurrent *Clostridium difficile* diarrhoea. Gut **51:**456.

16. **Bebbington, C., and G. Yarranton.** 2008. Antibodies for the treatment of bacterial infections: current experience and future prospects. Curr Opin Biotechnol **19:**613-9.

17. **Bordoli, L., F. Kiefer, K. Arnold, P. Benkert, J. Battey, and T. Schwede.** 2009. Protein structure homology modeling using SWISS-MODEL workspace. Nat Protoc **4:**1-13.

18. **Calabi, E., F. Calabi, A. D. Phillips, and N. F. Fairweather.** 2002. Binding of *Clostridium difficile* surface layer proteins to gastrointestinal tissues. Infect Immun **70:**5770-8.

19. **Cegelski, L., G. R. Marshall, G. R. Eldridge, and S. J. Hultgren.** 2008. The biology and future prospects of antivirulence therapies. Nat Rev Microbiol **6:**17-27.

20. **Chan, P. H., E. Pardon, L. Menzer, E. De Genst, J. R. Kumita, J. Christodoulou, D. Saerens, A. Brans, F. Bouillenne, D. B. Archer, C. V. Robinson, S. Muyldermans, A. Matagne, C. Redfield, L. Wyns, C. M. Dobson, and M. Dumoulin.** 2008. Engineering a camelid antibody fragment that binds to the active site of human lysozyme and inhibits its conversion into amyloid fibrils. Biochemistry **47:**11041-54.

21. **Chandrasekar, T., N. Naqvi, A. Waddington, R. P. D. Cooke, H. Anijeet, C. W. Gradden, K. A. Abraham, and C. F. Wong.** 2008. Intravenous immunoglobulin

therapy for refractory *Clostridium difficile* toxin colitis in chronic kidney disease: case reports and literature review. NDT Plus **1:**3.

22. **Christ, D., K. Famm, and G. Winter.** 2007. Repertoires of aggregation-resistant human antibody domains. Protein Eng Des Sel **20:**413-6.

23. **Clatworthy, A. E., E. Pierson, and D. T. Hung.** 2007. Targeting virulence: a new paradigm for antimicrobial therapy. Nat Chem Biol **3:**541-8.

24. **Cooke, D. L., and S. P. Borriello.** 1998. Nonspecific binding of *Clostridium difficile* toxin A to murine immunoglobulins occurs via the fab component. Infect Immun **66:**1981-4.

25. **Cortez-Retamozo, V., N. Backmann, P. D. Senter, U. Wernery, P. De Baetselier, S. Muyldermans, and H. Revets.** 2004. Efficient cancer therapy with a nanobody-based conjugate. Cancer Res **64:**2853-7.

26. **Corthier, G., M. C. Muller, T. D. Wilkins, D. Lyerly, and R. L'Haridon.** 1991. Protection against experimental pseudomembranous colitis in gnotobiotic mice by use of monoclonal antibodies against *Clostridium difficile* toxin A. Infect Immun **59:**1192-5.

27. **Davidson, G. P., P. B. Whyte, E. Daniels, K. Franklin, H. Nunan, P. I. McCloud, A. G. Moore, and D. J. Moore.** 1989. Passive immunisation of children with bovine colostrum containing antibodies to human rotavirus. Lancet **2:**709-12.

28. **De Genst, E., D. Saerens, S. Muyldermans, and K. Conrath.** 2006. Antibody repertoire development in camelids. Dev Comp Immunol **30:**187-98.

29. **De Genst, E., K. Silence, K. Decanniere, K. Conrath, R. Loris, J. Kinne, S. Muyldermans, and L. Wyns.** 2006. Molecular basis for the preferential cleft recognition by dromedary heavy-chain antibodies. Proc Natl Acad Sci U S A **103:**4586-91.

30. **Deckers, N., D. Saerens, K. Kanobana, K. Conrath, B. Victor, U. Wernery, J. Vercruysse, S. Muyldermans, and P. Dorny.** 2009. Nanobodies, a promising tool for species-specific diagnosis of Taenia solium cysticercosis. Int J Parasitol **39:**625-33.

31. **Demarest, S. J., M. Hariharan, M. Elia, J. Salbato, P. Jin, C. Bird, J. M. Short, B. E. Kimmel, M. Dudley, G. Woodnutt, and G. Hansen.** 2010. Neutralization of *Clostridium difficile* toxin A using antibody combinations. MAbs **2**.

32. **Deng, X. K., L. A. Nesbit, and K. J. Morrow, Jr.** 2003. Recombinant single-chain variable fragment antibodies directed against *Clostridium difficile* toxin B produced by use of an optimized phage display system. Clin Diagn Lab Immunol **10:**587-95.

33. **Desmyter, A., T. R. Transue, M. A. Ghahroudi, M. H. Thi, F. Poortmans, R. Hamers, S. Muyldermans, and L. Wyns.** 1996. Crystal structure of a camel single-domain VH antibody fragment in complex with lysozyme. Nat Struct Biol **3:**803-11.

34. **Dingle, T., S. Wee, G. L. Mulvey, A. Greco, E. N. Kitova, J. Sun, S. Lin, J. S. Klassen, M. M. Palcic, K. K. Ng, and G. D. Armstrong.** 2008. Functional properties of the carboxy-terminal host cell-binding domains of the two toxins, TcdA and TcdB, expressed by *Clostridium difficile*. Glycobiology **18:**698-706.

35. **Dooley, H., and M. F. Flajnik.** 2006. Antibody repertoire development in cartilaginous fish. Dev Comp Immunol **30:**43-56.

36. **Doyle, P. J., M. Arbabi-Ghahroudi, N. Gaudette, G. Furzer, M. E. Savard, S. Gleddie, M. D. McLean, C. R. Mackenzie, and J. C. Hall.** 2008. Cloning, expression, and characterization of a single-domain antibody fragment with affinity for 15-acetyl-deoxynivalenol. Mol Immunol **45:**3703-13.

37. **Dumoulin, M., K. Conrath, A. Van Meirhaeghe, F. Meersman, K. Heremans, L. G. Frenken, S. Muyldermans, L. Wyns, and A. Matagne.** 2002. Single-domain antibody fragments with high conformational stability. Protein Sci **11:**500-15.

38. **Egerer, M., T. Giesemann, T. Jank, K. J. Satchell, and K. Aktories.** 2007. Auto-catalytic cleavage of *Clostridium difficile* toxins A and B depends on cysteine protease activity. J Biol Chem **282:**25314-21.

39. **Famm, K., L. Hansen, D. Christ, and G. Winter.** 2008. Thermodynamically stable aggregation-resistant antibody domains through directed evolution. J Mol Biol **376:**926-31.

40. **Famm, K., and G. Winter.** 2006. Engineering aggregation-resistant proteins by directed evolution. Protein Eng Des Sel **19:**479-81.

41. **Farver, D. K., D. D. Hedge, and S. C. Lee.** 2005. Ramoplanin: a lipoglycodepsipeptide antibiotic. Ann Pharmacother **39:**863-8.

42. **Florin, I., and M. Thelestam.** 1983. Internalization of *Clostridium difficile* cytotoxin into cultured human lung fibroblasts. Biochim Biophys Acta **763:**383-92.

43. **Forsman, A., E. Beirnaert, M. M. Aasa-Chapman, B. Hoorelbeke, K. Hijazi, W. Koh, V. Tack, A. Szynol, C. Kelly, A. McKnight, T. Verrips, H. de Haard, and R. A. Weiss.** 2008. Llama antibody fragments with cross-subtype human immunodeficiency virus type 1 (HIV-1)-neutralizing properties and high affinity for HIV-1 gp120. J Virol **82:**12069-81.

44. **Frenken, L. G., M. R. Egmond, A. M. Batenburg, and C. T. Verrips.** 1993. Pseudomonas glumae lipase: increased proteolytic stability by protein engineering. Protein Eng **6:**637-42.

45. **Garaicoechea, L., A. Olichon, G. Marcoppido, A. Wigdorovitz, M. Mozgovoj, L. Saif, T. Surrey, and V. Parreno.** 2008. Llama-derived single-chain antibody fragments directed to rotavirus VP6 protein possess broad neutralizing activity in vitro and confer protection against diarrhea in mice. J Virol **82:**9753-64.

46. **Gardiner, D. F., T. Rosenberg, J. Zaharatos, D. Franco, and D. D. Ho.** 2009. A DNA vaccine targeting the receptor-binding domain of *Clostridium difficile* toxin A. Vaccine **27:**3598-604.

47. **Garey, K. W., M. Salazar, D. Shah, R. Rodrigue, and H. L. DuPont.** 2008. Rifamycin antibiotics for treatment of *Clostridium difficile*-associated diarrhea. Ann Pharmacother **42:**827-35.

48. **Gerding, D. N.** 2005. Metronidazole for *Clostridium difficile*-associated disease: is it okay for Mom? Clin Infect Dis **40:**1598-600.

49. **Giannasca, P. J., and M. Warny.** 2004. Active and passive immunization against *Clostridium difficile* diarrhea and colitis. Vaccine **22:**848-56.

50. **Giannasca, P. J., Z. X. Zhang, W. D. Lei, J. A. Boden, M. A. Giel, T. P. Monath, and W. D. Thomas, Jr.** 1999. Serum antitoxin antibodies mediate systemic and mucosal protection from *Clostridium difficile* disease in hamsters. Infect Immun **67:**527-38.

51. **Goldman, E. R., G. P. Anderson, J. Conway, L. J. Sherwood, M. Fech, B. Vo, J. L. Liu, and A. Hayhurst.** 2008. Thermostable llama single domain antibodies for detection of botulinum A neurotoxin complex. Anal Chem **80:**8583-91.

52. **Goldman, E. R., G. P. Anderson, J. L. Liu, J. B. Delehanty, L. J. Sherwood, L. E. Osborn, L. B. Cummins, and A. Hayhurst.** 2006. Facile generation of heat-stable antiviral and antitoxin single domain antibodies from a semisynthetic llama library. Anal Chem **78:**8245-55.

53. **Greco, A., J. G. Ho, S. J. Lin, M. M. Palcic, M. Rupnik, and K. K. Ng.** 2006. Carbohydrate recognition by *Clostridium difficile* toxin A. Nat Struct Mol Biol **13:**460-1.

54. **Greenfield, N. J.** 2006. Analysis of the kinetics of folding of proteins and peptides using circular dichroism. Nat Protoc **1:**2891-9.

55. **Greenfield, N. J.** 2006. Using circular dichroism spectra to estimate protein secondary structure. Nat Protoc **1:**2876-90.

56. **Guarino, A., A. Lo Vecchio, and R. B. Canani.** 2009. Probiotics as prevention and treatment for diarrhea. Curr Opin Gastroenterol **25:**18-23.

57. **Hagihara, Y., S. Mine, and K. Uegaki.** 2007. Stabilization of an immunoglobulin fold domain by an engineered disulfide bond at the buried hydrophobic region. J Biol Chem **282:**36489-95.

58. **Hamers-Casterman, C., T. Atarhouch, S. Muyldermans, G. Robinson, C. Hamers, E. B. Songa, N. Bendahman, and R. Hamers.** 1993. Naturally occurring antibodies devoid of light chains. Nature **363:**446-8.

59. **Harmsen, M. M., and H. J. De Haard.** 2007. Properties, production, and applications of camelid single-domain antibody fragments. Appl Microbiol Biotechnol **77:**13-22.

60. **Harmsen, M. M., H. P. Fijten, B. Engel, A. Dekker, and P. L. Eble.** 2009. Passive immunization with llama single-domain antibody fragments reduces foot-and-mouth disease transmission between pigs. Vaccine **27:**1904-11.

61. **Harmsen, M. M., R. C. Ruuls, I. J. Nijman, T. A. Niewold, L. G. Frenken, and B. de Geus.** 2000. Llama heavy-chain V regions consist of at least four distinct subfamilies revealing novel sequence features. Mol Immunol **37:**579-90.

62. **Harmsen, M. M., C. B. van Solt, and H. P. Fijten.** 2009. Enhancement of toxin- and virus-neutralizing capacity of single-domain antibody fragments by N-glycosylation. Appl Microbiol Biotechnol **84:**1087-94.

63. **Harmsen, M. M., C. B. van Solt, A. Hoogendoorn, F. G. van Zijderveld, T. A. Niewold, and J. van der Meulen.** 2005. *Escherichia coli* F4 fimbriae specific llama single-domain antibody fragments effectively inhibit bacterial adhesion *in vitro* but poorly protect against diarrhoea. Vet Microbiol **111:**89-98.

64. **Harmsen, M. M., C. B. van Solt, A. M. van Zijderveld-van Bemmel, T. A. Niewold, and F. G. van Zijderveld.** 2006. Selection and optimization of proteolytically stable

llama single-domain antibody fragments for oral immunotherapy. Appl Microbiol Biotechnol **72:**544-51.

65. **Hassoun, A., and F. Ibrahim.** 2007. Use of intravenous immunoglobulin for the treatment of severe *Clostridium difficile* colitis. Am J Geriatr Pharmacother **5:**48-51.

66. **Hecht, G., A. Koutsouris, C. Pothoulakis, J. T. LaMont, and J. L. Madara.** 1992. *Clostridium difficile* toxin B disrupts the barrier function of T84 monolayers. Gastroenterology **102:**416-23.

67. **Hinkson, P. L., C. Dinardo, D. DeCiero, J. D. Klinger, and R. H. Barker, Jr.** 2008. Tolevamer, an anionic polymer, neutralizes toxins produced by the BI/027 strains of *Clostridium difficile*. Antimicrob Agents Chemother **52:**2190-5.

68. **Hmila, I., R. B. Abdallah, D. Saerens, Z. Benlasfar, K. Conrath, M. E. Ayeb, S. Muyldermans, and B. Bouhaouala-Zahar.** 2008. VHH, bivalent domains and chimeric Heavy chain-only antibodies with high neutralizing efficacy for scorpion toxin AahI'. Mol Immunol **45:**3847-56.

69. **Hmila, I., D. Saerens, R. Ben Abderrazek, C. Vincke, N. Abidi, Z. Benlasfar, J. Govaert, M. El Ayeb, B. Bouhaouala-Zahar, and S. Muyldermans.** 2010. A bispecific nanobody to provide full protection against lethal scorpion envenoming. FASEB J **24:**3479-89.

70. **Ho, J. G., A. Greco, M. Rupnik, and K. K. Ng.** 2005. Crystal structure of receptor-binding C-terminal repeats from *Clostridium difficile* toxin A. Proc Natl Acad Sci U S A **102:**18373-8.

71. **Ho, S. N., H. D. Hunt, R. M. Horton, J. K. Pullen, and L. R. Pease.** 1989. Site-directed mutagenesis by overlap extension using the polymerase chain reaction. Gene **77:**51-9.

72. **Holliger, P., and P. J. Hudson.** 2005. Engineered antibody fragments and the rise of single domains. Nat Biotechnol **23:**1126-36.

73. **Holt, L. J., C. Herring, L. S. Jespers, B. P. Woolven, and I. M. Tomlinson.** 2003. Domain antibodies: proteins for therapy. Trends Biotechnol **21:**484-90.

74. **Hoogenboom, H. R.** 2005. Selecting and screening recombinant antibody libraries. Nat Biotechnol **23:**1105-16.

75. **Hubbard, S. J., R. J. Beynon, and J. M. Thornton.** 1998. Assessment of conformational parameters as predictors of limited proteolytic sites in native protein structures. Protein Eng **11:**349-59.

76. **Hudson, D. L., A. N. Layton, T. R. Field, A. J. Bowen, H. Wolf-Watz, M. Elofsson, M. P. Stevens, and E. E. Galyov.** 2007. Inhibition of type III secretion in *Salmonella enterica* serovar Typhimurium by small-molecule inhibitors. Antimicrob Agents Chemother **51:**2631-5.

77. **Hussack, G., M. Arbabi-Ghahroudi, H. van Faassen, J. G. Songer, K. K. Ng, R. Mackenzie, and J. Tanha.** 2011. Neutralization of *Clostridium difficile* toxin A with single-domain antibodies targeting the cell receptor binding domain. J Biol Chem **286:**8961-76.

78. **Hussack, G., Y. Lou, L. Veldhuis, J. C. Hall, J. Tanha, and R. MacKenzie.** 2009. Multivalent anchoring and oriented display of single-domain antibodies on cellulose. Sensors **9:**4351-5367.

79. **Hussack, G., C. R. Mackenzie, and J. Tanha.** 2011. Characterization of single-domain antibodies with an engineered disulfide bond. Methods Mol Biol (in press).

80. **Jank, T., and K. Aktories.** 2008. Structure and mode of action of clostridial glucosylating toxins: the ABCD model. Trends Microbiol **16:**222-9.

81. **Jank, T., T. Giesemann, and K. Aktories.** 2007. Rho-glucosylating *Clostridium difficile* toxins A and B: new insights into structure and function. Glycobiology **17:**15R-22R.

82. **Jermutus, L., A. Honegger, F. Schwesinger, J. Hanes, and A. Pluckthun.** 2001. Tailoring in vitro evolution for protein affinity or stability. Proc Natl Acad Sci U S A **98:**75-80.

83. **Jespers, L., O. Schon, K. Famm, and G. Winter.** 2004. Aggregation-resistant domain antibodies selected on phage by heat denaturation. Nat Biotechnol **22:**1161-5.

84. **Johal, S. S., C. P. Lambert, J. Hammond, P. D. James, S. P. Borriello, and Y. R. Mahida.** 2004. Colonic IgA producing cells and macrophages are reduced in recurrent and non-recurrent *Clostridium difficile* associated diarrhoea. J Clin Pathol **57:**973-9.

85. **Johnson, S.** 2009. Recurrent *Clostridium difficile* infection: a review of risk factors, treatments, and outcomes. J Infect **58:**403-10.

86. **Johnson, S., W. D. Sypura, D. N. Gerding, S. L. Ewing, and E. N. Janoff.** 1995. Selective neutralization of a bacterial enterotoxin by serum immunoglobulin A in response to mucosal disease. Infect Immun **63:**3166-73.

87. **Juang, P., S. J. Skledar, N. K. Zgheib, D. L. Paterson, E. N. Vergis, W. D. Shannon, N. T. Ansani, and R. A. Branch.** 2007. Clinical outcomes of intravenous immune globulin in severe *Clostridium difficile*-associated diarrhea. Am J Infect Control **35:**131-7.

88. **Jung, S., A. Honegger, and A. Pluckthun.** 1999. Selection for improved protein stability by phage display. J Mol Biol **294:**163-80.

89. **Just, I., J. Selzer, M. Wilm, C. von Eichel-Streiber, M. Mann, and K. Aktories.** 1995. Glucosylation of Rho proteins by *Clostridium difficile* toxin B. Nature **375:**500-3.

90. **Kamiya, S., K. Yamakawa, X. Q. Meng, H. Ogura, and S. Nakamura.** 1991. Production of monoclonal antibody to *Clostridium difficile* toxin A which neutralizes enterotoxicity but not haemagglutination activity. FEMS Microbiol Lett **65:**311-5.

91. **Katchar, K., C. P. Taylor, S. Tummala, X. Chen, J. Sheikh, and C. P. Kelly.** 2007. Association between IgG2 and IgG3 subclass responses to toxin A and recurrent *Clostridium difficile*-associated disease. Clin Gastroenterol Hepatol **5:**707-13.

92. **Keel, M. K., and J. G. Songer.** 2007. The distribution and density of *Clostridium difficile* toxin receptors on the intestinal mucosa of neonatal pigs. Vet Pathol **44:**814-22.

93. **Kelly, C. P., C. Pothoulakis, and J. T. LaMont.** 1994. *Clostridium difficile* colitis. N Engl J Med **330:**257-62.

94. **Kelly, C. P., C. Pothoulakis, J. Orellana, and J. T. LaMont.** 1992. Human colonic aspirates containing immunoglobulin A antibody to *Clostridium difficile* toxin A inhibit toxin A-receptor binding. Gastroenterology **102:**35-40.

95. **Kelly, C. P., C. Pothoulakis, F. Vavva, I. Castagliuolo, E. F. Bostwick, J. C. O'Keane, S. Keates, and J. T. LaMont.** 1996. Anti-*Clostridium difficile* bovine immunoglobulin concentrate inhibits cytotoxicity and enterotoxicity of *C. difficile* toxins. Antimicrob Agents Chemother **40:**373-9.

96. **Kim, D. Y., W. Ding, and J. Tanha.** 2011. Solubility and stability engineering of human VH domains. Methods Mol Biol **Submitted**.

97. **Kim, P. H., J. P. Iaconis, and R. D. Rolfe.** 1987. Immunization of adult hamsters against *Clostridium difficile*-associated ileocecitis and transfer of protection to infant hamsters. Infect Immun **55:**2984-92.

98. **Kim, P. H., and R. D. Rolfe.** 1989. Characterization of protective antibodies in hamsters immunized against *C. difficile* toxins A and B. Microb. Ecol. Health Dis. **2:**13.

99. **Kink, J. A., and J. A. Williams.** 1998. Antibodies to recombinant *Clostridium difficile* toxins A and B are an effective treatment and prevent relapse of *C. difficile*-associated disease in a hamster model of infection. Infect Immun **66:**2018-25.

100. **Koch-Nolte, F., J. Reyelt, B. Schossow, N. Schwarz, F. Scheuplein, S. Rothenburg, F. Haag, V. Alzogaray, A. Cauerhff, and F. A. Goldbaum.** 2007. Single domain antibodies from llama effectively and specifically block T cell ecto-ADP-ribosyltransferase ART2.2 in vivo. FASEB J **21:**3490-8.

101. **Koide, A., V. Tereshko, S. Uysal, K. Margalef, A. A. Kossiakoff, and S. Koide.** 2007. Exploring the capacity of minimalist protein interfaces: interface energetics and affinity maturation to picomolar KD of a single-domain antibody with a flat paratope. J Mol Biol **373:**941-53.

102. **Koulaouzidis, A., R. Tatham, J. Moschos, and C. W. Tan.** 2008. Successful treatment of *Clostridium difficile* colitis with intravenous immunoglobulin. J Gastrointestin Liver Dis **17:**353-5.

103. **Krivan, H. C., G. F. Clark, D. F. Smith, and T. D. Wilkins.** 1986. Cell surface binding site for *Clostridium difficile* enterotoxin: evidence for a glycoconjugate containing the sequence Gal alpha 1-3Gal beta 1-4GlcNAc. Infect Immun **53:**573-81.

104. **Kruger, C., Y. Hu, Q. Pan, H. Marcotte, A. Hultberg, D. Delwar, P. J. van Dalen, P. H. Pouwels, R. J. Leer, C. G. Kelly, C. van Dollenweerd, J. K. Ma, and L. Hammarstrom.** 2002. In situ delivery of passive immunity by lactobacilli producing single-chain antibodies. Nat Biotechnol **20:**702-6.

105. **Kruger, C., A. Hultberg, H. Marcotte, P. Hermans, S. Bezemer, L. G. Frenken, and L. Hammarstrom.** 2006. Therapeutic effect of llama derived VHH fragments against *Streptococcus mutans* on the development of dental caries. Appl Microbiol Biotechnol **72:**732-7.

106. **Kuehne, S. A., S. T. Cartman, J. T. Heap, M. L. Kelly, A. Cockayne, and N. P. Minton.** 2010. The role of toxin A and toxin B in *Clostridium difficile* infection. Nature **467:**711-3.

107. **Kurtz, C. B., E. P. Cannon, A. Brezzani, M. Pitruzzello, C. Dinardo, E. Rinard, D. W. Acheson, R. Fitzpatrick, P. Kelly, K. Shackett, A. T. Papoulis, P. J. Goddard, R. H. Barker, Jr., G. P. Palace, and J. D. Klinger.** 2001. GT160-246, a toxin binding polymer for treatment of *Clostridium difficile* colitis. Antimicrob Agents Chemother **45:**2340-7.

108. **Kyne, L.** 2010. *Clostridium difficile*--beyond antibiotics. N Engl J Med **362:**264-5.

109. **Kyne, L., M. B. Hamel, R. Polavaram, and C. P. Kelly.** 2002. Health care costs and mortality associated with nosocomial diarrhea due to *Clostridium difficile*. Clin Infect Dis **34:**346-53.

110. **Kyne, L., M. Warny, A. Qamar, and C. P. Kelly.** 2001. Association between antibody response to toxin A and protection against recurrent *Clostridium difficile* diarrhoea. Lancet **357:**189-93.

111. **Lee, A. S., and K. P. Song.** 2005. LuxS/autoinducer-2 quorum sensing molecule regulates transcriptional virulence gene expression in *Clostridium difficile*. Biochem Biophys Res Commun **335:**659-66.

112. **Leffler, D. A., and J. T. Lamont.** 2009. Treatment of *Clostridium difficile*-associated disease. Gastroenterology **136:**1899-912.

113. **Leung, D. Y., C. P. Kelly, M. Boguniewicz, C. Pothoulakis, J. T. LaMont, and A. Flores.** 1991. Treatment with intravenously administered gamma globulin of chronic relapsing colitis induced by *Clostridium difficile* toxin. J Pediatr **118:**633-7.

114. **Li, S., W. Zheng, R. Kuolee, T. Hirama, M. Henry, S. Makvandi-Nejad, T. Fjallman, W. Chen, and J. Zhang.** 2009. Pentabody-mediated antigen delivery induces antigen-specific mucosal immune response. Mol Immunol **46:**1718-26.

115. **Liu, J. L., G. P. Anderson, and E. R. Goldman.** 2007. Isolation of anti-toxin single domain antibodies from a semi-synthetic spiny dogfish shark display library. BMC Biotechnol **7:**78.

116. **Liu, T., Z. Guo, Q. Yang, S. Sad, and H. J. Jennings.** 2000. Biochemical engineering of surface alpha 2-8 polysialic acid for immunotargeting tumor cells. J Biol Chem **275:**32832-6.

117. **Louie, T. J., M. A. Miller, K. M. Mullane, K. Weiss, A. Lentnek, Y. Golan, S. Gorbach, P. Sears, and Y. K. Shue.** 2011. Fidaxomicin versus vancomycin for *Clostridium difficile* infection. N Engl J Med **364:**422-31.

118. **Lowy, I., D. C. Molrine, B. A. Leav, B. M. Blair, R. Baxter, D. N. Gerding, G. Nichol, W. D. Thomas, Jr., M. Leney, S. Sloan, C. A. Hay, and D. M. Ambrosino.** 2010. Treatment with monoclonal antibodies against *Clostridium difficile* toxins. N Engl J Med **362:**197-205.

119. **Lyerly, D. M., E. F. Bostwick, S. B. Binion, and T. D. Wilkins.** 1991. Passive immunization of hamsters against disease caused by *Clostridium difficile* by use of bovine immunoglobulin G concentrate. Infect Immun **59:**2215-8.

120. **Lyerly, D. M., P. E. Carrig, and T. D. Wilkins.** 1989. Nonspecific binding of mouse monoclonal antibodies to *Clostridium difficile* toxins A and B. Curr Microbiol **19:**303-6.

121. **Lyerly, D. M., J. L. Johnson, S. M. Frey, and T. D. Wilkins.** 1990. Toxin A of *Clostridium difficile* is a potent cytotoxin. Curr Microbiol **21:**29-32.

122. **Lyerly, D. M., C. J. Phelps, J. Toth, and T. D. Wilkins.** 1986. Characterization of toxins A and B of *Clostridium difficile* with monoclonal antibodies. Infect Immun **54:**70-6.

123. **Lyerly, D. M., K. E. Saum, D. K. MacDonald, and T. D. Wilkins.** 1985. Effects of *Clostridium difficile* toxins given intragastrically to animals. Infect Immun **47:**349-52.

124. **Lynch, S. V., and J. P. Wiener-Kronish.** 2008. Novel strategies to combat bacterial virulence. Curr Opin Crit Care **14:**593-9.

125. **Lyon, G. J., J. S. Wright, T. W. Muir, and R. P. Novick.** 2002. Key determinants of receptor activation in the agr autoinducing peptides of *Staphylococcus aureus*. Biochemistry **41:**10095-104.

126. **Lyras, D., J. R. O'Connor, P. M. Howarth, S. P. Sambol, G. P. Carter, T. Phumoonna, R. Poon, V. Adams, G. Vedantam, S. Johnson, D. N. Gerding, and J. I. Rood.** 2009. Toxin B is essential for virulence of *Clostridium difficile*. Nature **458:**1176-9.

127. **Matsuura, T., and A. Pluckthun.** 2003. Selection based on the folding properties of proteins with ribosome display. FEBS Lett **539:**24-8.

128. **Mattila, E., V. J. Anttila, M. Broas, H. Marttila, P. Poukka, K. Kuusisto, L. Pusa, K. Sammalkorpi, J. Dabek, O. P. Koivurova, M. Vahatalo, V. Moilanen, and T. Widenius.** 2008. A randomized, double-blind study comparing *Clostridium difficile* immune whey and metronidazole for recurrent *Clostridium difficile*-associated

diarrhoea: efficacy and safety data of a prematurely interrupted trial. Scand J Infect Dis **40:**702-8.

129. **McDonald, L. C., G. E. Killgore, A. Thompson, R. C. Owens, Jr., S. V. Kazakova, S. P. Sambol, S. Johnson, and D. N. Gerding.** 2005. An epidemic, toxin gene-variant strain of *Clostridium difficile*. N Engl J Med **353:**2433-41.

130. **McPherson, S., C. J. Rees, R. Ellis, S. Soo, and S. J. Panter.** 2006. Intravenous immunoglobulin for the treatment of severe, refractory, and recurrent *Clostridium difficile* diarrhea. Dis Colon Rectum **49:**640-5.

131. **Moncino, M. D., and J. M. Falletta.** 1992. Multiple relapses of *Clostridium difficile*-associated diarrhea in a cancer patient. Successful control with long-term cholestyramine therapy. Am J Pediatr Hematol Oncol **14:**361-4.

132. **Murphy, C., M. Vernon, and M. Cullen.** 2006. Intravenous immunoglobulin for resistant *Clostridium difficile* infection. Age Ageing **35:**85-6.

133. **Muschiol, S., L. Bailey, A. Gylfe, C. Sundin, K. Hultenby, S. Bergstrom, M. Elofsson, H. Wolf-Watz, S. Normark, and B. Henriques-Normark.** 2006. A small-molecule inhibitor of type III secretion inhibits different stages of the infectious cycle of *Chlamydia trachomatis*. Proc Natl Acad Sci U S A **103:**14566-71.

134. **Musher, D. M., N. Logan, R. J. Hamill, H. L. Dupont, A. Lentnek, A. Gupta, and J. F. Rossignol.** 2006. Nitazoxanide for the treatment of *Clostridium difficile* colitis. Clin Infect Dis **43:**421-7.

135. **Muyldermans, S., C. Cambillau, and L. Wyns.** 2001. Recognition of antigens by single-domain antibody fragments: the superfluous luxury of paired domains. Trends Biochem Sci **26:**230-5.

136. **Nguyen, V. K., A. Desmyter, and S. Muyldermans.** 2001. Functional heavy-chain antibodies in Camelidae. Adv Immunol **79:**261-96.

137. **Ni Eidhin, D. B., J. B. O'Brien, M. S. McCabe, V. Athie-Morales, and D. P. Kelleher.** 2008. Active immunization of hamsters against *Clostridium difficile* infection using surface-layer protein. FEMS Immunol Med Microbiol **52:**207-18.

138. **Nowakowski, A., C. Wang, D. B. Powers, P. Amersdorfer, T. J. Smith, V. A. Montgomery, R. Sheridan, R. Blake, L. A. Smith, and J. D. Marks.** 2002. Potent neutralization of botulinum neurotoxin by recombinant oligoclonal antibody. Proc Natl Acad Sci U S A **99:**11346-50.

139. **Numan, S. C., P. Veldkamp, E. J. Kuijper, R. J. van den Berg, and J. T. van Dissel.** 2007. *Clostridium difficile*-associated diarrhoea: bovine anti-*Clostridium difficile* whey protein to help aid the prevention of relapses. Gut **56:**888-9.

140. **O'Connor, J. R., S. Johnson, and D. N. Gerding.** 2009. *Clostridium difficile* infection caused by the epidemic BI/NAP1/027 strain. Gastroenterology **136:**1913-24.

141. **O'Horo, J., and N. Safdar.** 2009. The role of immunoglobulin for the treatment of *Clostridium difficile* infection: a systematic review. Int J Infect Dis **13:**663-7.

142. **Ochsner, U. A., S. J. Bell, A. L. O'Leary, T. Hoang, K. C. Stone, C. L. Young, I. A. Critchley, and N. Janjic.** 2009. Inhibitory effect of REP3123 on toxin and spore formation in *Clostridium difficile*, and in vivo efficacy in a hamster gastrointestinal infection model. J Antimicrob Chemother **63:**964-71.

143. **Pace, C. N., F. Vajdos, L. Fee, G. Grimsley, and T. Gray.** 1995. How to measure and predict the molar absorption coefficient of a protein. Protein Sci **4:**2411-23.

144. **Panchal, R. G., A. R. Hermone, T. L. Nguyen, T. Y. Wong, R. Schwarzenbacher, J. Schmidt, D. Lane, C. McGrath, B. E. Turk, J. Burnett, M. J. Aman, S. Little, E. A. Sausville, D. W. Zaharevitz, L. C. Cantley, R. C. Liddington, R. Gussio, and S. Bavari.** 2004. Identification of small molecule inhibitors of anthrax lethal factor. Nat Struct Mol Biol **11:**67-72.

145. **Pant, N., A. Hultberg, Y. Zhao, L. Svensson, Q. Pan-Hammarstrom, K. Johansen, P. H. Pouwels, F. M. Ruggeri, P. Hermans, L. Frenken, T. Boren, H. Marcotte, and L. Hammarstrom.** 2006. Lactobacilli expressing variable domain of llama heavy-chain antibody fragments (lactobodies) confer protection against rotavirus-induced diarrhea. J Infect Dis **194:**1580-8.

146. **Parkes, G. C., J. D. Sanderson, and K. Whelan.** 2009. The mechanisms and efficacy of probiotics in the prevention of *Clostridium difficile*-associated diarrhoea. Lancet Infect Dis **9:**237-44.

147. **Pelaez, T., L. Alcala, R. Alonso, M. Rodriguez-Creixems, J. M. Garcia-Lechuz, and E. Bouza.** 2002. Reassessment of *Clostridium difficile* susceptibility to metronidazole and vancomycin. Antimicrob Agents Chemother **46:**1647-50.

148. **Pepin, J., L. Valiquette, and B. Cossette.** 2005. Mortality attributable to nosocomial *Clostridium difficile*-associated disease during an epidemic caused by a hypervirulent strain in Quebec. CMAJ **173:**1037-42.

149. **Peterson, J. W., K. E. Hejtmancik, D. E. Markel, J. P. Craig, and A. Kurosky.** 1979. Antigenic specificity of neutralizing antibody to cholera toxin. Infect Immun **24:**774-9.

150. **Pothoulakis, C.** 2000. Effects of *Clostridium difficile* toxins on epithelial cell barrier. Ann N Y Acad Sci **915:**347-56.

151. **Powers, D. B., P. Amersdorfer, M. Poul, U. B. Nielsen, M. R. Shalaby, G. P. Adams, L. M. Weiner, and J. D. Marks.** 2001. Expression of single-chain Fv-Fc fusions in Pichia pastoris. J Immunol Methods **251:**123-35.

152. **Pruitt, R. N., M. G. Chambers, K. K. Ng, M. D. Ohi, and D. B. Lacy.** 2010. Structural organization of the functional domains of *Clostridium difficile* toxins A and B. Proc Natl Acad Sci U S A **107:**13467-72.

153. **Rasko, D. A., and V. Sperandio.** 2010. Anti-virulence strategies to combat bacteria-mediated disease. Nat Rev Drug Discov **9:**117-28.

154. **Rea, M. C., C. S. Sit, E. Clayton, P. M. O'Connor, R. M. Whittal, J. Zheng, J. C. Vederas, R. P. Ross, and C. Hill.** 2010. Thuricin CD, a posttranslationally modified bacteriocin with a narrow spectrum of activity against *Clostridium difficile*. Proc Natl Acad Sci U S A **107:**9352-7.

155. **Reilly, R. M., R. Domingo, and J. Sandhu.** 1997. Oral delivery of antibodies. Future pharmacokinetic trends. Clin Pharmacokinet **32:**313-23.

156. **Reineke, J., S. Tenzer, M. Rupnik, A. Koschinski, O. Hasselmayer, A. Schrattenholz, H. Schild, and C. von Eichel-Streiber.** 2007. Autocatalytic cleavage of *Clostridium difficile* toxin B. Nature **446:**415-9.

157. **Rupnik, M., M. H. Wilcox, and D. N. Gerding.** 2009. *Clostridium difficile* infection: new developments in epidemiology and pathogenesis. Nat Rev Microbiol **7:**526-36.

158. **Ryan, S., A. J. Kell, H. van Faassen, L. L. Tay, B. Simard, R. MacKenzie, M. Gilbert, and J. Tanha.** 2009. Single-domain antibody-nanoparticles: promising architectures for increased *Staphylococcus aureus* detection specificity and sensitivity. Bioconjug Chem **20:**1966-74.

159. **Saerens, D., K. Conrath, J. Govaert, and S. Muyldermans.** 2008. Disulfide bond introduction for general stabilization of immunoglobulin heavy-chain variable domains. J Mol Biol **377:**478-88.

160. **Saerens, D., J. Kinne, E. Bosmans, U. Wernery, S. Muyldermans, and K. Conrath.** 2004. Single domain antibodies derived from dromedary lymph node and peripheral blood lymphocytes sensing conformational variants of prostate-specific antigen. J Biol Chem **279:**51965-72.

161. **Salcedo, J., S. Keates, C. Pothoulakis, M. Warny, I. Castagliuolo, J. T. LaMont, and C. P. Kelly.** 1997. Intravenous immunoglobulin therapy for severe *Clostridium difficile* colitis. Gut **41:**366-70.

162. **Salnikova, M. S., S. B. Joshi, J. H. Rytting, M. Warny, and C. R. Middaugh.** 2008. Physical characterization of *Clostridium difficile* toxins and toxoids: effect of the formaldehyde crosslinking on thermal stability. J Pharm Sci **97:**3735-52.

163. **Sambrook, J., E. F. Fritsch, and T. Maniatis (ed.).** 1989. Molecular Cloning: A Laboratory Manual. Cold Spring Harbor Laboratory, Cold Spring Harbor, NY.

164. **Scheinfeld, N., and K. Biggers.** 2008. Tolevamer, an orally administered, toxin-binding polymer for *Clostridium difficile*-associated diarrhea. Curr Opin Investig Drugs **9:**913-24.

165. **Schmidt, P., V. Wiedemann, R. Kuhlmann, R. Wanke, E. Linckh, and U. Losch.** 1989. Chicken egg antibodies for prophylaxis and therapy of infectious intestinal diseases. II. *In vitro* studies on gastric and enteric digestion of egg yolk antibodies specific against pathogenic Escherichia coli strains. Zentralbl Veterinarmed B **36:**619-28.

166. **Schneemann, A., and M. Manchester.** 2009. Anti-toxin antibodies in prophylaxis and treatment of inhalation anthrax. Future Microbiol **4:**35-43.

167. **Shoop, W. L., Y. Xiong, J. Wiltsie, A. Woods, J. Guo, J. V. Pivnichny, T. Felcetto, B. F. Michael, A. Bansal, R. T. Cummings, B. R. Cunningham, A. M. Friedlander, C. M. Douglas, S. B. Patel, D. Wisniewski, G. Scapin, S. P. Salowe, D. M. Zaller, K. T. Chapman, E. M. Scolnick, D. M. Schmatz, K. Bartizal, M. MacCoss, and J. D. Hermes.** 2005. Anthrax lethal factor inhibition. Proc Natl Acad Sci U S A **102:**7958-63.

168. **Sieber, V., A. Pluckthun, and F. X. Schmid.** 1998. Selecting proteins with improved stability by a phage-based method. Nat Biotechnol **16:**955-60.

169. **Songer, J. G.** 2004. The emergence of *Clostridium difficile* as a pathogen of food animals. Anim Health Res Rev **5:**321-6.

170. **Sougioultzis, S., L. Kyne, D. Drudy, S. Keates, S. Maroo, C. Pothoulakis, P. J. Giannasca, C. K. Lee, M. Warny, T. P. Monath, and C. P. Kelly.** 2005. *Clostridium*

difficile toxoid vaccine in recurrent *C. difficile*-associated diarrhea. Gastroenterology **128:**764-70.

171. **Spinelli, S., L. G. Frenken, P. Hermans, T. Verrips, K. Brown, M. Tegoni, and C. Cambillau.** 2000. Camelid heavy-chain variable domains provide efficient combining sites to haptens. Biochemistry **39:**1217-22.

172. **Stanfield, R. L., H. Dooley, M. F. Flajnik, and I. A. Wilson.** 2004. Crystal structure of a shark single-domain antibody V region in complex with lysozyme. Science **305:**1770-3.

173. **Steidler, L., S. Neirynck, N. Huyghebaert, V. Snoeck, A. Vermeire, B. Goddeeris, E. Cox, J. P. Remon, and E. Remaut.** 2003. Biological containment of genetically modified *Lactococcus lactis* for intestinal delivery of human interleukin 10. Nat Biotechnol **21:**785-9.

174. **Stewart, C. S., C. R. MacKenzie, and J. C. Hall.** 2007. Isolation, characterization and pentamerization of alpha-cobrotoxin specific single-domain antibodies from a naive phage display library: preliminary findings for antivenom development. Toxicon **49:**699-709.

175. **Stijlemans, B., K. Conrath, V. Cortez-Retamozo, H. Van Xong, L. Wyns, P. Senter, H. Revets, P. De Baetselier, S. Muyldermans, and S. Magez.** 2004. Efficient targeting of conserved cryptic epitopes of infectious agents by single domain antibodies. African trypanosomes as paradigm. J Biol Chem **279:**1256-61.

176. **Stone, E., T. Hirama, W. Chen, A. L. Soltyk, J. Brunton, C. R. MacKenzie, and J. Zhang.** 2007. A novel pentamer versus pentamer approach to generating neutralizers of verotoxin 1. Mol Immunol **44:**2487-91.

177. **Strockbine, N. A., L. R. Marques, R. K. Holmes, and A. D. O'Brien.** 1985. Characterization of monoclonal antibodies against Shiga-like toxin from *Escherichia coli*. Infect Immun **50:**695-700.

178. **Sullivan, K. M., and L. M. Spooner.** 2010. Fidaxomicin: a macrocyclic antibiotic for the management of *Clostridium difficile* infection. Ann Pharmacother **44:**352-9.

179. **Svensson, A., A. Larsson, H. Emtenas, M. Hedenstrom, T. Fex, S. J. Hultgren, J. S. Pinkner, F. Almqvist, and J. Kihlberg.** 2001. Design and evaluation of pilicides: potential novel antibacterial agents directed against uropathogenic *Escherichia coli*. Chembiochem **2:**915-8.

180. **Tacket, C. O., S. B. Binion, E. Bostwick, G. Losonsky, M. J. Roy, and R. Edelman.** 1992. Efficacy of bovine milk immunoglobulin concentrate in preventing illness after Shigella flexneri challenge. Am J Trop Med Hyg **47:**276-83.

181. **Tacket, C. O., G. Losonsky, H. Link, Y. Hoang, P. Guesry, H. Hilpert, and M. M. Levine.** 1988. Protection by milk immunoglobulin concentrate against oral challenge with enterotoxigenic Escherichia coli. N Engl J Med **318:**1240-3.

182. **Thiagarajah, J. R., and A. S. Verkman.** 2005. New drug targets for cholera therapy. Trends Pharmacol Sci **26:**172-5.

183. **Tjellstrom, B., L. Stenhammar, S. Eriksson, and K. E. Magnusson.** 1993. Oral immunoglobulin A supplement in treatment of *Clostridium difficile* enteritis. Lancet **341:**701-2.

184. **To, R., T. Hirama, M. Arbabi-Ghahroudi, R. MacKenzie, P. Wang, P. Xu, F. Ni, and J. Tanha.** 2005. Isolation of monomeric human V(H)s by a phage selection. J Biol Chem **280:**41395-403.

185. **Tucker, K. D., and T. D. Wilkins.** 1991. Toxin A of *Clostridium difficile* binds to the human carbohydrate antigens I, X, and Y. Infect Immun **59:**73-8.

186. **Tung, J. M., L. R. Dolovich, and C. H. Lee.** 2009. Prevention of *Clostridium difficile* infection with Saccharomyces boulardii: a systematic review. Can J Gastroenterol **23:**817-21.

187. **Tung, W. L., and K. C. Chow.** 1995. A modified medium for efficient electrotransformation of *E. coli*. Trends Genet **11:**128-9.

188. **Van Bockstaele, F., J. B. Holz, and H. Revets.** 2009. The development of nanobodies for therapeutic applications. Curr Opin Investig Drugs **10:**1212-24.

189. **van der Vaart, J. M., N. Pant, D. Wolvers, S. Bezemer, P. W. Hermans, K. Bellamy, S. A. Sarker, C. P. van der Logt, L. Svensson, C. T. Verrips, L. Hammarstrom, and B. J. van Klinken.** 2006. Reduction in morbidity of rotavirus induced diarrhoea in mice by yeast produced monovalent llama-derived antibody fragments. Vaccine **24:**4130-7.

190. **van Dissel, J. T., N. de Groot, C. M. Hensgens, S. Numan, E. J. Kuijper, P. Veldkamp, and J. van 't Wout.** 2005. Bovine antibody-enriched whey to aid in the prevention of a relapse of *Clostridium difficile*-associated diarrhoea: preclinical and preliminary clinical data. J Med Microbiol **54:**197-205.

191. **Viscidi, R., B. E. Laughon, R. Yolken, P. Bo-Linn, T. Moench, R. W. Ryder, and J. G. Bartlett.** 1983. Serum antibody response to toxins A and B of *Clostridium difficile*. J Infect Dis **148:**93-100.

192. **Voth, D. E., and J. D. Ballard.** 2005. *Clostridium difficile* toxins: mechanism of action and role in disease. Clin Microbiol Rev **18:**247-63.

193. **Vu, K. B., M. A. Ghahroudi, L. Wyns, and S. Muyldermans.** 1997. Comparison of llama VH sequences from conventional and heavy chain antibodies. Mol Immunol **34:**1121-31.

194. **Ward, E. S., D. Gussow, A. D. Griffiths, P. T. Jones, and G. Winter.** 1989. Binding activities of a repertoire of single immunoglobulin variable domains secreted from Escherichia coli. Nature **341:**544-6.

195. **Ward, S. J., G. Douce, G. Dougan, and B. W. Wren.** 1999. Local and systemic neutralizing antibody responses induced by intranasal immunization with the nontoxic binding domain of toxin A from *Clostridium difficile*. Infect Immun **67:**5124-32.

196. **Warny, M., A. Fatimi, E. F. Bostwick, D. C. Laine, F. Lebel, J. T. LaMont, C. Pothoulakis, and C. P. Kelly.** 1999. Bovine immunoglobulin concentrate-*Clostridium difficile* retains *C. difficile* toxin neutralising activity after passage through the human stomach and small intestine. Gut **44:**212-7.

197. **Warny, M., J. Pepin, A. Fang, G. Killgore, A. Thompson, J. Brazier, E. Frost, and L. C. McDonald.** 2005. Toxin production by an emerging strain of *Clostridium difficile* associated with outbreaks of severe disease in North America and Europe. Lancet **366:**1079-84.

198. **Warny, M., J. P. Vaerman, V. Avesani, and M. Delmee.** 1994. Human antibody response to *Clostridium difficile* toxin A in relation to clinical course of infection. Infect Immun **62:**384-9.

199. **Werle, M., A. Makhlof, and H. Takeuchi.** 2009. Oral protein delivery: a patent review of academic and industrial approaches. Recent Pat Drug Deliv Formul **3:**94-104.

200. **Wesolowski, J., V. Alzogaray, J. Reyelt, M. Unger, K. Juarez, M. Urrutia, A. Cauerhff, W. Danquah, B. Rissiek, F. Scheuplein, N. Schwarz, S. Adriouch, O. Boyer, M. Seman, A. Licea, D. V. Serreze, F. A. Goldbaum, F. Haag, and F. Koch-Nolte.** 2009. Single domain antibodies: promising experimental and therapeutic tools in infection and immunity. Med Microbiol Immunol **198:**157-74.

201. **Wilcox, M. H.** 2004. Descriptive study of intravenous immunoglobulin for the treatment of recurrent *Clostridium difficile* diarrhoea. J Antimicrob Chemother **53:**882-4.

202. **Wilkins, T. D., and D. M. Lyerly.** 2003. *Clostridium difficile* testing: after 20 years, still challenging. J Clin Microbiol **41:**531-4.

203. **Worn, A., and A. Pluckthun.** 1998. Mutual stabilization of VL and VH in single-chain antibody fragments, investigated with mutants engineered for stability. Biochemistry **37:**13120-7.

204. **Wu, S. L., H. Jiang, Q. Lu, S. Dai, W. S. Hancock, and B. L. Karger.** 2009. Mass spectrometric determination of disulfide linkages in recombinant therapeutic proteins using online LC-MS with electron-transfer dissociation. Anal Chem **81:**112-22.

205. **Yokoyama, H., R. C. Peralta, R. Diaz, S. Sendo, Y. Ikemori, and Y. Kodama.** 1992. Passive protective effect of chicken egg yolk immunoglobulins against experimental enterotoxigenic Escherichia coli infection in neonatal piglets. Infect Immun **60:**998-1007.

206. **Yoshida, M., K. Kobayashi, T. T. Kuo, L. Bry, J. N. Glickman, S. M. Claypool, A. Kaser, T. Nagaishi, D. E. Higgins, E. Mizoguchi, Y. Wakatsuki, D. C. Roopenian, A. Mizoguchi, W. I. Lencer, and R. S. Blumberg.** 2006. Neonatal Fc receptor for IgG regulates mucosal immune responses to luminal bacteria. J Clin Invest **116:**2142-2151.

207. **Young, N. M., C. R. MacKenzie, S. A. Narang, R. P. Oomen, and J. E. Baenziger.** 1995. Thermal stabilization of a single-chain Fv antibody fragment by introduction of a disulphide bond. FEBS Lett **377:**135-9.

208. **Zhang, J., R. MacKenzie, and Y. Durocher.** 2009. Production of chimeric heavy-chain antibodies. Methods Mol Biol **525:**323-36, xv.

CONTRIBUTIONS OF COLLABORATORS

The following section details individual collaborators and their role in this thesis.

1. Glenn Songer (University of Arizona) provided recombinant and native *C. difficile* toxins.
2. Mehdi Arbabi-Ghahroudi, Hong Tong-Sevinc, and Nathalie Gaudette (NRC) assisted with llama immunization and V_HH immune library construction.
3. Sonia Leclerc (NRC) performed all DNA sequencing.
4. Tomoko Hirama and Henk van Fassen (NRC) assisted with SEC and SPR analyses.
5. Kenneth Ng and colleagues (University of Alberta) provided the TcdA-binding carbohydrates.
6. Jamshid Tanha and Artine Keklikian (NRC) provided the synthetic V_L display library.
7. John Kelly and Wen Ding (NRC) assisted with mass spectrometry experiments.

APPENDIX 1

Appendix 1 contains recipes for all culture medium, buffers, and other solutions used in this work.

CULTURE MEDIUM AND ANTIBIOTICS

Ampicillin
100 mg/mL, filter-sterilize, store at -20°C in 1 mL aliquots.

ddH_2O
Distilled, deionized H_2O.

Kanamycin
50 mg/mL, filter-sterilize, store at -20°C in 1 mL aliquots.

LB-Amp medium
10 g tryptone, 5 g yeast extract, 10 g NaCl, in 1 L of ddH_2O. Autoclave, cool to ~55°C, add ampicillin to 100 μg/mL final.

LB-Amp plates
10 g tryptone, 5 g yeast extract, 10 g NaCl, 15 g agar, in 1 L of ddH_2O. Autoclave, cool to ~55°C, add ampicillin to 100 μg/mL final, pour plates, store at 4°C for up to a month.

M9 salts (10x)
60 g Na_2HPO_4, 30 g KH_2PO_4, 10 g NH_4Cl, 5 g NaCl, in 1 L of ddH_2O. Filter-sterilize and store at room temperature.

M9 expression medium
100 mL 10x M9 salts, 1 mL ampicillin (100 mg/mL stock), 1 mL 1 M $MgCl_2$, 0.1 mL 1 M $CaCl_2$, 5 mL vitamin B1 (1 mg/mL stock), 10 mL 20% (w/v) glucose, 20 mL 20% (w/v) casamino acids, in 1 L of ddH_2O. Autoclave 864 mL of ddH_2O and 100 mL of M9 salts, cool to room temperature and add remaining ingredients.

SOC medium
20 g tryptone, 5 g yeast extract, 0.58 g NaCl, 0.19 g KCl, in 1 L of ddH_2O. Autoclave, cool and add 0.4% filter-sterilized glucose, 10 mM filter-sterilized $MgCl_2$. Store at -20°C in 1 mL aliquots.

2xYT medium
16 g tryptone, 10 g yeast extract, 5 g NaCl, in 1 L of ddH_2O. Autoclave to sterilize.

2xYT-Amp-Kan medium
2xYT + 100 μg/mL ampicillin + 50 μg/mL kanamycin.

2xYT-Amp-Glu medium
2xYT + 100 μg/mL ampicillin + 2% (w/v) filter-sterilized glucose.

2xYT-Amp plates
2xYT medium, 15 g agar, in 1 L of ddH_2O. Autoclave, cool to ~55°C, add ampicillin to a final concentration of 100 μg/mL, pour plates, store at 4°C for up to a month.

BUFFERS

Blocking buffer A
5% (w/v) BSA in PBS-T. Filter-sterilize, store at 4°C.

Blocking buffer B
PBS + 1% (w/v) casein. Autoclave to sterilize.

Blocking buffer C
PBS + 3% (w/v) skim milk powder.

BSA (5 mg/mL)
5 mg BSA in 1 mL PBS. Filter-sterilize, store at 4°C.

Buffer P
1.4 g Na_2HPO_4, 0.24 g KH_2PO_4, pH 7.3, in 1 L ddH_2O. Filter-sterilize, store at room temperature.

Citrate buffer (100 mM)
3.11 g citric acid, 1.53 g sodium citrate, pH 3.5, in 200 mL of ddH_2O. Adjust to pH 3.5 with 1 M NaOH, filter-sterilize, store at 4°C.

Glycine buffer (100 mM)
1.5 g glycine, pH 2.7, in 200 mL of ddH_2O. Adjust to pH 2.7 with 3 M HCl, filter-sterilize, store at 4°C.

HBS-EP buffer
10 mM HEPES pH 7.4, 150 mM NaCl, 3 mM EDTA, 0.005% (v/v) P20 surfactant. This buffer can be purchased from GE Healthcare. The buffer should be thoroughly degassed before use.

IMAC buffer A
29.4 g NaCl, 10 mL 1 M HEPES pH 8.0, in 1 L of ddH_2O. Filter-sterilize, degass, and store at room temperature.

IMAC buffer B
IMAC buffer A, 500 mM imidazole, pH 8.0, in 1 L of ddH_2O. Filter-sterilize, degass, and store at room temperature.

Lysis buffer
50 mL 1 M Tris-HCl pH 7.4, 1.46 g NaCl, 4 mL 0.5 M EDTA, in 1 L of ddH_2O.

NaPi buffer (20 mM)
8.46 mL 1 M NaH_2PO_4, 11.54 mL 1 M Na_2HPO_4, in 1 L of ddH_2O (pH 7.0).

Phosphate-buffered saline (PBS)
8 g NaCl, 0.2 g KCl, 1.4 g Na_2HPO_4, 0.24 g KH_2PO_4, in 1 L of ddH_2O (pH 7.3).

PBS-T
PBS + 0.05% (v/v) Tween 20.

PEG/NaCl
20% (v/v) PEG 8000, 146.1 g NaCl, in 1 L of ddH_2O. Autoclave, store at room temperature.

PreScission™ protease cleavage buffer (10x)
500 mM Tris-HCl pH 7, 1.5 M NaCl, 10 mM EDTA, 10 mM DTT. Filter-sterilize, store at 4°C.

Reduced glutathione elution buffer
1.51 g Tris-HCl, 0.77 g reduced glutathione, in 250 mL of ddH_2O. Adjust to pH 8.0 with 3 M HCl and store at room temperature protected from light.

Sodium acetate buffer (100 mM)
2.7 g sodium acetate, pH 4.5, in 200 mL of ddH_2O. Adjust to pH 4.5 with acetic acid, filter-sterilize, store at 4°C.

TES buffer
0.2 M Tris-HCl buffer pH 8.0, 20% (w/v) sucrose, 0.5 mM EDTA. Filter-sterilize, and store at room temperature.

Tris-HCl buffer (1 M, pH 8.8)
24.1 g Tris-base, pH 8.8, in 200 mL of ddH_2O. Adjust to pH 8.8 with 3 M HCl, filter-sterilize, store at 4°C.

Tris-HCl buffer (1 M, pH 7.4)
121.4 g Tris-base, pH 7.4, in 1 L of ddH_2O. Adjust to pH 7.4 with 3 M HCl, filter-sterilize, store at 4°C.

OTHER SOLUTIONS

Cyanogen bromide (CNBr)
10 mg/mL CNBr stock prepared in 0.1 M HCl. Protect from light and store at 4°C.

Native-PAGE sample buffer (3x)
0.5 mL 1% (w/v) Bromophenol Blue, 0.6 mL 0.5 M Tris-HCl, pH 6.8, 2.9 mL 50% glycerol, 1 mL ddH_2O.

Native-PAGE running buffer
14.4 g glycine, 3.03 g Tris-base, in 1 L of ddH_2O. Store at room temperature.

SDS-PAGE sample buffer (3x)
0.5 mL 1% (w/v) Bromophenol Blue, 0.6 mL 0.5 M Tris-HCl (pH 6.8), 2.9 mL 50% glycerol, 0.5 mL 10% (w/v) SDS, 0.5 mL ddH_2O.

SDS-PAGE running buffer
14.4 g glycine, 3.03 g Tris-base, 1 g SDS, in 1 L of ddH_2O. Store at room temperature.

APPENDIX 2

Appendix 2 contains the amino acid sequences of all toxins, recombinant toxins, and single-domain antibodies (V_HHs and V_LS) used in this work.

TcdA (*C. difficile* strain 10463)

MSLISKEELIKLAYSIRPRENEYKTILTNLDEYNKLTTNNNENKYLQLKKLNESIDVFMNKYKTSSRNRALSNL
KKDILKEVILIKNSNTSPVEKNLHFVWIGGEVSDIALEYIKQWADINAEYNIKLWYDSEAFLVNTLKKAIVESS
TTEALQLLEEEIQNPQFDNMKFYKKRMEFIYDRQKRFINYYKSQINKPTVPTIDDIIKSHLVSEYNRDETVLES
YRTNSLRKINSNHGIDIRANSLFTEQELLNIYSQELLNRGNLAAASDIVRLLALKNFGGVYLDVDMLPGIHSDL
FKTISRPSSIGLDRWEMIKLEAIMKYKKYINNYTSENFDKLDQQLKDNFKLIIESKSEKSEIFSKLENLNVSDL
EIKIAFALGSVINQALISKQGSYLTNLVIEQVKNRYQFLNQHLNPAIESDNNFTDTTKIFHDSLFNSATAENSM
FLTKIAPYLQVGFMPEARSTISLSGPGAYASAYYDFINLQENTIEKTLKASDLIEFKFPENNLSQLTEQEINSL
WSFDQASAKYQFEKYVRDYTGGSLSEDNGVDFNKNTALDKNYLLNNKIPSNNVEEAGSKNYVHYIIQLQGDDIS
YEATCNLFSKNPKNSIIIQRNMNESAKSYFLSDDGESILELNKYRIPERLKNKEKVKVTFIGHGKDEFNTSEFA
RLSVDSLSNEISSFLDTIKLDISPKNVEVNLLGCNMFSYDFNVEETYPGKLLLSIMDKITSTLPDVNKNSITIG
ANQYEVRINSEGRKELLAHSGKWINKEEAIMSDLSSKEYIFFDSIDNKLKAKSKNIPGLASISEDIKTLLLDAS
VSPDTKFILNNLKLNIESSIGDYIYYEKLEPVKNIIHNSIDDLIDEFNLLENVSDELYELKKLNNLDEKYLISF
EDISKNNSTYSVRFINKSNGESVYVETEKEIFSKYSEHITKEISTIKNSIITDVNGNLLDNIQLDHTSQVNTLN
AAFFIQSLIDYSSNKDVLNDLSTSVKVQLYAQLFSTGLNTIYDSIQLVNLISNAVNDTINVLPTITEGIPIVST
ILDGINLGAAIKELLDEHDPLLKKELEAKVGVLAINMSLSIAATVASIVGIGAEVTIFLLPIAGISAGIPSLVN
NELILHDKATSVVNYFNHLSESKKYGPLKTEDDKILVPIDDLVISEIDFNNNSIKLGTCNILAMEGGSGHTVTG
NIDHFFSSPSISSHIPSLSIYSAIGIETENLDFSKKIMMLPNAPSRVFWWETGAVPGLRSLENDGTRLLDSIRD
LYPGKFYWRFYAFFDYAITTLKPVYEDTNIKIKLDKDTRNFIMPTITTNEIRNKLSYSFDGAGGTYSLLLSSYP
ISTNINLSKDDLWIFNIDNEVREISIENGTIKKGKLIKDVLSKIDINKNKLIIGNQTIDFSGDIDNKDRYIFLT
CELDDKISLIIEINLVAKSYSLLLSGDKNYLISNLSNTIEKINTLGLDSKNIAYNYTDESNNKYFGAISKTSQK
SIIHYKKDSKNILEFYNDSTLEFNSKDFIAEDINVFMKDDINTITGKYYVDNNTDKSIDFSISLVSKNQVKVNG
LYLNESVYSSYLDFVKNSDGHHNTSNFMNLFLDNISFWKLFGFENINFVIDKYFTLVGKTNLGYVEFICDNNKN
IDIYFGEWKTSSSKSTIFSGNGRNVVVEPIYNPDTGEDISTSLDFSYEPLYGIDRYINKVLIAPDLYTSLININ
TNYYSNEYYPEIIVLNPNTFHKKVNINLDSSSFEYKWSTEGSDFILVRYLEESNKKILQKIRIKGILSNTQSFN
KMSIDFKDIKKLSLGYIMSNFKSFNSENELDRDHLGFKIIDNKTYYYDEDSKLVKGLININNSLFYFDPIEFNL
VTGWQTINGKKYYFDINTGAALTSYKIINGKHFYFNNDGVMQLGVFKGPDGFEYFAPANTQNNNIEGQAIVYQS
KFLTLNGKKYYFDNNSKAVTGWRIINNEKYYFNPNNAIAAVGLQVIDNNKYYFNPDTAIISKGWQTVNGSRYYF
DTDTAIAFNGYKTIDGKHFYFDSDCVVKIGVFSTSNGFEYFAPANTYNNNIEGQAIVYQSKFLTLNGKKYYFDN
NSKAVTGLQTIDSKKYYFNTNTAEAATGWQTIDGKKYYFNTNTAEAATGWQTIDGKKYYFNTNTAIASTGYTII
NGKHFYFNTDGIMQIGVFKGPNGFEYFAPANTDANNIEGQAILYQNEFLTLNGKKYYFGSDSKAVTGWRIINNK
KYYFNPNNAIAAIHLCTINNDKYYFSYDGILQNGYITIERNNFYFDANNESKMVTGVFKGPNGFEYFAPANTHN
NNIEGQAIVYQNKFLTLNGKKYYFDNDSKAVTGWQTIDGKKYYFNLNTAEAATGWQTIDGKKYYFNLNTAEAAT
GWQTIDGKKYYFNTNTFIASTGYTSINGKHFYFNTDGIMQIGVFKGPNGFEYFAPANTDANNIEGQAILYQNKF
LTLNGKKYYFGSDSKAVTGLRTIDGKKYYFNTNTAVAVTGWQTINGKKYYFNTNTSIASTGYTIISGKHFYFNT
DGIMQIGVFKGPDGFEYFAPANTDANNIEGQAIRYQNRFLYLHDNIYYFGNNSKAATGWVTIDGNRYYFEPNTA
MGANGYKTIDNKNFYFRNGLPQIGVFKGSNGFEYFAPANTDANNIEGQAIRYQNRFLHLLGKIYYFGNNSKAVT
GWQTINGKVYYFMPDTAMAAAGGLFEIDGVIYFFGVDGVKAPGIYG

TcdB (*C. difficile* stain 10463)

MSLVNRKQLEKMANVRFRTQEDEYVAILDALEEYHNMSENTVVEKYLKLKDINSLTDIYIDTYKKSGRNKALKK
FKEYLVTEVLELKNNNLTPVEKNLHFVWIGGQINDTAINYINQWKDVNSDYNVNVFYDSNAFLINTLKKTVVES
AINDTLESFRENLNDPRFDYNKFFRKRMEIIYDKQKNFINYYKAQREENPELIIDDIVKTYLSNEYSKEIDELN

TYIEESLNKITQNSGNDVRNFEEFKNGESFNLYEQELVERWNLAAASDILRISALKEIGGMYLDVDMLPGIQPD
LFESIEKPSSVTVDFWEMTKLEAIMKYKEYIPEYTSEHFDMLDEEVQSSFESVLASKSDKSEIFSSLGDMEASP
LEVKIAFNSKGIINQGLISVKDSYCSNLIVKQIENRYKILNNSLNPAISEDNDFNTTTNTFIDSIMAEANADNG
RFMMELGKYLRVGFFPDVKTTINLSGPEAYAAAYQDLLMFKEGSMNIHLIEADLRNFEISKTNISQSTEQEMAS
LWSFDDARAKAQFEEYKRNYFEGSLGEDDNLDFSQNIVVDKEYLLEKISSLARSSERGYIHYIVQLQGDKISYE
AACNLFAKTPYDSVLFQKNIEDSEIAYYYNPGDGEIQEIDKYKIPSIISDRPKIKLTFIGHGKDEFNTDIFAGF
DVDSLSTEIEAAIDLAKEDISPKSIEINLLGCNMFSYSINVEETYPGKLLLKVKDKISELMPSISQDSIIVSAN
QYEVRINSEGRRELLDHSGEWINKEESIIKDISSKEYISFNPKENKITVKSKNLPELSTLLQEIRNNSNSSDIE
LEEKVMLTECEINVISNIDTQIVEERIEEAKNLTSDSINYIKDEFKLIESISDALCDLKQQNELEDSHFISFED
ISETDEGFSIRFINKETGESIFVETEKTIFSEYANHITEEISKIKGTIFDTVNGKLVKKVNLDTTHEVNTLNAA
FFIQSLIEYNSSKESLSNLSVAMKVQVYAQLFSTGLNTITDAAKVVELVSTALDETIDLLPTLSEGLPIIATII
DGVSLGAAIKELSETSDPLLRQEIEAKIGIMAVNLTTATTAIITSSLGIASGFSILLVPLAGISAGIPSLVNNE
LVLRDKATKVVDYFKHVSLVETEGVFTLLDDKIMMPQDDLVISEIDFNNNSIVLGKCEIWRMEGGSGHTVTDDI
DHFFSAPSITYREPHLSIYDVLEVQKEELDLSKDLMVLPNAPNRVFAWETGWTPGLRSLENDGTKLLDRIRDNY
EGEFYWRYFAFIADALITTLKPRYEDTNIRINLDSNTRSFIVPIITTEYIREKLSYSFYGSGGTYALSLSQYNM
GINIELSESDVWIIDVDNVVRDVTIESDKIKKGDLIEGILSTLSIEENKIILNSHEINFSGEVNGSNGFVSLTF
SILEGINAIIEVDLLSKSYKLLISGELKILMLNSNHIQQKIDYIGFNSELQKNIPYSFVDSEGKENGFINGSTK
EGLFVSELPDVVLISKVYMDDSKPSFGYYSNNLKDVKVITKDNVNILTGYYLKDDIKISLSLTLQDEKTIKLNS
VHLDESGVAEILKFMNRKGNTNTSDSLMSFLESMNIKSIFVNFLQSNIKFILDANFIISGTTSIGQFEFICDEN
DNIQPYFIKFNTLETNYTLYVGNRQNMIVEPNYDLDDSGDISSTVINFSQKYLYGIDSCVNKVVISPNIYTDEI
NITPVYETNNTYPEVIVLDANYINEKINVNINDLSIRYVWSNDGNDFILMSTSEENKVSQVKIRFVNVFKDKTL
ANKLSFNFSDKQDVPVSEIILSFTPSYYEDGLIGYDLGLVSLYNEKFYINNFGMMVSGLIYINDSLYYFKPPVN
NLITGFVTVGDDKYYFNPINGGAASIGETIIDDKNYYFNQSGVLQTGVFSTEDGFKYFAPANTLDENLEGEAID
FTGKLIIDENIYYFDDNYRGAVEWKELDGEMHYFSPETGKAFKGLNQIGDYKYYFNSDGVMQKGFVSINDNKHY
FDDSGVMKVGYTEIDGKHFYFAENGEMQIGVFNTEDGFKYFAHHNEDLGNEEGEEISYSGILNFNNKIYYFDDS
FTAVVGWKDLEDGSKYYFDEDTAEAYIGLSLINDGQYYFNDDGIMQVGFVTINDKVFYFSDSGIIESGVQNIDD
NYFYIDDNGIVQIGVFDTSDGYKYFAPANTVNDNIYGQAVEYSGLVRVGEDVYYFGETYTIETGWIYDMENESD
KYYFNPETKKACKGINLIDDIKYYFDEKGIMRTGLISFENNNYYFNENGEMQFGYINIEDKMFYFGEDGVMQIG
VFNTPDGFKYFAHQNTLDENFEGESINYTGWLDLDEKRYYFTDEYIAATGSVIIDGEEYYFDPDTAQLVISE

TcdA-RBD-f1 antigen

HHHHHHQNKFLTLNGKKYYFDNDSKAVTGWQTIDGKKYYFNLNTAEAATGWQTIDGKKYYFNLNTAEAATGWQT
IDGKKYYFNTNTFIASTGYTSINGKHFYFNTDGIMQIGVFKGPNGFEYFAPANTDANNIEGQAILYQNKFLTLN
GKKYYFGSDSKAVTGLRTIDGKKYYFNTNTAVAVTGWQTINGKKYYFNTNTSIASTGYTIISGKHFYFNTDGIM
QIGVFKGPDGFEYFAPANTDANNIEGQAIRYQNRFLYLHDNIYYFGNNSKAATGWVTIDGNRYYFEPNTAMGAN
GYKTIDNKNFYFRNGLPQIGVFKGSNGFEYFAPANTDANNIEGQAIRYQNRFLHLLGKIYYFGNNSKAVTGWQT
INGKVYYFMPDTAMAAAGGLFEIDGVIYFFGVDGVKAPGIYG

TcdB-RBD-f1 antigen

HHHHHHEDGVMQIGVFNTPDGFKYFAHQNTLDENFEGESINYTGWLDLDEKRYYFTDEYIAATGSVIIDGEEYY
FDPDTAQLVISE

GST

MSPILGYWKIKGLVQPTRLLLEYLEEKYEEHLYERDEGDKWRNKKFELGLEFPNLPYYIDGDVKLTQSMAIIRY
IADKHNMLGGCPKERAEISMLEGAVLDIRYGVSRIAYSKDFETLKVDFLSKLPEMLKMFEDRLCHKTYLNGDHV
THPDFMLYDALDVVLYMDPMCLDAFPKLVCFKKRIEAIPQIDKYLKSSKYIAWPLQGWQATFGGGDHPPKSDLE
VLFQGPLGSPGIPGSTRAAAS

GST-TcdB-F80

MSPILGYWKIKGLVQPTRLLLEYLEEKYEEHLYERDEGDKWRNKKFELGLEFPNLPYYIDGDVKLTQSMAIIRY
IADKHNMLGGCPKERAEISMLEGAVLDIRYGVSRIAYSKDFETLKVDFLSKLPEMLKMFEDRLCHKTYLNGDHV
THPDFMLYDALDVVLYMDPMCLDAFPKLVCFKKRIEAIPQIDKYLKSSKYIAWPLQGWQATFGGGDHPPKSDLE
VLFQGPLGSEDGVMQIGVFNTPDGFKYFAHQNTLDENFEGESINYTGWLDLDEKRYYFTDEYIAATGSVIIDGE
EYYFDPDTAQLVISE

A1.3 VHH

QVKLEESGGGLVQAGGSLRLSCAASIRSFSYRNMGWFRQPPGKEREFVAAITWDGGSTRYADSVKGRFTVSRDN
AKKTVYLQMNSLKPEDAAVYYCAAGFGHTLATSSDEYDYWGQGIQVTVSS

A4.2 VHH

QVKLEESGGGLVQAGGSLRLSCAASGRTFNTLSMGWFRQAPGKEREFVAAVSRSGGSTYYADSVKGRFTISRDN
AKNTVYLQMNSLKPEDTAVYYCAAAATKSNTTAYRLSFDYWGQGTQVTVSS

A5.1 VHH

QVKLEESGGGLVQAGGSLRLSCAASGRTFSMYRMGWFRQAPGKEREFVGVITRNGSSTYYADSVKGRFTISRDN
AKNTVYLQMNSLKPEDTALYYCAATSGSSYLDAAHVYDYWGQGTQVTVSS

A19.2 VHH

QVKLEESGGGLVQPGGSLRLSCAASGRTLSSYIVAWFRQAPGKEREFVAGISRRGGNSAYVESVKGRFTISRDN
AKNTVYLQMNSLKPEDTAVYYCAADGSVAGWGRRSVSVSSYDYWGQGTQVTVSS

A20.1 VHH

QVQLVESGGGLAQAGGSLRLSCAASGRTFSMDPMAWFRQPPGKEREFVAAGSSTGRTTYYADSVKGRFTISRDN
AKNTVYLQMNSLKPEDTAVYYCAAAPYGANWYRDEYAYWGQGTQVTVSS

A24.1 VHH

QVQLVESGGGLVQAGGSLRLSCAASIRSFSNRNMGWFRQPPGKEREFVAGISWGGGSTRYADSVKGRFTISRDN
AKKTVYLQMNSLKPEDTAVYYCAAEFGHNIATSSDEYDYWGQGTQVTVSS

A26.8 VHH

QVKLEESGGGLVQAGGSLRLSCAASERTFSRYPVAWFRQAPGAEREFVAVISSTGTSTYYADSVKGRFTISRDN
AKVTVYLQMNNLKREDTAVYFCAVNSQRTRLQDPNEYDYWGQGTQVTVSS

A4.2m VHH

QVKLEESGGGLVQAGGSLRLSCAASGRTFNTLSMGWFRQAPGKEREFVCAVSRSGGSTYYADSVKGRFTCSRDN
AKNTVYLQMNSLKPEDTAVYYCAAAATKSNTTAYRLSFDYWGQGTQVTVSS

A5.1m V_HH

QVKLEESGGGLVQAGGSLRLSCAASGRTFSMYRMGWFRQAPGKEREFVCVITRNGSSTYYADSVKGRFTCSRDN
AKNTVYLQMNSLKPEDTALYYCAATSGSSYLDAAHVYDYWGQGTQVTVSS

A19.2m V_HH

QVKLEESGGGLVQPGGSLRLSCAASGRTLSSYIVAWFRQAPGKEREFVCGISRRGGNSAYVESVKGRFTCSRDN
AKNTVYLQMNSLKPEDTAVYYCAADGSVAGWGRRSVSVSSYDYWGQGTQVTVSS

A20.1m V_HH

QVQLVESGGGLAQAGGSLRLSCAASGRTFSMDPMAWFRQPPGKEREFVCAGSSTGRTTYYADSVKGRFTCSRDN
AKNTVYLQMNSLKPEDTAVYYCAAAPYGANWYRDEYAYWGQGTQVTVSS

A24.1m V_HH

QVQLVESGGGLVQAGGSLRLSCAASIRSFSNRNMGWFRQPPGKEREFVCGISWGGGSTRYADSVKGRFTCSRDN
AKKTVYLQMNSLKPEDTAVYYCAAEFGHNIATSSDEYDYWGQGTQVTVSS

A26.8m V_HH

QVKLEESGGGLVQAGGSLRLSCAASERTFSRYPVAWFRQAPGAEREFVCVISSTGTSTYYADSVKGRFTCSRDN
AKVTVYLQMNNLKREDTAVYFCAVNSQRTRLQDPNEYDYWGQGTQVTVSS

B5.2 V_HH

QVQLVESGGGLVQPGGSLRLSCAASGNIFSINTMGWYRQAPGKQLELVAAITSGGTTSYTDSVEGRFTISRDNA
KNAVYLQMNSLKAEDTAVYYCNTVKVVGGRLDNPDYWGQGTQVTVSS

B7.3 V_HH

QVKLEESGGGLVQPGGSLRLSCAASGRTASGYGMGWFRQAPGKEREFVAAISRSGAGTLNADFVKGRFTISRDN
AKNTVYLQMNSLKPEDTAVYYCVARPTKVDRDYATRREMYNYWGQGTQVTVSS

B13.2 V_HH

QVKLEESGGGSVQAGGSLRLSCAASGRDFSTLAMGWFRQAPGKEREFVATINWSGGTTHYADSVKGRFTISRDN
AKNTVYLQMGSLKPEDTAVYYCGRSKYAAGALTRAYDYNYWGQGTQVTVSS

B13.3 V_HH

QVKLEESGGGLVQAGGSLRLSCSASGSIFSINDMGWYRRAPGKRRELVAAITSGGIPNYADSVKGRFTISRDNA
KNTGYLQMNSLKPEDTAVYYCAAQFGTVAAALRRHEYDYWGQGTQVTVSS

B13.6 V_HH

QVKLEESGGGLVQAGGSLRLSCSASGRTFSSGVMGWFRQAPGKQRELVAAITTGGSTSYTDSVKGRFTISRDNA
KNTVYLQMNSLKPEDTAVYYCNSVAVVGGVIKSPDYWGQGTQVTVSS

B15.3 V_HH

QVQLVESGGGSVQAGGSLRLSCAASGLSRYAMAWFRQGTGKEREFVASTNWSSGNTPYADSVKGRFIISRDNAK
NTVYLQMNSLKPGDTAIYYCAARKLDVPSRYSQHYDYWGQGTQVTVSS

B15.5 V_HH

QVQLVESGGDLVQAGGSLRLSCAASGSISRISTMGWYRQAPGKQRELVATISTGGTTNYAESVKGRFTVSRDNA
KNTMYLQMNSLKPEDTAVYYCAAGWKVVRGSLEYEYSGQGTQVTVSS

B4.3 V_L

DIQMTQSPSSLSASVGDRVTITCRASQSISTYLNWYQQKPGKAPKLLIFRASRRPSGVPSRFSGSGSGTDFTLT
ISNLQPEDFATYYCGQSEPGPPRTFGHGTKVTVL

B5. 40 V_L

DIQMTQSPSSLSASVGDRVTITCRASQSISTYLNWYQQKPGKAPKLLIFRASRRVSGVPSRFSGSGSGTDFTLT
ISNLQPEDFATYYCTQSEPGPSRTFGHGTKVTVL

B12.51 V_L

DIQMTQSPSSLSASVGDRVTITCKASQGIASRLGWYQQKPGKAPKLLIFDASRRASGVPSRFSGSGSGTDFTLT
ISNLQPEDFATYYCGQFSSIPRTFGHGTKVTVL

B17.62 V_L

DIQMTQSPSSLSASVGDRVTITCVASQSIGMGLGWYQQKPGKAPKLLIFAASRRPSGVPSRFSGSGSGTDFTLT
ISNLQPEDFATYYCSQRKMRPFTFGHGTKVTVL

CURRICULUM VITAE

GREG HUSSACK, Ph.D.

EXPERTISE

- Extensive background in monoclonal antibody and recombinant antibody therapeutics.
- Ten years of industry, government, and academic research experience.
- Keen interest in the development of biological therapeutics (e.g., proteins, enzymes, antibodies).
- Extensive peer-reviewed publication record.
- Course development, lecturing and laboratory coordinator experience.

EXPERIENCE

2007-Present National Research Council Canada Ottawa, ON

Ph.D. Student / Visiting Scientist

- Isolated and characterized the first single-domain antibody inhibitors of *Clostridium difficile* toxin A & B.
- Developed a protein engineering technique that universally increases antibody thermal stability and reduces antibody degradation by the major gastrointestinal proteases.
- Initiated several key Canadian and international collaborations within NRC aimed at developing and implementing single-domain antibodies as oral therapeutics against infectious disease targets.
- Maintained effective communication and productive relationships with key collaborators to monitor project results, milestones and new directions.
- Presented key findings at several international scientific conferences.
- First-authored three (3) and co-authored one (1) peer reviewed publications.
- First-authored two (2) invited book chapters in *Methods in Molecular Biology* on the isolation and engineering of single-domain antibodies for therapeutic applications.
- Co-inventor on a *C. difficile* single-domain antibody patent.

2006-2007 Conestoga College Kitchener, ON

Lecturer and Course Developer

- Recruited to develop components of the Biotechnology Program curriculum at Conestoga College, a new 2-year applied science diploma program.
- Delivered weekly molecular biology lectures to 30+ students.
- Coordinated a weekly molecular biology lab, instructed and lead hands-on cloning and gene expression experiments in the lab, and graded weekly reports.

2005-2007 University of Guelph Guelph, ON

M.Sc. Student / Research Assistant

- Developed and implemented a novel, cost-effective purification technique for the isolation of therapeutic monoclonal antibodies from transgenic tobacco.
- Provided technical direction / critique and lead team meetings with collaborators from OMAFRA and McMaster University.
- Developed and tested a novel antibody-based water purification device for the removal of small organic pesticides from water samples.

- First-authored one (1) peer-reviewed publication.
- Supervised and mentored two summer students on various molecular biology and protein engineering projects.

2003 Samuel Lunenfeld Research Institute, Mount Sinai Hospital Toronto, ON

Research Assistant

- Elucidated a role of kallikrein serine proteases in normal skin and psoriatic skin in the laboratory of Dr. E. P. Diamandis.
- Co-authored one (1) peer reviewed publication.
- Generated and characterized monoclonal antibodies against several kallikreins, a family of novel serum biomarkers for cancer.
- Instrumental in assay development and molecular cloning projects.

2002 DuPont Canada Georgetown, ON

Research Assistant

- Conducted greenhouse canola trials for the double haploid canola breeding program at DuPont subsidiary Pioneer HiBred Limited.
- Performed statistical analysis on large data sets generated from greenhouse trials.
- Awarded a NSERC / University of Waterloo co-op work term placement award for performance.

2001 Toxin Alert Inc. Guelph, ON

Research Technician

- Assisted in the optimization and monitoring of large-scale monoclonal antibody production in hollow-fiber bioreactors for therapeutic and diagnostic applications.
- Developed immunological detection assays for food-borne pathogens.

EDUCATION

2007 – Present University of Ottawa Ottawa, ON
- Ph.D. (candidate) Biochemistry / Microbiology / Immunology
- Thesis: "Single-domain antibody inhibitors of *Clostridium difficile* toxins".
- Supervisor: Dr. Jamshid Tanha
- **Projected completion date: August 2011**

2005 - 2007 University of Guelph Guelph, ON
- M.Sc. Molecular Biology / Biochemistry
- Thesis: "Applications of cellulose binding domain fusion proteins: From antibody purification to bioactive filters".
- Supervisor: Dr. J. Christopher Hall

1999 - 2004 University of Waterloo Waterloo, ON
- B.Sc. (Honours) Biochemistry
- Co-op Program

HONOURS & AWARDS

2010 Second place winner. Student Poster Scholarship Program, IBC Antibody Engineering and Immunotherapeutics Conference, San Diego, CA.

2010 University of Ottawa travel award.

2010 Ontario Graduate Scholarship.

2010 University of Ottawa Excellence Scholarship.

2009 Silver medal award. CIHR National Student Health Research Forum, Winnipeg, MB.

2009 CIHR Infection and Immunity travel award, Winnipeg, MB.

2009 Mary Beatrice Houlihan Memorial Scholarship.

2008 First place winner. University of Ottawa Poster Day.

2007 Admission Scholarship, University of Ottawa.

2006 Latronell Graduate Scholarship, University of Guelph.

2004 Dean's honour list, University of Waterloo.

2003 Dean's honour list, University of Waterloo.

2002 NSERC co-op work placement award, DuPont Canada.

PATENTS

1. **Hussack G**, Arbabi-Ghahroudi M, MacKenzie CR, Tanha J. *Clostridium difficile*-specific antibodies and uses thereof. Application No. 61/406,254 (Filed Oct. 28, 2010).

PUBLICATIONS (PEER REVIEWED)

1. **Hussack G**, Hirama T, Ding W, MacKenzie R, Tanha J. (2011) Engineered single-domain antibodies with increased thermal stability and protease resistance. *PLoS ONE* (In press).
2. **Hussack G**, Arbabi-Ghahroudi M, van Faassen H, Songer JG, Ng KK, MacKenzie R, Tanha J. (2011) Neutralization of *Clostridium difficile* toxin A with single-domain antibodies targeting the cell receptor binding domain. *Journal of Biological Chemistry* 286, 8961-8976.
3. **Hussack G**, Tanha J. (2010) Toxin-specific antibodies for the treatment of *Clostridium difficile*: current status and future perspectives. *Toxins* 2, 998-1018.
4. **Hussack G**, Grohs BM, Almquist KC, McLean MD, Ghosh R, Hall JC. (2010) Purification of plant-derived antibodies through direct immobilization of affinity ligands on cellulose. *Journal of Agricultural and Food Chemistry* 58, 3451-3459.
5. Doyle PJ, Saeed H, Hermans A, Gleddie SC, **Hussack G**, Arbabi-Ghahroudi M, Seguin C, Savard ME, MacKenzie CR, Hall JC. (2009) Intracellular expression of a single-domain antibody reduces cytotoxicity of 15-acetyl-deoxynivalenol in yeast. *Journal of Biological Chemistry* 284, 35029-35039.
6. **Hussack G**, Lou Y, Ryan S, Veldhuis L, Hall JC, Tanha J, MacKenzie R. (2009) Multi-valent anchoring and oriented display of single-domain antibodies on cellulose. *Sensors* 9, 5351-5367.
7. Komatsu N, Saijoh K, Toyama T, Ohka R, Otsuki N, **Hussack G**, Takehara K, Diamandis EP. (2005) Multiple tissue kallikrein mRNA and protein expression in normal skin and skin diseases. *British Journal of Dermatology* 153, 274-281.

PUBLICATIONS (SUBMITTED OR IN PREPARATION)

1. **Hussack G**, Keklikian A, van Faassen H, Tanha J. (2011) Construction of a synthetic human V_L single-domain antibody library and isolation of soluble, non-aggregating V_Ls against several protein targets. *Prot Eng Des Sel* (Submitted).
2. Parisien A, Dorval-Courchesne NM, **Hussack G**, Tanha J, Lan CQ. (2011) Optimized expression of a single-domain antibody against *Clostridium difficile* toxin A in *Escherichia coli*. (In preparation).

BOOK CHAPTERS

1. **Hussack G**, MacKenzie R, Arbabi-Ghahroudi M, Tanha J. (2011) Isolation and characterization of *Clostridium difficile* toxin-specific single-domain antibodies. *Methods in Molecular Biology* (In press).
2. **Hussack G**, MacKenzie R, Tanha J. (2011) Characterization of single-domain antibodies with an engineered disulfide bond. *Methods in Molecular Biology* (In press).

PRESENTATIONS

1. **Hussack G.** Single-domain antibody inhibitors of *Clostridium difficile* toxin A bind to sites other than the carbohydrate binding pocket. Oral presentation. 7th National Carbohydrate Symposium (AICCS), Banff, AB (05/2011).
2. **Hussack G**, MacKenzie CR, Tanha J. Engineered single-domain antibodies with increased thermal stability and protease resistance. IBC Antibody Engineering Conference, San Diego, CA (12/2010).
3. **Hussack G**, MacKenzie CR, Tanha J. Engineered single-domain antibodies with increased thermal stability and protease resistance. University of Ottawa, BMI Department Poster Day, Ottawa, ON (05/2010).
4. **Hussack G**, Arbabi M, Songer G, MacKenzie CR, Tanha J. Isolation and characterization of single-domain antibodies against *Clostridium difficile* toxin A and B. NRC Poster Day, National Research Council Canada, Ottawa, ON (03/2010).
5. Logan SM, Twine SM, Reid C, Chen W, **Hussack G**, Austin J, Aubry A, KuoLee R, Fulton K. Flagellar glycosylation in *Clostridium difficile*. ClosPath, Rome, Italy (10/2009).
6. **Hussack G**, Arbabi M, Songer G, MacKenzie CR, Tanha J. Isolation and characterization of single-domain antibodies against *Clostridium difficile* toxin A and B. CIHR National Student Health Research Forum, Winnipeg, MB (06/2009).
7. Doyle PJ, Saeed H, Hermans A, Gleddie S, **Hussack G**, Arbabi-Ghahroudi M, Savard ME, MacKenzie CR, Hall JC. Intracellular expression of a single domain antibody fragment confers resistance to 15-acetyl-deoxynivalenol. Gordon Mycotoxins and Phycotoxins Conference, New London, NH (05/2009).
8. **Hussack G.** Isolation and characterization of single-domain antibodies against *Clostridium difficile* toxins A and B. Oral presentation, National Research Council Canada Seminar Series, Ottawa, ON (05/2009).
9. **Hussack G**, Arbabi M, Songer G, MacKenzie CR, Tanha J. Isolation and characterization of single-domain antibodies against *Clostridium difficile* toxin A and B. Keystone Antibodies as Drugs Conference, Whistler, BC (03/2009).
10. **Hussack G**. Isolation and characterization of single-domain antibodies against *Clostridium difficile* toxins A and B. Oral presentation, University of Ottawa, BMI Department Seminar Day, Ottawa, ON (02/2009).
11. Doyle PJ, Saeed H, Hermans A, Gleddie S, **Hussack G**, Arbabi-Ghahroudi M, Savard ME, MacKenzie CR, Hall JC. Intracellular expression of a single domain antibody fragment confers resistance to 15-acetyl-deoxynivalenol. IBC Antibody Engineering Conference, San Diego, CA (12/2008).
12. **Hussack G**, Arbabi-Ghahroudi M, MacKenzie CR, Tanha J. Isolation and characterization of single-domain antibodies against *Clostridium difficile* toxin A and B. University of Ottawa, BMI Department Poster Day, Ottawa, ON (05/2008).
13. **Hussack G**, Almquist KC, McLean MD, Hall JC. Single-step preparation of a novel affinity column for recombinant antibody purification from *Pichia pastoris* and tobacco. IBC Antibody Engineering Conference, San Diego, CA (12/2006).
14. **Hussack G**, Almquist KC, Hall JC. Antibody-based biofilters: An emerging technology for the selected removal of organic contaminants from water. Society of Environmental Toxicology and Chemistry (SETAC) AGM, Sudbury, ON (05/2006).
15. Memari N, **Hussack G**, Cui S, Grass L, Diamandis EP. Production of polyclonal antibodies against human tissue kallikrein 9. American Association for Cancer Research (AACR), Orlando, FL (03/2004).